SCAFFOLDLESS TISSUE ENGINEERING: A MODEL TO STUDY TISSUE FORMATION AND A DEVICE FOR TISSUE REGENERATION

by

Fatima Naz Syed-Picard

B.S. Materials Science and Engineering, University of Michigan, 2004

M.S. Materials Science and Engineering, University of Michigan 2006

Submitted to the Graduate Faculty of

Swanson School of Engineering in partial fulfillment

of the requirements for the degree of

Doctor of Philosophy

University of Pittsburgh

2013

UNIVERSITY OF PITTSBURGH

SWANSON SCHOOL OF ENGINEERING

This dissertation was presented

by

Fatima N. Syed-Picard

It was defended on

November 27, 2012

and approved by

Elia Beniash, PhD, Associate Professor, Department of Oral Biology

Lance Davidson, PhD, Associate Professor, Department of Bioengineering

Pamela Robey, PhD, Chief, Craniofacial and Skeletal Diseases Branch, NIDCR

Yadong Wang, PhD, Associate Professor, Department of Bioengineering

Dissertation Director: Charles Sfeir, DDS, PhD, Department of Bioengineering

SCAFFOLDLESS TISSUE ENGINEERING: A MODEL OF TISSUE FORMATION AND A DEVICE FOR TISSUE REGENERATION

Fatima N. Syed-Picard, PhD

University of Pittsburgh, 2013

Traditional tissue engineering methods involve the combination of cells, growth factors and a scaffold to regenerate 3D tissues for therapeutic purposes. Naturally, cells utilize their endogenous matrix as a scaffold to form 3D structures. The goals of this thesis were to study scaffoldless 3D constructs as a model of tissue formation and as a device for dental and bone regenerative therapies. Scaffoldless 3D constructs were first used as a model that showed that calcium phosphates are osteoinductive and alter 3D spatial differentiation patterns of dental pulp cells through modulations of connexin 43 expression. Scaffoldless 3D constructs were next used as a model system that showed tissues formed from an isolated population of dental pulp pericyte stem cells regenerated structurally and molecularly different 3D tissues than the total population of dental pulp cells. These studies emphasize the importance of scaffold and cell selection for regenerative therapies. Scaffoldless 3D dental pulp cell tissues were then used as a device that regenerated pulp-like tissue in the root canals of human tooth root segments. Dental pulp cells delivered into the root canals with calcium phosphate particles as a delivery system formed a mixture of dentin and pulp-like tissues. These two cell delivery systems show promise for various endodontic therapies. Finally,

scaffoldless bone marrow stromal cell sheets were wrapped around calcium phosphate cements to create a structurally and molecularly relevant periosteum-like tissue that will aid in bone regeneration. These studies show the significance of using engineered tissues generated and organized entirely by the cells themselves and emphasize that scaffoldless engineered tissues are powerful tools for dental and bone research and regeneration.

TABLE OF CONTENTS

LIST OF TABLES

LIST OF FIGURES

ACKNOWLEDGEMENTS

This dissertation is dedicated to my father, the late Kutub Syed, and my mother Talat Syed. I will never be able to thank my parents enough for all of the sacrifices they made for me and my siblings and for their never ending support and love.

This dissertation represents years of research that could not have been done without the support and encouragement of several people. I would like to first thank my research advisor, Dr. Charles Sfeir for providing an amazing learning environment. I would like to thank him for all of his research guidance and encouragement and most of all thank him for being a mentor for my career. I would also like to thank him for always supplying good music. I would like to thank Dr. Elia Beniash, Dr. Lance Davidson, Dr. Pamela Robey, and Dr. Yadong Wang for being on my thesis committee and provide feedback and unique perspectives on this research. I would like to especially thank Dr. Robey for making the multiple trips to Pittsburgh for my committee meetings.

This work could not have been done with the support of Center for Craniofacial Regeneration and the Sfeir laboratory past and present. I would like to thank Bonnie Teng, Hong Wu, Jinhua Li, Lynzy Maruca, Linda Zhang, Shinsuke Onishi, Amy Chaya, Wenju Cui, Andrew Brown, Samer Zaky, Jay Jayaraman, Sayuri Yoshizawa, Sabrina Noorani, Sylvain Bougoin, Ray Lam, Shannen Liu, Dandan Hong, Sarah Henderson, Avinash Patel, Catherine Hagendora, and Nicole Myers for their support and camaraderie. I would like to thank the dental students, Neil Robertson, Gaurav Shah,

Steven Cudney, and Tong Liu for working with me on these projects. I would like to also thank the CCR faculty, Dr. Elia Beniash, Dr. Alejandro Almarza, Dr. Juan Toboas, Dr. Kostas Verdelis, Dr. Hongjiao Ouyang, and Dr. Heather Szabo-Rogers for their support and feedback on this research. I would like to thank Dr. Herbert Ray for introducing me to the world of endodontics. This work could not have been done without the support of our administrators Diane Turner and Michele Leahy.

I would like to acknowledge my previous mentors for all of the career guidance they have provided me and for all of the training that I received in their laboratories. Thank you to Dr. Marian Young, Dr, Ellen Arruda and Dr. Lisa Larkin.

I would like to thank the National Institute of Dental and Craniofacial Research for providing financial support for my graduate studies.

None of this could have been done without the support from my family and friends. I would like to thank my amazing siblings, my sister, Amena, and my brother, Ajaz, for all of their encouragement. I would like to thank my awesome mother and father-in-law Zareena and Ibrahim Picard for all of their support. Finally, I can not thank my loving husband, Yoosuf, enough for all of his support and encouragement.

1.0 CHAPTER 1: INTRODUCTION

1.1 NEED FOR TISSUE ENGINEERING

1.1.1 Need for dental tissue engineering

It is estimated that 85% of adults in the Western countries have endured dental treatment and by the age of 50, the average adult has lost 12 teeth (Sharpe and Young, 2005).Currently, missing teeth are replaced with either conventional fixed, removable prosthesis or titanium metal implants with ceramic crowns. These strategies are adequate but also have many limitations such as insufficient tissue integration and complications at the tissue/material interface (Scheller et al., 2009). Thus, many research groups are developing strategies to utilize biological approaches to engineer dental tissues.

Regenerative therapies for endodontics would prolong the life of the entire tooth organ. The field of endodontics focuses on the treatment of the inner most, soft tissue of the tooth, the dental pulp. During an endodontic treatment the dental pulp is extracted due to Infection and an inert material is used to fill the dental pulp chamber. While these treatments are generally successful (Friedman et al., 2003), the removal of the dental pulp compromises the health of remaining tooth organ. One of the main causes of the

future extraction of treated teeth is the formation of caries that potentially could have been repaired by progenitor cells in the pulp (Zadik et al., 2008). The surrounding hard tissue of the pulp, the dentin, becomes mechanically altered after an endodontic treatment due potentially to the loss of moisture and interstitial pressure provided by the pulp tissue, which leads to higher fracture susceptibility to the tooth (Akkayan and Gulmez, 2002; Heyeraas and Berggreen, 1999; Soares et al., 2007). Additional problems arise from the placement of an inert material in the pulp space. Often, endodontically treated teeth require retreatment due to bacterial penetration through the material (Ray and Trope, 1995; Stockton, 1999; Torabinejad et al., 1990). The presence of a vital pulp would provide a biological defense and maintain interstitial pulp pressure to deter such invasions (Heyeraas and Berggreen, 1999). The complications associated with current endodontic treatments could be avoided by the regeneration of a vital pulp.

Another facet of endodontics is the protection of the dental pulp after exposures. Current methods involve using a cement to form a barrier between the dental pulp and the oral flora; however, there are several complications with the current materials used for this application such as bacterial leakage over long periods or difficulty in handling due to long setting times (Bakland and Andreasen; Torabinejad and Chivian, 1999). The ideal biomaterial for the protection of exposed pulps would induce dentin bridge formation from the remaining healthy pulp tissue that would inhibit future bacterial penetration and would be easy to handle for clinical application (Chong and Pitt Ford, 2005; Takita et al., 2006).

1.1.2 Need for bone tissue engineering

There are over 6.3 million bone fractures annually in the United States (Stevens et al., 2008). Currently, the main treatment for bone repair involves autografts and allografts; however, there is often limited graft availability and these therapies can lead to donor site morbidity or immune rejection. Tissue engineered bone substitutes could avoid such complications.

The presence of a functional periosteum in a bone defect has been shown to accelerate repair (Eyre-Brook, 1984; Knothe Tate et al., 2007; Zhang et al., 2008). The periostuem is a soft tissue enclosing the bone that provides vasculature and progenitor cells that can facilitate bone formation(Allen et al., 2004; Ellender et al., 1988; Marks and Popoff, 1988). Periosteum grafting has shown to be successful in aiding in bone healing, however, it inflicts similar limitations of total bone grafting (Fujii et al., 2006; Puckett et al., 1979; Reynders et al., 1999). An engineering periosteum-like tissue could be a promising method of cell delivery to a bone defect site or could be combined with load bearing scaffolds to facilitate functionality and repair.

1.2 TOOTH ANATOMY

Teeth are multi-tissue organs found in the mouth that function mainly in mastication. **Figure 1.1** shows a schematic of multiple tissues of the tooth. Enamel is the outer most structure of the crown region of the tooth and is the hardest tissue in the body. It

develops prior to tooth eruption from ameloblasts, the epithelially derived enamel forming cells. After eruption however, the ameloblasts are lost, and therefore this structure is unable to renew itself. Dentin is an avascular, mineralized tissue that lies below the enamel spanning both the crown and root regions of the tooth. The function of dentin is to provide mechanical support during mastication to the surrounding more brittle enamel (Nanci, 2003). The center of the tooth is composed of a soft connective tissue, the dental pulp, that maintains the surrounding dentin by providing a population of progenitor cells and a source of moisture to the surrounding tissues. The pulp is considered the most vital part of the tooth organ since it is vascular and can

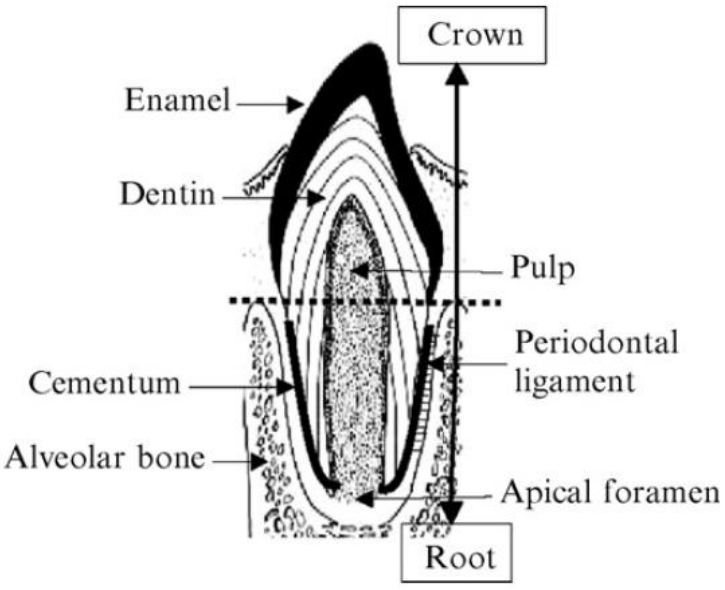

Figure 1.1: Schematic of tooth(Liu et al., 2006)

therefore provide nutrients to its surrounding tissues, and also facilitates the sensory mechanisms of the tooth. The dentin and dental pulp are important components of the tooth organ with reparative capacity, therefore, the regeneration of these tissues after trauma and disease is of great focus for dental tissue engineering.

1.2.1 Dental pulp

The dental pulp is a vascular, connective tissue found in the center of the tooth with fibroblastic cells, nerves, capillaries, macrophages, and a population of stem cells that aid in regeneration of the pulp and the surrounding dentin(Goldberg and Smith, 2004; Liu et al., 2006). The extracellular matrix of the dental pulp comprises mainly types I and III collagen. The pulp space also constitutes interstitial fluids that provide moisture to the surrounding dentin and aids in the transport of nutrients or waste between the cells and the vasculature and (Heyeraas and Berggreen, 1999). The neural components of the dental pulp protect the tooth organ by registering a response to external temperatures and forces(Hildebrand et al., 1995). The outer region of the dental pulp is lined with odontoblasts, the cells that generate and maintain the dentin. After maturation, these cells become post mitotic and can only aid in the repair of minor defects in the dentin, however, upon larger trauma to the dentin, progenitor cells in the dental pulp facilitate the repair of the surrounding hard tissue (Liu et al., 2006; Ruch, 1998).

1.2.2 Dentin

Dentin is composed of approximately 50 vol% of low crystallinity carbonated hydroxyapatite mineral, 30 vol% organic material which is mainly type I collagen, and 20 vol % fluid (Marshall et al., 1997). There are several non-collagenous proteins also present in dentin that are thought to be involved in dentin formation and mineralization

processes (Boskey, 1998), one of which being dentin matrix protein 1 (DMP1). This protein was originally discovered in dentin and considered to be dentin specific, however it has since been found in other hard tissues such as bone (Qin et al., 2007). Two of the most notable non-collagenous proteins found in dentin are dentin phosphoprotein (DPP) and dentin sialoprotein (DSP). Unlike most components of dentin which are present in similar concentrations to other mineralized tissues, DPP and DSP are found in high amounts in dentin, whereas only trace amounts are found in other hard tissues such as bone. These two proteins are specific cleavage products of a single gene called dentin sialophosphoprotein (DSPP) (Suzuki et al., 2009). The expression of this gene and its products are often used as a dentin marker.

During dentinogenesis, odontoblasts, the dentin-forming cells, differentiate from dental papilla at the dentin-enamel interface. These cells organize between the dentin and dental pulp and continually deposit dentin towards the center of the tooth in the direction of the pulp chamber. As the odontoblasts produce dentin they leave behind tracks termed tubules containing single cytoplasmic projections from the cells that extend from the enamel or cementum to the pulp chamber. These tubules and the single cytoplasmic projections of the odontoblasts are distinct structures of dentin and its cells (Marshall et al., 1997; Nanci, 2003). During their final stages of cell maturation, the cells undergo terminal differentiation and become post-mitotic. Upon mild trauma, odontoblasts can produce reactionary dentin which share many similarities to primary dentin (Liu et al., 2006; Ruch, 1998). If dentin is significantly damaged, progenitor cells from the pulp migrate into the dentin and differentiate into odontoblast-like cells to produce reparative dentin. Reparative dentin can be produced with the similar tubular

structure of primary dentin, or in an atubular form. Often times the odontoblast-like cells will become trapped within the reparative dentin matrix. In this case the cells have a more cuboidal morphology (Hwang et al., 2008; Lee et al., 2006). It has been shown that the precursors involved in dentin repair are stem cells (Gronthos et al., 2000). It is hypothesized that growth factors in the transforming growth factor beta (TGF-β) super family such as TGF-β1 and bone morphogenetic protein 2 (BMP2) are released from the dentin matrix during trauma and these signaling molecules stimulate the stem cells from the dentin pulp to differentiate into odontoblasts (About et al., 2002).

1.3 Bone Anatomy

Bone is mineralized tissue of the musculoskeletal system that provides structure, protects internal organs, and facilitates muscle action and movement. This tissue is also involved in cell formation, mineral storage, and calcium metabolism (Frankel, 2001). The tissue is predominately composed of type I collagen and low crystallinity carbonated hydroxyapatite mineral. Several non-collagenous components are also present in bone, the most notable being osteocalcin, osteonectin, and bone sialoprotein (Clarke, 2008). Bone is maintained by three different cell types: osteoblasts, osteocytes, and osteoclasts. Osteoblasts are involved in the deposition and mineralization of type I collagen. Once the osteoblast is fully surrounded by mineralized matrix, it differentiates into an osteocyte. Osteocytes sit in open lacunae within the mineralized tissue and maintain the bone. Finally, osteoclasts are large multinucleated cells that resorb mineralized bone (Marks and Popoff, 1988). The multiple cell types of

bone allow it to remodel itself. Bone is therefore able to withstand functional loads because of its ability to alter its architecture with changes in the loading environment. Also, when inflicted with a small defect, bone can easily heal by the combination of processes of collagen deposition, mineralization, and resorption (Ehrlich and Lanyon, 2002).

Bones are surrounded by an outer fibrous sheath known as the periosteum. This tissue serves as an interface between bone and surrounding tissues, provides precursor bone cells, and is involved in the radial growth of bone through intramembranous ossification. An intact periosteum in bone defects aids in accelerated bone healing by providing a cell source (Marks and Popoff, 1988). The periosteum is composed of two different layers. The outer fibrous layer is composed of connective tissue with elongated fibroblasts oriented parallel to the axis of the bone (Hall, 2000). The inner cambium layer is composed of mesenchymal progenitor cells, fibroblasts, pre-osteoblasts and osteoblasts. The periosteum can be characterized through both morphological and molecular mechanisms. The cambium layer of the periosteum directly lines the outer surface of the bone and can be morphologically characterized by the presence of cuboidal osteoblasts organized in rows(Allen et al., 2004; Ellender et al., 1988; Marks and Popoff, 1988). Periostin, also known as osteoblast-specific factor-2, is an extracellular matrix protein that is found in high levels in the cambium layer and in lower amounts in the fibrous layers of the periosteum but not in the bone matrix or the endosteum. This protein is thought to be expressed by the periosteal pre-osteoblasts and osteoblasts and may act as cell adhesion molecules (Allen et al., 2004; Horiuchi et al., 1999). Periostin is also found in the periodontal ligament, during embryonic

development of heart valves, in the myocardium of patients with heart failure, and is over expressed in tumors, however, since it is not expressed in any other bone region, it can be used as a periosteum specific marker (Horiuchi et al., 1999; Kuhn et al., 2007).

1.4 CALCIUM PHOSPHATE

Calcium phosphates constitute the mineral component of vertebrate hard tissues and are therefore considered an obvious scaffolding choice for hard tissue engineering(LeGeros, 2002; Rezwan et al., 2006). Hydroxyapatite is the crystalline form of calcium phosphate found in mature tissues, however, during tissue maturation calcium phosphate transforms through several phases before crystallizing into its final form. The initial phase of calcium phosphate found during vertebrate biomineralization is amorphous calcium phosphate which transforms through transient mineral phases such as octacalcium phosphate before finally stabilizing into hydroxyapatite(Boskey, 1998; Crane et al., 2006; Jager et al., 2006). The biological role of each individual phase of calcium phosphate in biomineralization is not fully understood, therefore, several different phases of calcium phosphates are being investigated as scaffolding materials.

Until recently, calcium phosphates were considered to be osteoconductive but not osteoinductive(Damien and Parsons, 1991; LeGeros, 2002), meaning that these materials would act as a substrate for bone deposition in the presence of osteogenic factors, however, could not alone induce osteogenic differentiation *in vitro* or in an ectopic site *in vivo* (LeGeros, 2008). Studies have now started to show that some calcium phosphates do exhibit osteoinductive-like properties but the exact mechanism

is largely unknown (Muller et al., 2008; Yuan et al., 2000; Yuan et al., 2010). It has been postulated that this property is based on topography and the interconnectivity of porosity of the material as these geometrical factors may aid in the ability of calcium phosphates to provide a substrate for the adsorption and entrapment of circulating osteogenic factors such as bone morphogenic proteins (BMP) (LeGeros, 2008; Li et al., 2011). However, in these cases the osteoinductivity is not intrinsic to the material itself rather the result of the ability of material to adsorb biological factors. Additional studies though have shown that certain types of calcium phosphates have increased capacity to induce osteogenic differentiation in spite of surface morphologies and potentially due to the release of soluble ions suggesting that calcium phosphates may direct differentiation at a more molecular level(Knabe et al., 2004; Knabe et al., 2008; Sun et al., 2004). A deeper understanding on the mechanisms facilitation the osteoinductivity of calcium phosphates would aid in future tissue engineering scaffold design.

1.5 STEM CELLS

Regenerative therapies for dental and bone restoration require an autologous source of cells that are easily accessible and maintain a reparative capacity. One of the body's natural methods of repair involves stem cells that remain quiescent in the body until needed for growth, renewal, and maintenance of tissues. Stem cells are cells with self renewal capabilities and can differentiate down multiple cell lineages. These cells can be derived from many different sources, the most valuable source being from blastocyte stage embryos. Embryonic stem cells are involved in initial organ formation during development. They have the greatest long term proliferation capacity and can

transform into any fully differentiated cell in the body (Zandstra and Nagy, 2001). However, the therapeutic use of embryonic stem cells is limited due to the ethical issues related with their isolation. Adult stem cells maintain and repair tissues and can be found in several different regions of the body such as bone marrow, adipose, skin, blood, and muscle tissues. These cells do not have the same level of plasticity as embryonic stem cells, but can still differentiate into several different cell types.

In situ, the microenvironment of stem cells, or the stem cell niche, is thought to be composed of other cells and matrix that maintain the stem cells in a quiescent state. Disruptions of this niche due such things as trauma may trigger the stem cell to multiply or differentiate and the resulting progenitor or differentiated cells aid in tissue repair and remodeling(Moore and Lemischka, 2006; Watt and Hogan, 2000). A more fundamental understanding of the factors that stimulate stem cell differentiation down various pathways and their capacity for tissue formation will lead to improved cellular therapies and tissue engineering approaches for dental and craniofacial regeneration. Stem cells have been discovered and characterized in several different adult dental tissues including dental pulp and bone marrow (Gronthos et al., 2000; Miura et al., 2003; Pittenger et al., 1999).

Traditional methods of harvesting cells involve the collection of the total population of the cells after enzymatic digestion of tissues or cell outgrowth from tissue biopsies. However, stem cells comprise only a small fraction of the cells in a tissue. Different mechanisms exist to purify the population of stem cells. Cell can be cultured at low density and due to their clonogenic nature, stem cells can to survive and divide at this low density whereas differentiated cells can not. These clonogenic cells will form

individual colonies and if cultured properly, these groups of cells will maintain their stem cell nature. Stem cells can also be characterized by cell surface proteins, and different cell sorting techniques, such as fluorescence activated cell sorting or magnetic activated cell sorting, have been developed to separate cells based on the expressions of these markers. It has been shown that one stem cell niches is located in the perivascular regions of tissues. Therefore, cell surface proteins specific for pericytes are used to isolate stem cell populations such as STRO-1 and CD146 (Crisan et al., 2008b; Shi and Gronthos, 2003). However, the remaining cells from the originating tissue may provide support during cell differentiation and tissue formation. Therefore, it is unknown whether the total population of cells isolated from a tissue should be used for regenerative therapies or if the stem cell population should be isolated alone. Studies need to be performed with both the stem cell populations and total populations of cells.

1.5.1 Bone Marrow Stromal Cells

Bone marrow stromal cells (BMSC) are the adherent cells from bone marrow and contain a population of stem cells with the ability to differentiate into bone, cartilage, tendon, ligament, adipose, and muscle(Pittenger et al., 1999). At this time, this population of stem cells is the most widely studied since they are easily isolated from autologous sources and have a large potential for expansion. Currently the differentiation of BMSCs to into a specific cell type in vitro can be controlled by the different factors in the culture environment such as growth factors and mechanical stimulation. Studies where these cells have been subcutaneously implanted into

immunocompromised mice with a calcium phosphate carrier have shown that BMSC can form bone-like and bone marrow-like tissues indicating the capability of these cells to be used for bone regenerative therapies(Batouli et al., 2003).

1.5.2 Dental Pulp Stem Cells

A subset of cells from the dental pulp of adult and deciduous teeth have been characterized as stem cells due to their clonogenic nature and ability to differentiate into many cell types including odontoblast, fibroblast, adipocyte and neural-like cells (Gronthos et al., 2000; Miura et al., 2003). In vivo studies where the DPSC were subcutaneously implanted into immunocompromised mice with a calcium phosphate carrier revealed that these cells maintain the capacity to regenerate dentin-like and pulp-like tissues (Gronthos et al., 2000).

1.6 SCAFFOLDLESS TISSUE ENGINEERING

Tissue engineering is the combination of cells, growth factors, and a scaffold to recapitulate functional tissues. The scaffolding component serves many roles for tissue regeneration that include facilitating three-dimensional (3D) tissue formation, bearing the mechanical loads placed on the regenerated tissue, and ideally degrading at a similar rate as tissue deposition. The materials used in scaffold design and their degradation properties can have strong effects on cell behavior and tissue formation.

Naturally during tissue formation, cells produce their own 3D structure with their preferred microenvironment. The natural cell microenvironment is extremely complex thus only a fraction of information is known about its several multifaceted components. Scaffoldless 3D tissue engineering, where cells generate a 3D structure using their endogenous matrix as a scaffold would avoid the complexities of designing ideal exogenous materials for regenerative therapies. Furthermore, these constructs could also be used as model systems to study the natural cellular microenvironment.

There are several different types of 3D scaffoldless culture systems such as cell pellet systems, cell sheet cultures, and self assembled 3D cellular constructs (Bosnakovski et al., 2004; Calve et al., 2004; Dennis and Kosnik, 2000; Elloumi Hannachi et al., 2009; Muraglia et al., 2003; Syed-Picard et al., 2009; Yamato et al., 2002; Yu et al., 2006). Pellet cultures involve centrifuging cells in a tube to form a condensed cellular pellet. Although these systems are scaffoldless, the cells still endure external factors that can affect their behavior. In these systems, the cells are forced into a 3D system with a high cellular density prior to matrix deposition, and the increased cellular associations can affect cellular behavior. Cell sheet technology has been used for many applications such as myocardial tissue repair (Masuda et al., 2008) and cornea regeneration (Nishida, 2003). This technique involves culturing cells until hyperconfluence and inducing matrix production for the formation of a robust tissue sheet (See et al.). At this point tissue sheets can be either peeled from the dish with forceps or released from the dish if cultured on a thermo-responsive polymer such as poly(N-isopropylacrylamide) (Akiyama et al., 2004). These cells sheets are a useful method for cell delivery for regenerative therapies.

The self-assembled 3D cellular constructs offer many advantages as a regenerative device and as a model system to study stem cell differentiation and tissue organization. These constructs are formed by plating cells onto a two-dimensional substrate and culturing them to confluence. Once a monolayer is formed, the cell sheet lifts from the substrate and contracts towards two pins placed in the dish to self assemble into a solid cylindrical tissue anchored to the plate by the pins (Dennis et al., 2001; Hairfield-Stein et al., 2007; Kosnik et al., 2001). Unlike pellet systems where the cells are forced into a 3D structure prior to matrix production, in the scaffoldless self-assembled constructs, the cells are able to secrete and organize their matrix into their preferred 3D structure. These engineered tissues are generated and organized entirely by the cells themselves. In addition, these constructs can be used to assess potential scaffold material since material particles can be incorporated into the final engineered tissue by being placed on the cell sheet prior to 3D construct formation. This model provides a means to directly study 3D tissue organization with and without scaffold material. Currently this method is mainly researched as a potential device for musculoskeletal and neural regeneration (Adams et al.; Calve et al., 2004; Dennis et al., 2001; Hairfield-Stein et al., 2007; Syed-Picard et al., 2009). However, it has great potential for dental and bone repair and also as a model system to study 3D cell differentiation and tissue formation.

1.7 HYPOTHESES AND SPECIFIC AIMS OF CURRENT STUDY

The goals of this thesis are to use scaffoldless tissue engineered constructs as a model to study cellular behavior and as a device for regenerative dental and bone therapies. In the first portion (Chapters 2 and 3) of the dissertation, the following hypotheses are tested with the subsequent specific aims using scaffoldless 3D self-assembled constructs as a model.

1.7.1 Hypothesis 1: Calcium phosphates are osteoinductive and alter cell differentiation patterns and tissue organization in 3D engineered tissues

1.7.1.1 Specific Aim 1: Compare cell differentiation patterns and tissue formation of scaffoldless 3D self-assembled constructs formed from dental pulp cells with and without the incorporation of amorphous calcium phosphate.

The results from the first aim are reported in Chapter 2. Scaffoldless self-assembled constructs are formed from the total population of cells with and without the incorporation of amorphous calcium phosphate particles (ACP). The ACP particles induce cellular differentiation towards an osteogenic lineage. In this study, the effects of ACP on cellular behavior and tissue formation are also mechanistically assessed at a molecular level.

1.7.2 Hypothesis 2: An isolated population of dental pulp stem cells will regenerate molecularly and structurally different tissues than those generated from the total population of dental pulp cells

1.7.2.1 Specific Aim 2: Structurally and molecularly compare scaffoldless 3D self-assembled constructs formed from a population of dental pulp stem cells versus the total population of dental pulp cells

The results from the second aim are described in Chapters 2 and 3. In Chapter 2 the total population of DPC is used to engineer 3D self-assembled scaffoldless constructs and these constructs are assessed after both in vitro culture and in vivo implantations. In Chapter 3, a population of pericytes is isolated from the dental pulp based on cell surface protein expression and characterized as stem cells. These stem cells are used to form scaffoldless 3D self-assembled constructs. The constructs formed from the total population of dental pup cells in Chapter 2 are structurally and molecularly compared to constructs formed from the purified population of dental pulp pericytes in Chapter 3.

The latter portion of the dissertation (Chapters 4-6) explores the use scaffoldless tissue engineered constructs as a device for regenerative therapies and the following hypothesis is tested.

1.7.3 Hypothesis 3: Scaffoldless tissue engineered constructs can be used as devices for dental and bone regenerative therapies

1.7.3.1 Specific Aim 3: Use of 3D scaffoldless tissue constructs as a device to deliver DPC into tooth root canal space for pulp regenerative therapy and assess differences when DPC are delivered with calcium phosphate cement carrier

This aim is investigated in Chapters 4 and 5. In these studies a tooth root model is created from human tooth root segments. DPC are delivered into the root canal space via either scaffoldless 3D tissue engineered constructs (Chapter 4) or with a calcium phosphate carrier (Chapter 5) and the tooth root system is implanted subcutaneously in mice. The types of tissues formed using the two different delivery systems are compared.

1.7.3.2 Specific Aim 4: Use of engineered scaffoldless tissues as a device to engineer a functional periosteum tissue for bone regeneration.

This last aim is tested in Chapter 6. Calcium phosphate disks are wrapped with cell sheets formed from bone marrow stromal cells and implanted subcutaneously in mice. The formation of a bone-like tissue and functional periosteum-like structure are morphologically and molecularly analyzed.

2.0 CHAPTER 2: THE OSTEOINDUCTIVE PROPERTY OF CALCIUM PHOSPHATES ARE MODULATED BY CONNEXIN 43

2.1 ABSTRACT

Recently few reports alluded to the osteoinductive properties of calcium phosphate, yet the cellular processes behind this are not well understood. To gain insight into the molecular mechanisms of this phenomenon, we have conducted a series of *in vitro* and *in vivo* experiments using a scaffoldless three dimensional (3D) dental pulp cell (DPC) construct as a physiologically relevant model. We demonstrate that amorphous calcium phosphate (ACP) alters cellular functions and 3D spatial tissue differentiation patterns by increasing local calcium concentration, which modulates connexin 43 (Cx43)-mediated gap junctions. To the best of our knowledge this is the first report proposing a chemical mechanism of osteoinductivity of calcium phosphates. These results provide new insights for possible roles of mineral phases in bone formation and remodeling and are expected to aid in development of novel tissue engineered materials. These data also emphasize the strong effect of scaffold materials on cellular functions.

2.2 INTRODUCTION

Calcium phosphates constitute the major mineral component of bones and teeth and are considered by many researchers as promising scaffold materials for hard tissue engineering (LeGeros, 2002; Rezwan et al., 2006). Until recently, calcium phosphates were considered to be osteoconductive but not osteoinductive (Damien and Parsons, 1991; LeGeros, 2002), meaning that these materials can act as substrates for bone deposition but can not alone induce osteogenic differentiation *in vitro* or in an ectopic site *in vivo* (LeGeros, 2008). In contrast, an osteoinductive scaffold material directs cell differentiation for tissue regeneration alone without the addition of an inductive growth factor. Studies now show that some calcium phosphates do exhibit osteoinductive properties, however the exact mechanisms of this are not yet understood (Muller et al., 2008; Yuan et al., 2000; Yuan et al., 2010). It has been postulated that this property is based on the topography and the interconnectivity of porosity of the material as these geometrical factors may aid in the ability of calcium phosphates to provide a substrate for the adsorption and entrapment of circulating osteogenic factors such as bone morphogenic proteins (BMP) (LeGeros, 2008; Li et al., 2011). However, in these cases the osteoinductivity is not intrinsic to the material itself, but is rather the result of the ability of material to adsorb biological factors. Additional studies though have shown that certain types of calcium phosphates can induce osteogenic differentiation irrespective of surface morphology and potentially due to the release of soluble ions. This suggests that calcium phosphates may direct differentiation at a more molecular level (Knabe et

al., 2004; Knabe et al., 2008; Sun et al., 2004). Amorphous calcium phosphate (ACP) is the mineral phase found at the sites of initial mineral deposition in bones and teeth (Beniash et al., 2009; Crane et al., 2006; Mahamid et al., 2008) and it is believed to be a precursor to more stable carbonated hydroxyapatite which is the major mineral phase in mature mineralized tissues of vertebrates. ACP is widely used in grafting and remineralization applications (Knaack et al., 1998; Reynolds, 1997). Recently it has been viewed as a potential scaffold material due to its unique mechanical properties(Saber-Samandari and Gross) and has been shown to exhibit some osteogenic potential(Chatterjee et al.).

A number of studies have shown that cells behave differently when cultured in two dimensions (2D) versus three dimensions(3D) (Cukierman et al., 2001; Cukierman et al., 2002). Since generally an exogenous scaffold facilitates the formation of a 3D structure, it is difficult to directly compare the 3D behavior of cells with and without material. Self-assembled 3D scaffoldless tissue engineered constructs allow cells to generate and remodel their own preferred microenvironment without the interference of an exogenous material. These constructs offer many advantages as a model system to study cell differentiation and tissue organization over other 3D scaffoldless systems. Self-assembled 3D scaffoldless constructs are formed by first culturing cells to confluence on a 2D substrate. Once a monolayer is formed, the cell sheet lifts from the substrate and contract towards two pins placed in the dish. The cell sheet subsequently self-assembles into a solid cylindrical tissue anchored to the plate by the pins (Dennis et al., 2001; Hairfield-Stein et al., 2007; Kosnik et al., 2001). These 3D tissues are generated and organized entirely by the cells themselves. In this study these

engineered tissues assess the potential effects of scaffold materials; material particles are placed on the cell sheet prior to 3D construct formation and thereby get incorporated into the final construct itself. This model provides a means to directly study 3D tissue organization with and without scaffold material.

The tooth is an organ system comprising several distinct tissue types that function together mainly for mastication. Dental pulp is the inner most, and most vital tissue of the tooth, composed of a vascular connective tissue with fibroblastic cells, neural fibers, lymphatics, and a population of stem cells that aid in repairing defects in the surrounding dentin, one of the hard tissues of the tooth (Nanci, 2003). Both the dentin and pulp originate from neuromesenchymal cells of dental papilla, therefore it is expected that an engineered dentin-pulp complex could be formed from a single cell source. The generation of an engineered dentin-pulp complex would provide a therapeutic product for endodontic treatments where currently infected pulp tissue is replaced with an inert polymeric filler material (Zadik et al., 2008). In this study, we show that scaffoldless 3D self-assembled constructs engineered from human dental pulp cells (DPC) form a spatially organized dentin-pulp complex-like structure, and this organization is disrupted by the addition of calcium phosphate.

Proper spatial organization during tissue development requires cascades of spatial and temporal cues orchestrated in part by proper cell-cell interactions. Gap junctions are channels that form between neighboring cells allowing the passage of ions and small molecules. During development, these channels provide a conduit for molecules to form expression gradients in a community of cells thereby aiding in appropriate tissue patterning and morphogenesis (Lo, 1996; Lo et al., 1997). Connexins

are transmembrane proteins that organize into channels called connexons in the plasma membrane. When two connexons from neighboring cells align, gap junctions are formed. Connexin 43 (Cx43) mediated gap junctions are known to play an important role in hard tissue formation. These gap junctions allow the transfer of molecules up to 1.2 kDa in size including intracellular calcium (About et al., 2002; Minkoff et al., 1994). During development, Cx43 is upregulated prior to dentin and bone formation, and expressed in regions of limb development involved in patterning (Kamijo et al., 2006; Lecanda et al., 1998; Solan and Lampe, 2009). Cx43 null mouse embryos exhibit severe defects in mineralization in all bone types and have delayed tooth development and eruption (Lecanda et al., 2000; Stains and Civitelli, 2005). Currently, insufficient literature exists on the effects of different scaffold materials on connexin expression and gap junctional intercellular communication.

In this study, self-assembled scaffoldless 3D constructs were engineered from dental pulp cells that resulted in the formation of spatially organized dentin-pulp complex-like tissues after *in vitro* culture and *in vivo* implantation. The incorporation of ACP into the 3D constructs disrupted the formation of an organized dentin-pulp complex-like structure by inducing dentin-like tissue formation throughout the construct. We investigated the mechanistic phenomenon behind the osteoinductive behavior of ACP in this 3D model by examining the effects of ACP on cell-cell communication.

2.3 MATERIALS AND METHODS

2.3.1 Dental pulp cell isolation

Dental pulp cells (DPC) were isolated as previously described (Liu et al., 2006). Briefly, human adult third molars were obtained from the University of Pittsburgh, School of Dental Medicine. The molars were cracked open and the pulp was removed and minced. The pulp was digested in a collagenase-dispase enzyme solution and the cells were plated in Dulbecco's Modified Eagle Medium (DMEM; Gibco) containing 20% fetal bovine serum (FBS, Atlanta Biologics) and 1% penicillin/streptomycin (P/S; Gibco). Once approximately 80% confluence was met, the cells were enzymatically removed from the plate and either passaged or frozen for future studies. Cells were used in experiments between passages 2 and 6.

2.3.2 Formation of scaffoldless 3D engineered tissues

Scaffoldless 3D constructs were cultured as previously described (Syed-Picard et al., 2009). Briefly, tissue culture plastic dishes, 35 mm in diameter, were coated with SYLGARD (type 184 silicone elastomer; Dow). The SYLGARD was coated with 3µg/cm^2 natural mouse laminin (Invitrogen) for cell adhesion. DPSC were plated onto the construct dish at a density of 200,000 cells/dish in a media containing DMEM, 20%

FBS, 1% P/S, 50 µg/ml ascorbic acid (Fisher),10^{-8} M dexamethasone (dex; Sigma), 2 ng/ml basic fibroblast growth factor (bFGF; Peprotech), with or without 5 mM β-glycerophospate (βGP; MP Biomedicals). Once the cells reached confluence, two minutien pins, 0.2 mm diameter and 1 cm long, were pinned onto the cell monolayer, 7 mm apart, and 2 ng/ml transforming growth factor- β1 (TGFβ1; Peprotech) was added to the culture media. Constructs were either characterized or used for animal studies seven days after construct formation.

2.3.3 Incorporation of amorphous clcium phosphate particles into 3D scaffoldless tissues

Stock solutions of 20 mM calcium chloride dihydrate and 12 mM di-sodium hydrogen phosphate dehydrate with 0.8 mM pyrophosphate decahydrate were prepared. Amorphous calcium phosphate (ACP) nanoparticles were synthesized by adding the calcium chloride solution to the phosphate solution with vigorous stirring. The precipitate was isolated via centrifugation for 8 minutes. Once isolated, the particles were dipped into liquid nitrogen and lyophilized. Lyophilized powders were analyzed by FTIR in transmission mode using Bruker Vertex 70 spectrometer (Billerica, MA). ACP particles were added on top of the monolayer once cells were confluent in the amount of 0.6 mg/construct.

2.3.4 Animal studies

All animal studies were approved by the University of Pittsburgh Institutional Animal Care and Use Committee. Seven days following construct formation, samples were subcutaneously implanted into the backs of Balb/C nude mice. An incision of approximately 1cm in length was made through the skin on the dorsal surfaces of the animals. Subcutaneous pockets were made using blunt dissection. One construct was placed into each pocket, and four pockets were placed into each animal. The constructs were removed from the animals after four weeks.

2.3.5 Histology

Samples were fixed in a 4% paraformaldehyde solution for 4 hours, and then processed and embedded in paraffin. The constructs were sliced longitudinally at a thickness of approximately 5μm, and used for hematoxylin and eosin (H and E) staining or immunofluorescent staining for DMP-1 (LF148; provided by Dr. Larry Fisher, NIH), DSP (LF151, provided by Dr. Larry Fisher, NIH), or Cx43 (Abcam). Fluorescent intensity was quantified using Image J software (National Institutes of Health).

2.3.6 Scanning electron microscope

Samples were fixed 7 days after formation in 2.5% gluteraldehyde and also post fixed with 1% osmium tetroxide. Samples were than dehydrated in a graded series of alcohol

washes and finally using a critical point drier. Samples were sputter coated with gold and visualized using a JEOL 6335F Field Emission Scanning Electron Microscope.

2.3.7 Fourier transform infrared (FTIR) spectroscopy on constructs

Seven days after construct formation, samples were flash frozen in liquid nitrogen and lyophilized. Lyophilized powders were analyzed by FTIR by collecting 32 scans at a resolution of 4 cm^{-1} in transmission mode using Bruker Vertex 70 spectrometer (Billerica, MA). Plots were analyzed with Spectrum software (Perkin Elmer), and the absorbance was normalized to the amide I peak.

2.3.8 Western blot

Total protein was collected using M-PER mammalian protein extraction reagent (Thermo Scientific) containing Complete Protease Inhibitor (Roche). The proteins were separated using 8% SDS-polyacrylamide gel electrophoresis and transferred to polyvinylidene difluoride membrane (BioRad, Melvilla, N.Y.) using a Bio-Rad PowerPac HV. The membranes were blocked with 5% non-fat dried milk in TBST buffer with 0.5% Tween 20 and incubated for 2h in primary antibody. The antibodies used were rabbit polyclonal to Cx43 (Abcam; 1:20,000) and mouse monoclonal to β-actin (Santa Cruz; 1:1000). The blots were then incubated for 1h in donkey anti-rabbit IgG (Millipore) or goat anti-mouse IgG (Thermo Scientific) peroxidase conjugated secondary antibody. The blot was then treated with Western blotting detection reagent Western Lightning Plus-ECL (Perkin Elmer), and the blots were detected on Kodak scientific imaging film.

2.3.9 Quantitative real-time polymerase chain reaction

RNA was collected using an RNeasy Mini Kit (Qiagen) from monolayer cultures of human pulp cells treated with and without calcium chloride for 24h. Real-time RT-PCR was performed using TaqMan One-Step RT-PCR Master Mix Reagents (Applied Biosystems) and the primers and probes for GJA1, the gene for Cx43 (Applied Biosystems; Hs00748445_s1). The TaqMan Ribosomal RNA Control Reagents designed to detect the 18S ribosomal RNA gene(Applied Biosystems) was used as the endogenous control. Using a 7900 HT Fast Real-Time PCR System (Applied Biosystems) the RNA underwent reverse transcription for 30 minutes at 48°C, then polymerase activation for 10 minutes at 95°C, and finally PCR for 40 cycles with an initial denaturation for 15 seconds at 95°C then annealing/extending for 1 minute at 60°C. Results are presented as relative gene expression +/- standard deviation.

2.3.10 Inductively coupled plasma spectroscopy

The concentration of calcium in media used to culture 3D scaffold-less constructs with and without ACP was measured using inductively coupled plasma spectroscopy (ICP). Culture medium was collected from constructs three days after cell confluence and the addition of ACP. The culture medium was diluted (1:15) in 8% nitric acid. The calcium concentration was measured using an iCAP 6500 ICP Spectrometer (Thermo Scientific).

2.3.11 Dye transfer for GJIC

Fluorescent dye transfer was used to determine gap junction functionality. For staining, donor dental pulp cells were suspended in PBS containing 0.3M glucose with 1μM DiI (Sigma), a membrane tracker, and 5μM calcein-AM (Sigma), a gap junction-permeable dye, and incubated for 30 minutes at 37°C. Twenty thousand donor cells were added to each well of a 6-well plate already containing confluent dental pulp recipient cells. These recipient cells were cultured in DMEM with 20% FBS and 1% P/S and treated for 2 days with or without ACP and 1uM ethylene glycol tetraacetic acid (EGTA; Sigma). The co-culture was incubated for 3h, and then the cells were then collected and analyzed with an Accuri C6 Flow Cytometer. The transfer fraction was determined as the number of recipient cells (calcein+ and DiI-) per donor cell (DiI+). As a negative control, 18α-glycyrrhetinic acid (AGA; Sigma), a chemical gap junction uncoupler, was added at a concentration of 100μM.

2.3.12 Statistical analysis

Data was represented as the average +/- standard error. Statistical comparisons were performed using SPSS software. Independent samples t-tests and one-way independent ANOVA with Tukey's post hoc test were used to compare means. Significance was considered at $p < .05$.

2.4 RESULTS

Three-dimensional scaffoldless constructs were engineered from human dental pulp cells (DPC). Three different groups of constructs were formed, as described in **Table 2.1**. Group 1 (βGP-) was cultured in an osteogenic medium lacking beta glycerophosphate (βGP); without βGP the source of phosphate is omitted, impairing mineral deposition in the extracellular matrix (ECM) compartment. Group 2 (βGP - ACP+) is exactly the same as Group 1, but exogenous ACP particles were added on top of the monolayer prior to its rolling up and were incorporated into the final constructs.

Table 2.1 Culture conditions and expected outcomes of groups of constructs engineered in this study

Group	βGP -	βGP +	βGP - ACP+
Culture Condition	Osteogenic medium without beta glycerophosphate	Osteogenic medium with beta glycerophosphate	Osteogenic medium without beta glycerophosphate and with ACP particles
Outcome	No Mineral	Mineral organized by cells	Only exogenous mineral in samples

Group 3 (βGP+) was cultured in the full osteogenic medium including βGP, providing all the necessary physiological elements for mineral deposition in the ECM. The DPC formed a monolayer approximately 3-4 days after being plated onto the construct dishes, and started delaminating from the substrate at 5-6 days. The final 3D structures formed around 6-8 days after cells were plated. The resulting engineered tissues were 7mm in length**. Figure 2.1(a –c)** shows photographs of the monolayers during rolling without ACP particles, and of the final construct. **Figure 2.1(d-f)** shows images of a

construct formed in the presence of ACP; the ACP particles can be seen on top of the monolayer and can been seen incorporating into the construct as it rolls.

FTIR was used to assess the presence and character of mineral in 3D scaffoldless constructs. Constructs cultured without β glycerophosphate (βGP-) lacked mineral based on the absence of ν_4 PO_4 absorbance band in 500-600 cm^{-1} region and very weak absorbance in 1000-1200 cm-1 region corresponding to ν_3 PO_4 band. The weak ν_3 PO_4 is likely due to the absorbance of organic components of the construct or phosphates present in the culture medium **(Figure 2.2a)**. Samples in the βGP+ and the βGP-ACP+ groups show strong ν_3 PO_4 and ν_4 PO_4 peaks indicative of calcium phosphate mineral phases **(Figure 2.2b and c)** (Pleshko et al., 1991). The influence of organic components contributed peaks that overlap with the ν_3 PO_4 peaks making the PO_4 peak was used to characterize the crystallinity of the mineral as described by Termine and Posner (Termine and Posner, 1966). In the βGP-ACP+ samples, a single broad ν_4 PO_4 peak with maximum at 560 cm^{-1} is present indicating that the mineral phase in this sample is predominantly ACP. Whereas ν_4 PO_4 band in βGP- samples spit into two peaks with maxima at 560 and 601 cm^{-1} which is characteristic of low crystallinity hydroxyapatite (Termine and Posner, 1966).

Constructs were prepared for histological characterization seven days after formation. Hematoxylin and eosin (H and E) staining showed that constructs were composed of a highly cellular solid tissue **(Figure 2.3a-c)**. Scanning electron microscopy of cross sections of samples showed that samples not containing ACP have a smoother core and formed a separate peripheral structure. However, the samples

containing ACP had a more uniformly rough morphology and lacked any separate peripheral structure as seen in **Figure 2.3(d-i)**.

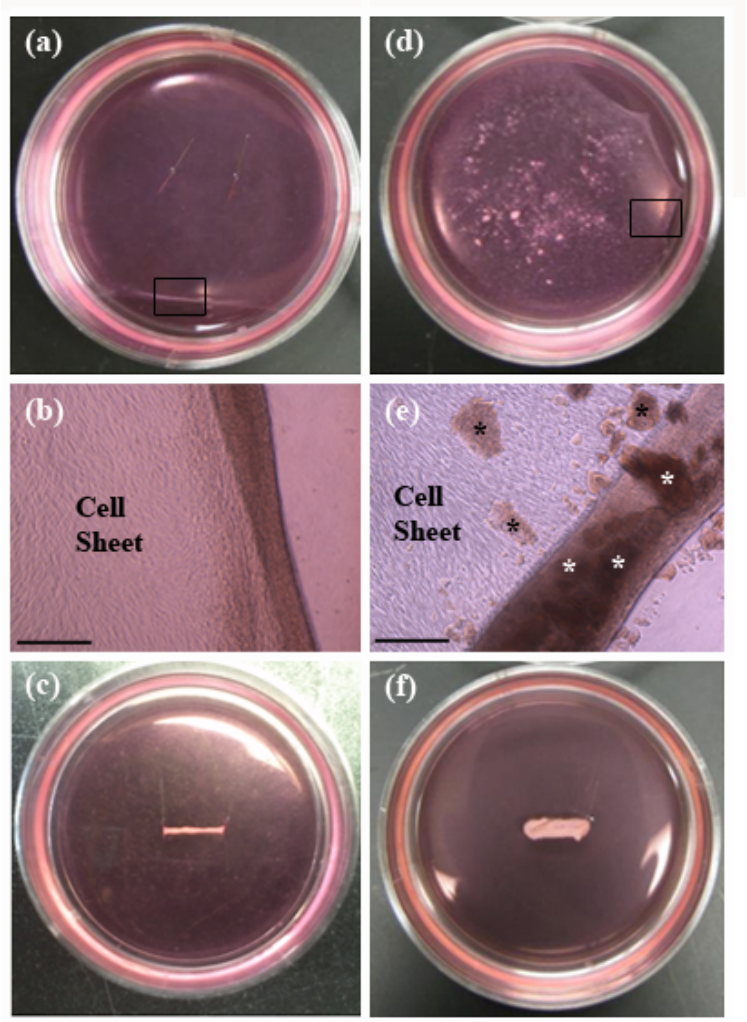

Figure 2.1: Images of scaffoldless 3D constructs as they roll up without ACP. Photograph of monolayer starting to roll up without ACP (A), outlined region in (A) is seen magnified in (B) where cell sheet can be seen with edge rolling up and the final formed construct without ACP is shown in (C). Photograph of monolayer starting to roll up in constructs with ACP, white ACP particles can be seen on monolayer (D), outline region in (D) is seen magnified in (E), ACP particles on top of monolayer can been seen (black stars), and ACP particles can be seen incorporated in the rolled up region (white stars), the final rolled up construct with ACP shown in (F). (B) and (E) scalebars = 225µm.

Confocal images of immunohistochemistry on longitudinal sections of the scaffoldless constructs showed that all three construct types expressed the dentin

proteins dentin sialoprotein (DSP) and dentin matrix protein 1 (DMP1) after *in vitro* culture. Immunofluorescence of DSP and DMP1 in the βGP- and βGP+ groups (the groups that did not contain ACP particles) was stronger on the periphery of the construct than in the center **(Figure 2.4)**. This data demonstrate that scaffoldless engineered DPC constructs develop specific patterns of dental proteins expression resembling their distribution in native dental pulp tissue where ododntoblast cells expressing dentin matrix proteins are localized at the periphery of the dentin-pulp complex. In contrast homogeneous immunofluorescencee of these proteins was observed throughout the constructs containing ACP (βGP- ACP+) **(Figure 2.4)**. This suggests that dentin-pulp complex tissue differentiation can be disrupted by the addition of exogenous ACP.

After 4 week subcutaneous implantation in mice, the βGP- and βGP+ samples that lack ACP formed a dense tissue on the periphery and a fibrous tissue in the center. These constructs also resembled the dentin-pulp complex where the cells on the dense peripheral structure expressed higher amounts of DSP and DMP1 than did the center fibrous tissues. In contrast, the βGP-ACP+ constructs formed a dense tissue that expressed of DMP1 and DSP throughout **(Figure 2.5)**. The structural development of the samples implanted into animals follows the organizational patterns seen after *in vitro* culture. These data indicate that ACP is an osteoinductive material that is disrupting the spatial tissue organization seen in scaffoldless constructs and causing the formation of constructs that express dentin specific proteins throughout.

During natural organ development cell-cell communication is a necessary component of proper tissue organization. Since the constructs lacking ACP formed

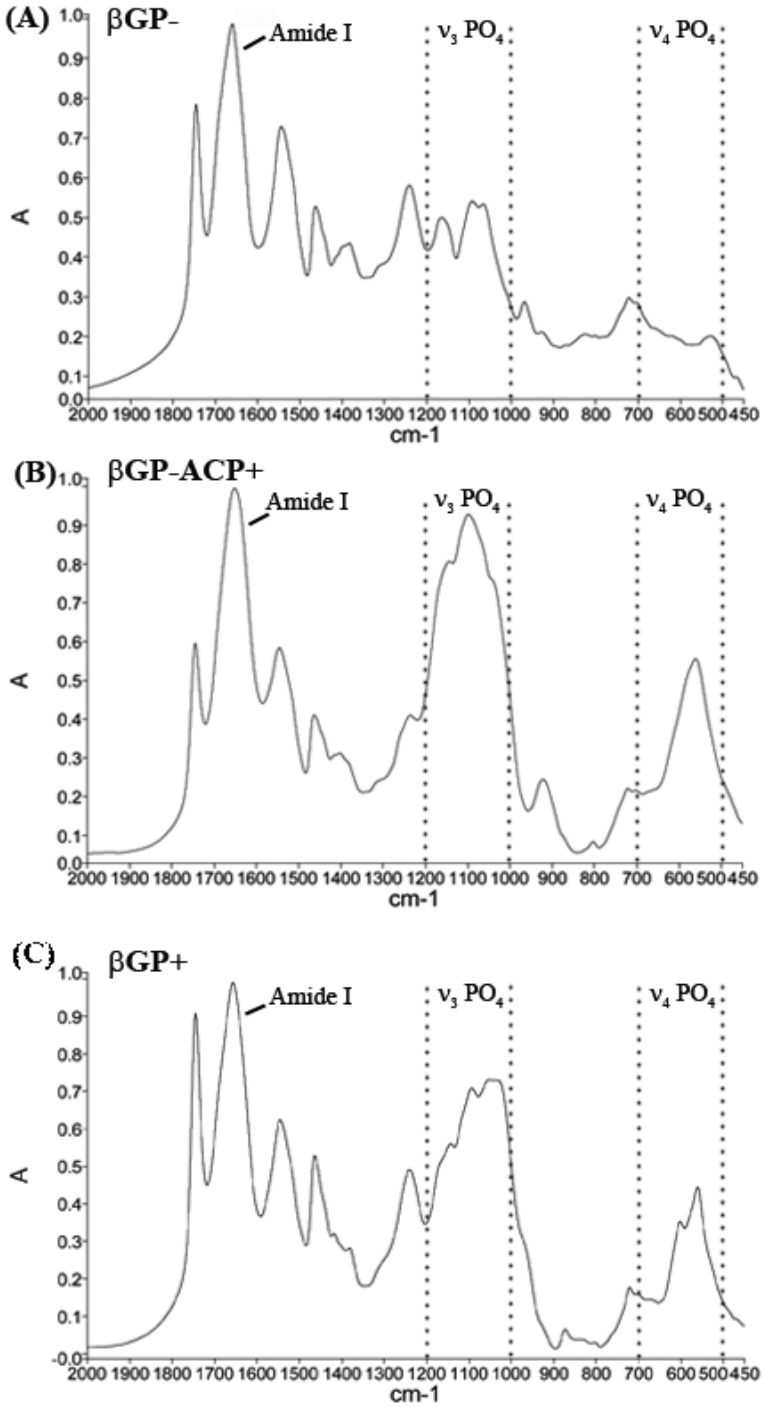

Figure 2.2: Fourier transform infrared spectroscopy confirms that βGP- constructs lack a mineral phase (A) as seen by minimal ν_4 PO_3 peak (1000-1200 cm^{-1}) and the lack of ν_4 PO_4 peak (500-700 cm^{-1}), where βGP-ACP+ (B) and βGP+ (C) samples contain a mineral phase as indicated by strong ν_3 PO_4 (1000-1200 cm^{-1}) and ν_4 PO_4 (500-700 cm^{-1}) peaks. The singular broad ν_4 PO_4 peak in βGP-ACP+ is indicative of amorphous mineral where as the splitting of ν_4 PO_4 into two peaks in βGP+ is signifies the presence of a more crystalline phase. Dotted lines enclose the regions corresponding with ν_3 PO_4 and ν_4 PO_4 peak ranges.

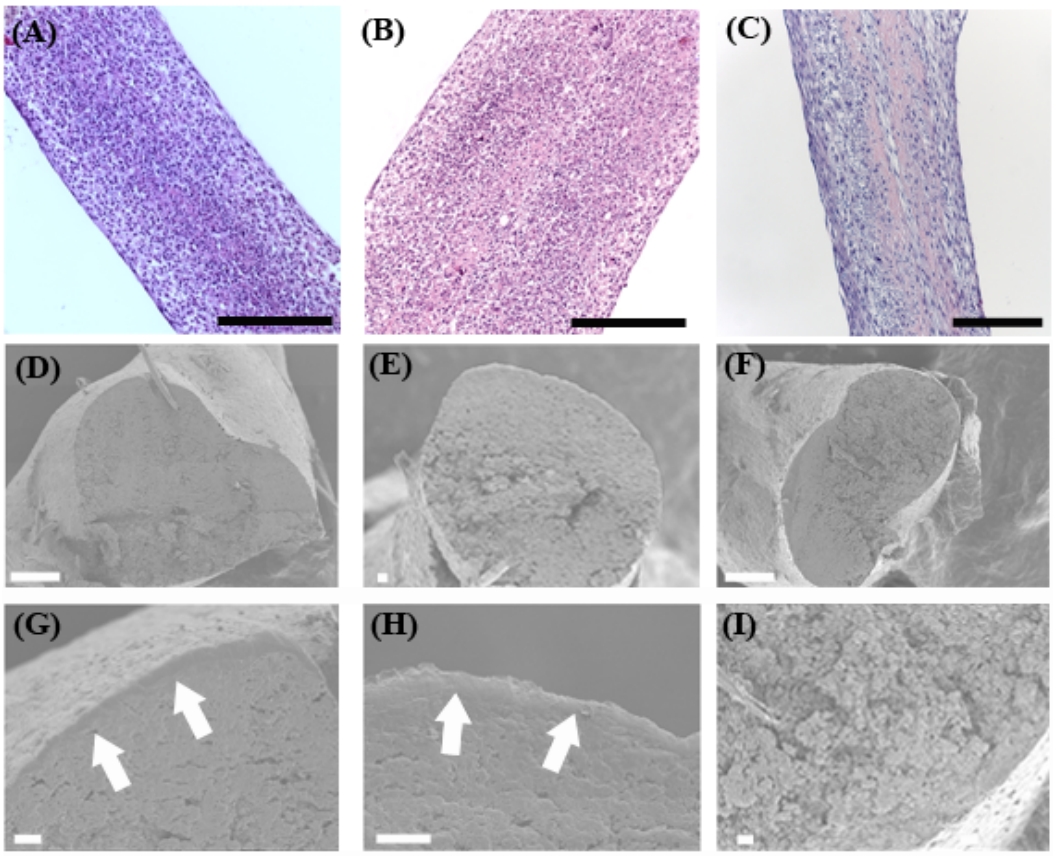

Figure 2.3: Structure of scaffoldless constructs. H and E staining shows that all constructs types are highly cellular as seen for βGP- (A), βGP+(B), and βGP-ACP+ (C). Scanning electron microscopy of the cross section of the of samples shows that constructs lacking ACP have a smooth dense center with a separate structure formed on the periphery as seen for βGP- at lower (D) and higher (G) magnifications and βGP+ at lower (E) and higher (H) magnifications, the arrows in (G) and (H) point to the peripheral structure. Whereas samples with ACP form a rough structure throughout and are lacking the separate peripherial structure as seen for βGP-ACP+ at lower (F) and higher (I) magnifications. Scalebars: A-C = 250 μm, D = 100 μm, E-I = 10 μm.

spatially organized structures whereas the βGP-ACP+ samples did not, it was hypothesized that ACP may be modulating the expression of connexin 43 (Cx43) mediated gap junctions. Immunofluorescent staining on sections of scaffoldless constructs with and without ACP particles showed that cell controlled groups (βGP- and βGP+) had increased Cx43 expression on the periphery, in contrast to constructs

containing ACP particles (βGP-ACP+) that exhibited the Cx43 throughout **(Figure 2.6a-g)**. The localization patterns of Cx43 follows that of the dentin proteins (DSP and DMP1) seen in **Figure 2.4**.

Cx43 has 3 different isoforms depending on the degree of phosphorylation. The largest P2 isoform of Cx43 is the functional form found in gap junctions and therefore the structure of interest. The P0 and P1 are transient isoforms seen during synthesis (Chung et al., 2007; Stains and Civitelli, 2005). Western blot analysis shows that cultures of DPCs with ACP have increased P2 isoform Cx43 expression compared to the DPCs cultured without ACP **(Figure 2.6h-i)**. These results indicate that ACP does affect gap junctional communication in DPC.

We hypothesized that an increase in localized extracellular calcium (Ca^{2+}) concentration around dissolving ACP particles may induce Cx43 expression. The Ca^{2+} concentration in the media collected from βGP-ACP+ samples was significantly increased as compared to samples lacking ACP **(Figure 2.7a)**. Western blot analysis showed increasing expression of Cx43 in DPC cultures with higher concentrations of Ca^{2+} **(Figure 2.7b and 2.7c)**. Quantitative real-time PCR results also showed that Cx43 gene expression was increased in DPC cultured with higher concentrations of Ca^{2+} **(Figure 2.7d)**. These results clearly demonstrate that Ca^{2+} regulates Cx43 expression.

To further investigate the affects of ACP and free Ca^{2+} on Cx43-mediated gap junction functionality, dye transfer assays were performed as a direct measure of gap junctional intracellular communication (GJIC) **(Figure 2.8)**. Indeed, DPCs show an increased transfer fraction when cultured with ACP illustrating an increase in the expression of functional gap junctions. This effect, however, was abolished with the

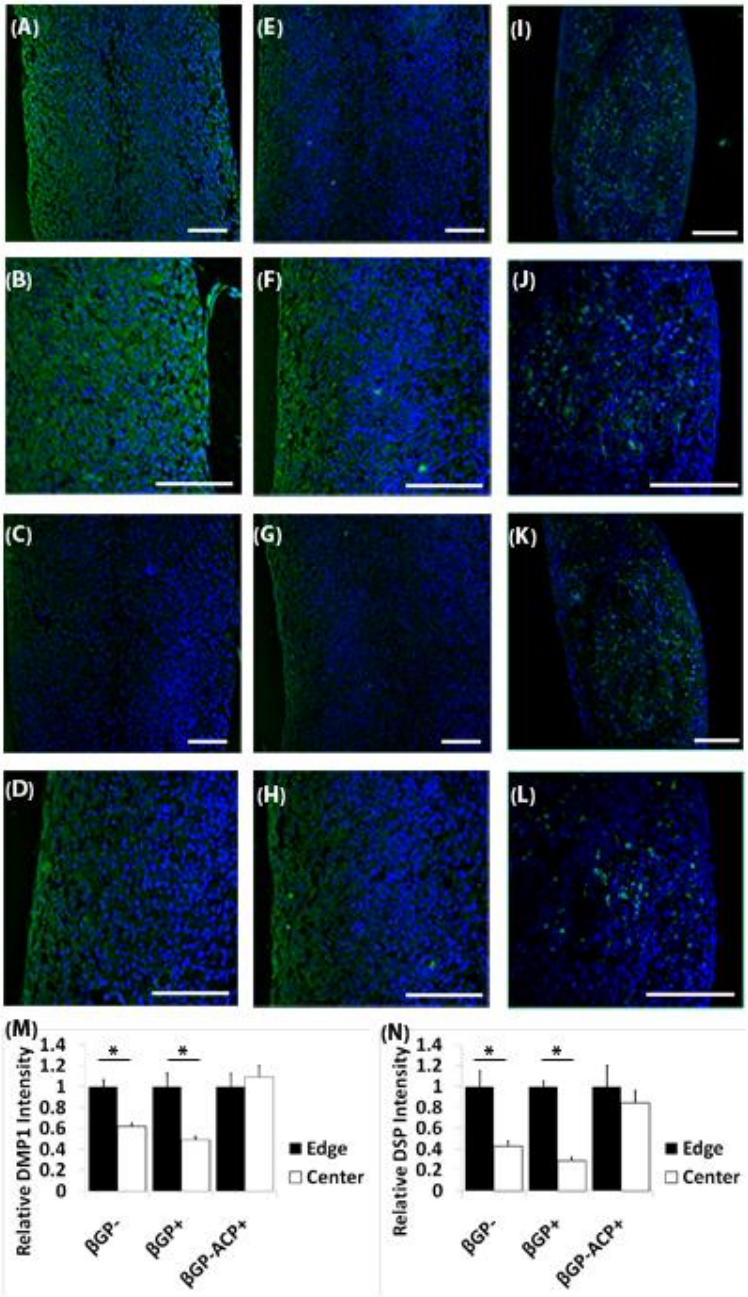

Figure 2.4: Confocal images of immunofluorescent staining of 3D scaffoldless constructs after in vitro culture. βGP- samples have higher expression of DMP1 expression (green) on the periphery than in the center as seen at lower (A) and higher magnifications (B), similar expression profile was seen with DSP (green) at lower (C) and higher magnification (D). βGP+ samples also had higher dentin protein expression on the periphery than in the center as seen with lower (E) and higher (F) magnfications of DMP1(green) and lower (G) and higher (H) magnifications of DSP(green). βGP-ACP+ samples expressed dentin proteins throughout the constructs as seen with DMP1(green) at lower (I) and higher (J) magnifications and DSP(green) at lower (K) and higher (L) magnifications. Fluorescent intensity was quantified at the edge and center of all construct types and differences were seen in βGP- and βGP+ samples but not βGP-ACP+ for DMP1 (M) and DSP (N). (A)-(L) Nuclei stained with DAPI (blue). Scale bars = 100 μm.

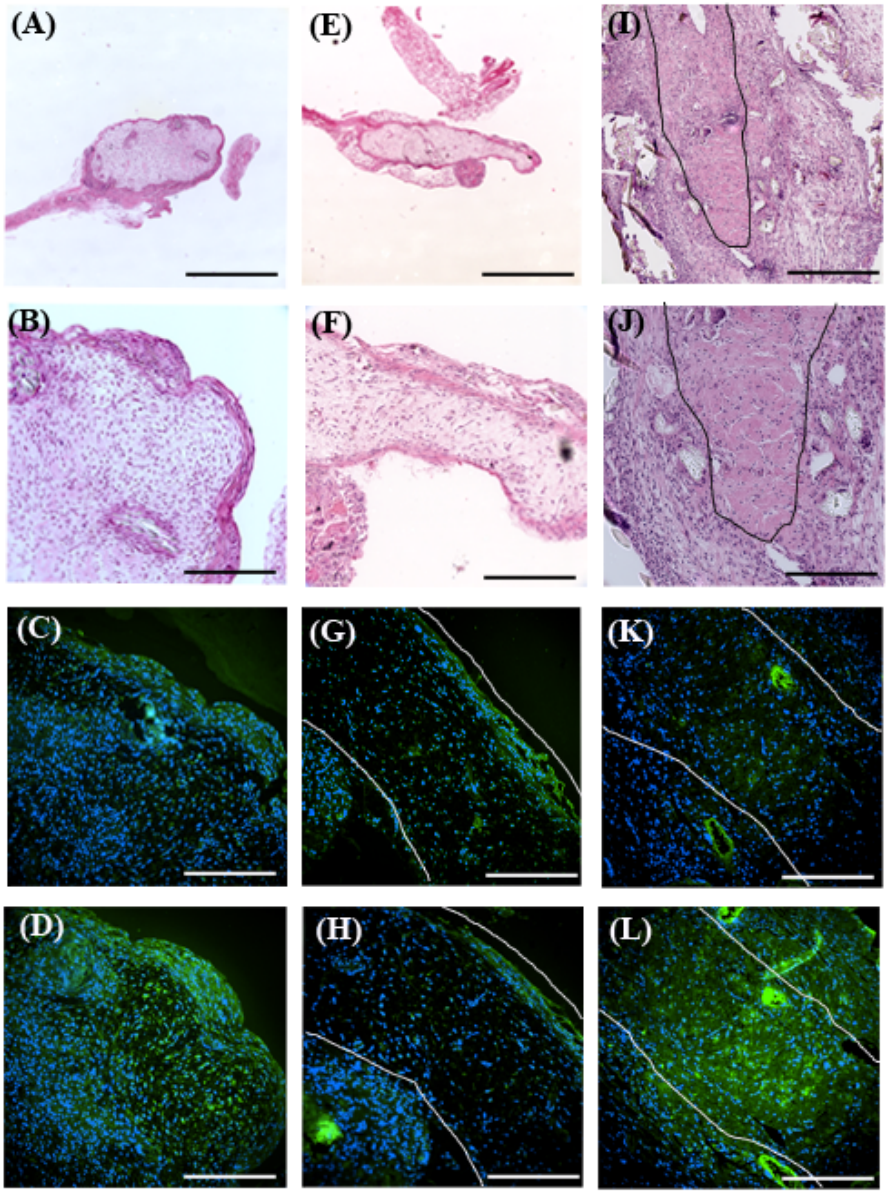

Figure 2.5: Histological analysis of 3D scaffoldless constructs after 4 week implantation. βGP- samples formed a dense structure on the periphery and a fibrous structure in the center as seen by H and E staining at lower (A) and higher (B) magnification. The dense peripherial structure expressed higher levels than the center of DMP1 (green) (C) and DSP (green) (D) in βGP- samples. Similar results were seen in βGP+ samples , H and E showed a dense structure on the periphery with a fibrous structure in the structure seen at lower (E) and higher (F) magnifications and the dense peripherial structure expressed higher levels of DMP1 (green) (G) and DSP (green) (H) that the fibrous center. βGP-ACP+ samples formed a uniform dense structure as seen by H and E images at lower (I) and higher (J) magnifications and expressed dentin proteins throughout as seen by DMP1 (green) (K) and DSP (green) (L). Black lines in (I) and (J) and white lines in (G), (H), (K), and (L) outline explants. (C), (D), (G), (H), (K), and (L) nuclei stained with DAPI (blue). Scalebars: (A), (E) = 1.25 mm, (I) = 500 μm, (B)-(D), (F)-(H), (J)-(L) = 250 μm.

addition of EGTA, a Ca^{2+} chelator. These data further support that ACP affects GJIC via increase in local Ca^{2+} concentration.

2.5 DISCUSSION

Calcium phosphates are a powerful material for hard tissue regeneration due to their osteoinductive properties. Understanding the underlying mechanism behind the osteoinductivity of these materials would greatly advance future biomaterial design. In this study, scaffoldless three-dimensional self-assembled constructs engineered from human DPC differentiated into spatially organized dentin-pulp complex-like tissues where dentin specific proteins are expressed on the periphery of the construct thereby exhibiting an odontoblastic cell phenotype. However, the addition of exogenous ACP particles altered the tissue differentiation patterns and disrupted this organization by altering the natural cell-cell communications within the community of cells.

Several studies have shown the formation of spatially organized multi-tissue constructs from single populations of cells using scaffoldless 3D culture models. Pellet culture systems have resulted in several types of multi-tissue structures. The formation of a spatially organized dentin-pulp complex-like structure was seen in a study where DPCs were cultured in pellet form in tooth germ conditioned media (Yu et al., 2006). In a study by Muraglia et al., pellets of human bone marrow stromal cells were coaxed to form a chondro-osseous organoid structure with a bone-like periphery and a cartilage core (Muraglia et al., 2003). In a separate study, pellets created from bovine bone

marrow stromal cells formed a periphery with stronger type I collagen expression and increased type II collagen expression in the core similar to a cartilage core with a perichondrium periphery. Another study showed that self-assembled 3D constructs, similar to the constructs formed in the present study, engineered from rat bone marrow stromal cells resulted in the formation of a bone core with a periosteum-like periphery (Syed-Picard et al., 2009). Potentially, the formation of spatially organized structures in scaffoldless models is a result of increased cellular control on the microenvironment without the interference of an exogenous material. We suggest that the addition of a scaffold alters natural nutrient gradients, change cell-cell or cell-matrix interactions, and introduce cell-material interactions which may have a strong influence on cell differentiation.

The addition of exogenous ACP to self assembled scaffoldless 3D engineered constructs supports that calcium phosphates have an effect on cellular behavior and furthermore we show that this phenomenon occurs through the modulation of cell-cell communication. The effects of exogenous ACP were also compared to inducing mineral formation by culturing the constructs in a mineralizing media (βGP+), this was to assess if any effects seen with ACP were specific to exogenous material. Constructs formed in the presence of beta glycerophosphate formed a spatially organized dentin-pulp complex-like structure similar to constructs that lacked mineral (βGP-). This indicates that the effects seen by the addition of exogenous ACP are specific to the presence of an exogenous calcium phosphate. It is considered that during hard tissue formation, mineralization may be controlled by the cells via matrix organization and the production of specific proteins (Weiner and Addadi, 1997). Potentially, the factors in the βGP+ and

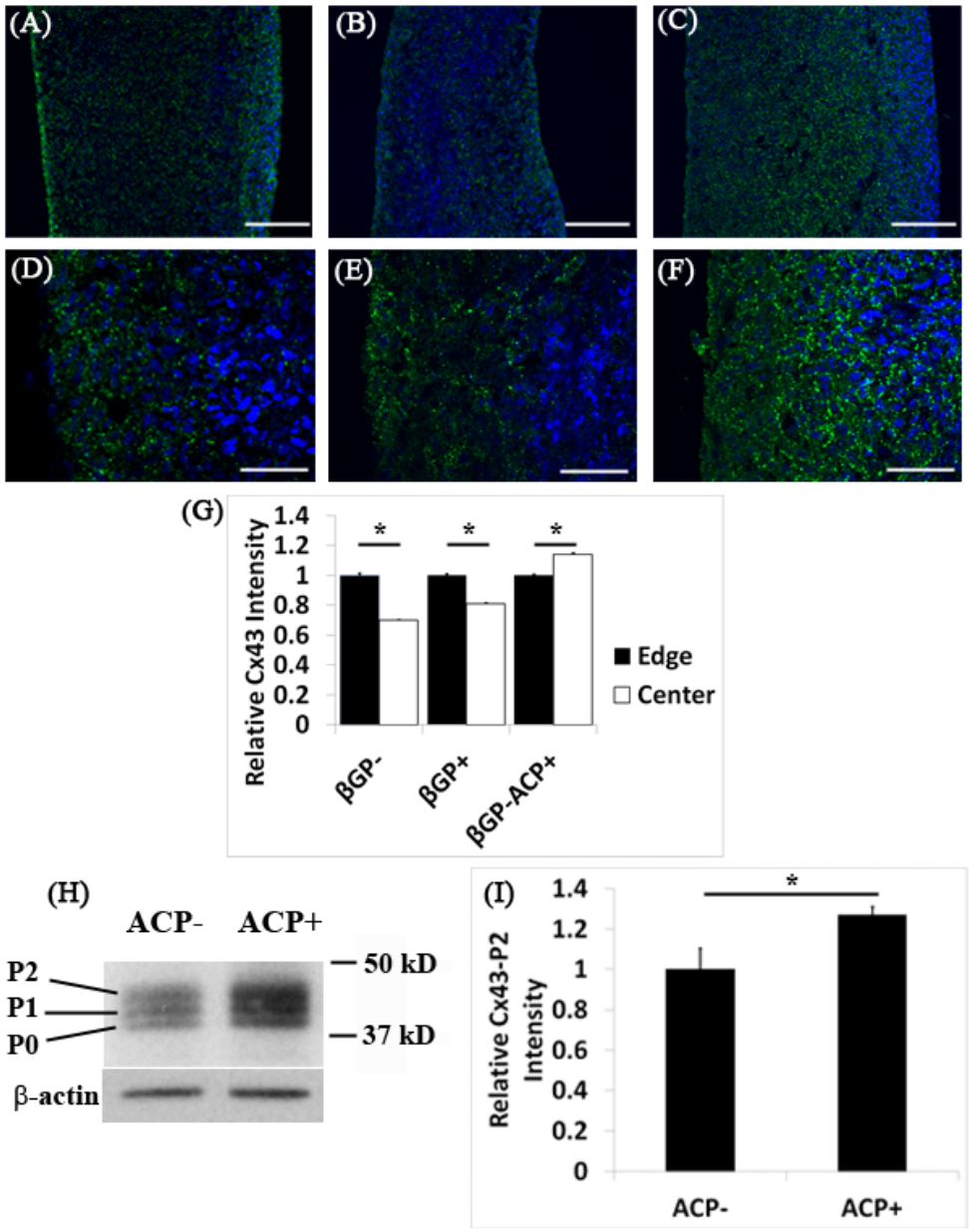

Figure 2.6: ACP alters Cx43 expression in DPC. Confocal images of immunofluorescent staining for Cx43 on sections of 3D scaffold-less constructs after *in vitro* culture shows that βGP- samples have higher expression of Cx43 expression (green) on the periphery than in the center as seen at lower (A) and higher (B) magnifications, similar expression profile was seen with βGP+ at lower (C) and higher (D) magnification. βGP-ACP+ samples expressed Cx43 throughout the constructs as seen with lower (E) and higher (F) magnifications. Fluorescent intensity was quantified at the edge and center of all construct types and differences were seen in βGP- and βGP+ samples with the edges expressing more Cx43 than the center ,whereas the opposite results were seen with the βGP-ACP+ (G). Western blot shows that ACP induces the expression of the P2 isoform of Cx43 in DPC as seen by Western blot (H) which was quantified using densitiometry (I), (A)-(G) Nuclei stained with DAPI (blue). Scale bars (A), (C), (E) = 150 μm, (B), (D), (E) = 50 μm

βGP- culture media are inducing cell differentiation and thereby directing the cells to produce the necessary matrix to facilitate mineralization, and these factors gradients causing differences in protein expression in the outer versus inner regions of the constructs. However, in the βGP-ACP+ group, the osteoinductive exogenous calcium phosphate phase is added to the cells at an early stage of construct formation thereby altering the microenvironment and differentiation conditions of the culture medium alone.

It is now accepted that exogenous calcium phosphates can induce hard tissue formation (Muller et al., 2008; Yuan et al., 1998; Yuan et al., 2000). The degree of osteoinductivity differs among the various types of calcium phosphate, which causes confusion on the mechanism behind this property (Knabe et al., 2004; Knabe et al., 2008; Sun et al., 2004; Wang et al., 2004). Amorphous calcium phosphate particles were selected for study in the scaffoldless constructs since they are one of the earliest calcium phosphate phases to form during natural biomineralization (Weiner et al., 2005). Crystalline hydroxyapatite (HA) particles were also attempted to be incorporated into scaffoldless constructs, however, the monolayer would not self assemble into a 3D structure in the presence of HA. Instead the monolayer would develop a thick structure that eventually fell apart. This indicates that the response of cells varies depending on the atomic structure of calcium phosphate. Amorphous calcium phosphate is a highly degradable form of calcium phosphate (LeGeros, 1993). In our study, the addition of ACP resulted in an increase in extracellular calcium as measured in the culture media. Since the global calcium concentration was increased it is expected that regions of the

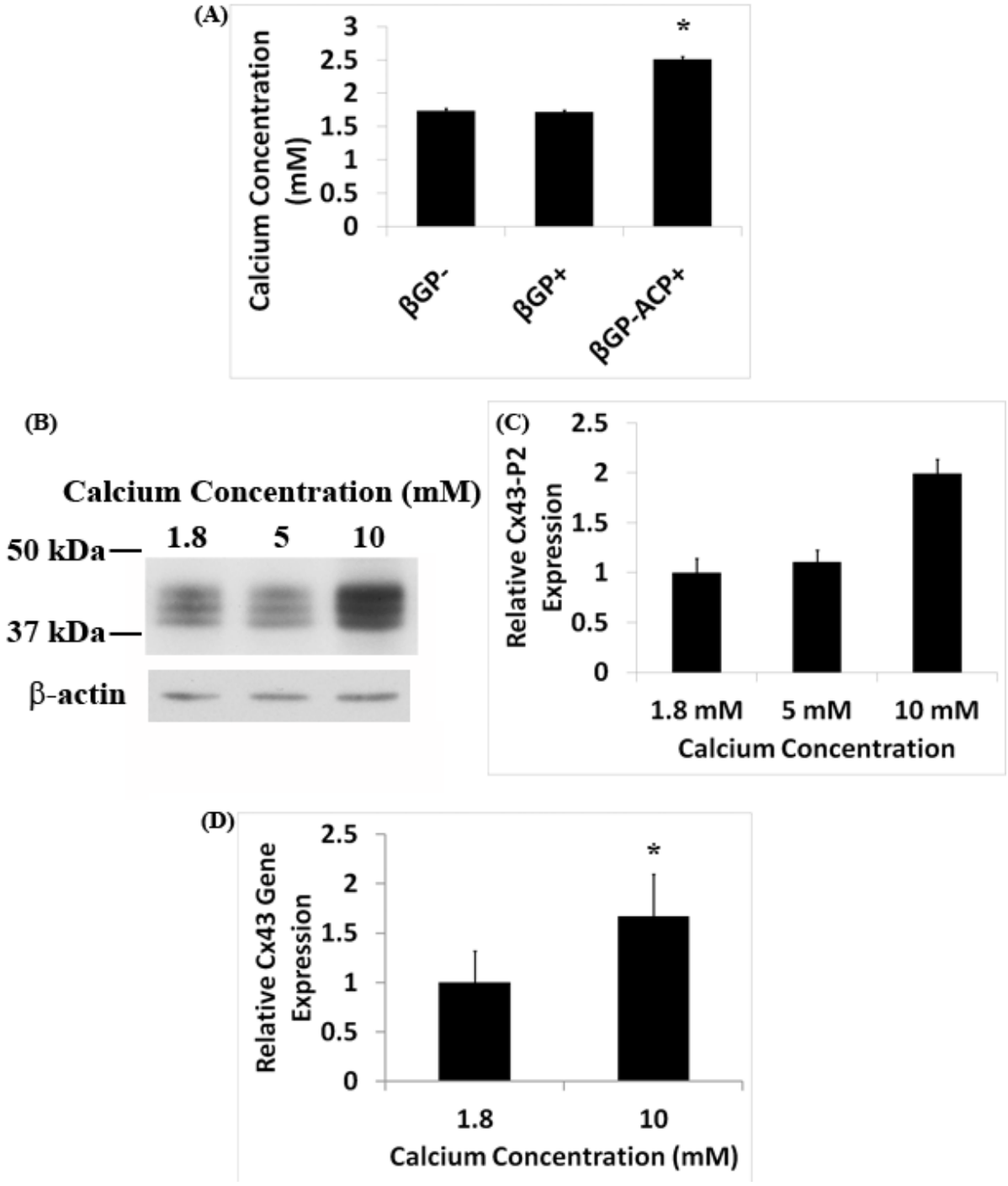

Figure 2.7: Extracellular calcium induces Cx43 expression. ICP spectroscopy shows that there is an increase in calcium concentration in the culture media collected from βGP-ACP+ samples, (A). Western blot shows that DPC cultured with increasing concentration of calcium result in an increased expression in the P2 isoform of Cx43 (B) which was also quantified using densitiometry (C). Quantitative real-time PCR of RNA isolated from DPC cultured with increased calcium concentration further verifies that calcium ion results in increased Cx43 expression (D).

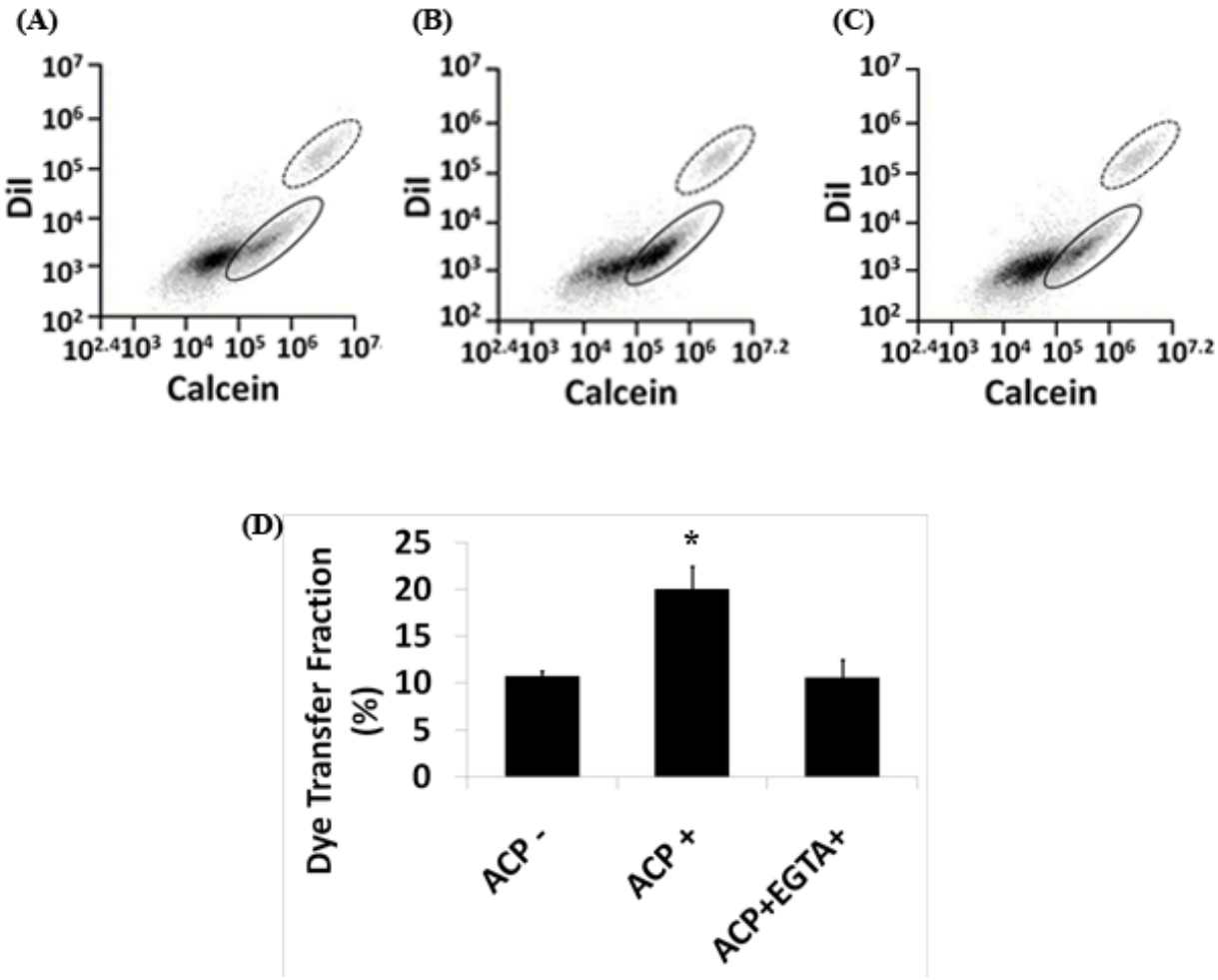

Figure 2.8: ACP causes an increase in functional gap junction expression caused by an increase in calcium concentration. Flow cytometry was used to assess the amount of calcein transfer via active gap junctions from donor cells characterized as DiI + to recipient cells characterized as Calcein+DiI- in ACP- (A), ACP+ (B), and ACP+EGTA+ (C) cultures. Dye transfer fraction calculated from the flow cytometery results indicate that the addition of ACP causes a significant increase in functional gap junctions, and that this is rescued by the addition of EGTA (D). (B), (C), (D): solid line ovals indicate recipient cells and dotted line ovals outline donor cells.

construct in direct contact to the ACP particles would sense an even higher concentration of extracellular calcium, and the different ACP particles would cause gradients of calcium ions within the construct. Extracellular Ca^{2+} was also shown in this study to modulate cell-cell communication in DPCs. Thus, the changes in extracellular

Ca^{2+} concentration and gradients could have resulted in the unorganized expression of dentin proteins in the βGP- ACP+ constructs.

Cx43 is necessary for proper bone and dentin differentiation from bone marrow stromal cells and dental pulp cells, respectively. Lecanda et al. showed that osteocalcin and bone sialoprotein gene expression increased in osteoblastic cells transfected with Cx43 (Lecanda et al., 1998). This is further supported by a study that showed that rat bone marrow stromal cells have decreased alkaline phosphatase activity and mineralization when cultured with the gap junctional inhibitor 18-α-glycyrrhetinic acid (Kamijo et al., 2006), and Cx43 inhibition in DPC with antisense oligonucleotides results in a decrease in alkaline phosphatase activity (Chung et al., 2007). These studies demonstrate that Cx43 plays a critical role in bone marrow and dental pulp stem cell differentiation and mineralization. This is in agreement with our data that samples cultured with ACP had increased Cx43 expression and gap junction formation which altered cell differentiation thereby causing the increased expression of dentin proteins throughout the βGP- ACP+ constructs.

This manuscript shows that calcium phosphates are osteoinductive materials that alter 3D tissue differentiation patterns through the release of Ca ions, which modulates Cx43-mediated gap junctions. These data emphasize that scaffolding material can strongly affect cellular functions and therefore great consideration should be taken when selecting this important tissue engineering component.

2.6 ACKNOWLEDGEMENTS

I would like to thank Dr. Charles Sfeir, Dr. Elia Beniash, Dr. Thottala Jayaraman, and Dr. Raymond Lam for their contributions to this research and Dr. Leslie Bannon for her editorial contribution.

3.0 CHAPTER 3: ESTABLISHMENT OF MULTILINEAGE PERICYTES SORTED FROM HUMAN DENTAL PULP AND THEIR POTENTIAL FOR CRANIOFACIAL REGENERATION

This chapter is currently in preparation for publication with Dr. Pang-ning (Bonnie) Teng and Ms. Fatima Syed-Picard as co-first authors. Dr. Teng contributed Figures 3.1-3.3 and Ms. Syed-Picard contributed Figures 3.4 and 3.5.

3.1 ABSTRACT

Pericytes of mesodermal origin have been isolated through CD146+CD34-CD45-CD56- expression and characterized as stem cells, however, it is unknown if neural crestal pericytes with this same expression profile behave similarly. In this study, we have established a perivascular stem cell population isolated from the human dental pulp utilizing fluorescence activated cell sorting by selection of cells that are positive for CD146 but negative for CD34, CD45, and CD56. Pericytes in human dental pulp were characterized by immunohistochemistry as expressing CD146, α-smooth muscle actin (α –SMA), NG2, but negative for CD34, von Willebrand factor (vWF), CD45 and CD56 expression. Long-term cultured dental pulp perivascular cells expressed the following stem cell markers including CD44, CD166 and CD90, and furthermore they gave rise to

osteoblasts, chondrocytes and adipocytes *in vitro*. The potential use of the dental pulp pericytes for tissue engineering applications was also assessed by culturing the cells in 3D self-assembled scaffoldless constructs. These 3D constructs expressed dentin proteins throughout indicating the potential utilization of dental pulp pericytes for craniofacial regeneration. Pericytes sorted to homogeneity from extracted dental pulp of the neural crest origin may represent a convenient source of therapeutic progenitor cells for future craniofacial tissue engineering.

3.2 INTRODUCTION

Regenerating tissues within the craniofacial complex could provide a therapy for bone loss resulting from periodontal disease, repair traumatic injuries to the face and treat congenital anomalies such as cleft lip and cleft palate. Currently, all of these anomalies require surgery where bony deficits are restored with synthetic materials. Innovative regenerative cellular therapies would improve tissue functionality. Identification of an easily available source of stem cells to repair and regenerate bone in the craniofacial complex is therefore a clinically important goal for tissue engineering. Populations of stem cells have been found in a number of craniofacial tissues such as the dental pulp of adult and deciduous teeth, the periodontal ligament, the apical papilla, and salivary glands (Gronthos et al., 2000; Lombaert et al., 2008; Miura et al., 2003; Seo et al., 2004; Sonoyama et al., 2008). However, the stem cells are subsets of the total heterogeneous population of cells comprising these tissues. Currently, it is unknown

whether the stem cells should be isolated from the remaining population of cells or if the total heterogeneous population will provide additional support to the stem cells and enhance tissue assembly during regenerative therapies.

Recently, two research groups have shown that perivascular cells can be purified from multiple human organs including placenta, pancreas, fat and muscle and can differentiate into multiple lineages including bone. These data suggest that the elusive mesenchymal stem cell (MSC) has a perivascular origin (Covas et al., 2008; Crisan et al.; Crisan et al., 2008b; Dellavalle et al., 2007; Hughes and Chan-Ling, 2004; Peault et al., 2007). Pericytes, also known as Rouget cells or mural cells, reside around the endothelium of microvessels (capillaries and postcapillary venules) and have diverse roles in the regulation of blood flow and vessel formation throughout the entire vasculature (Bergers and Song, 2005). Previously, pericytes were not sorted but were identified in primary cultures by the following characteristics: morphology, slow adhesion to plastic and expression of pericyte-associated antigens such as 3G5, NG2, CD146, Stro-1, α-SMA, desmin and osteonectin (Armulik et al., 2005; Bergers and Song, 2005; Howson et al., 2005; Hughes and Chan-Ling, 2004; Nayak et al., 1988; Shepro and Morel, 1993). The isolation of pericytes are therefore of interest for regenerative medicine.

The dental pulp of extracted teeth is a non-invasive, easily accessible source of stem cells. These cells, the dental pulp stem cells (DPSCs), differentiate into osteoblast-like cells *in vitro* and can form dentin-like and pulp-like structures *in vivo* (Gronthos et al., 2000). DPSCs are believed to be pericyte-like cells that migrate towards the pulpal injury site and aid its restoration (Fitzgerald et al., 1990; Tecles et al., 2005). Although

CD146 and Stro-1 have been markers used for magnetic-activated cell sorting of the mesenchymal stem cells from the dental pulp, these markers are not specific to pericytes (Shi and Gronthos, 2003). In addition to its expression in pericytes, CD146 is also expressed by the endothelium, smooth muscle, myofibroblasts, Schwann cells; while Stro-1 is also expressed by the endothelium, perineurium, and hematopoeitic cells (Shi and Gronthos, 2003) (Shih, 1999) (Crisan et al., 2008b) (Doherty et al., 1998). Therefore, identifying methods that can specifically identify and isolate dental pulp pericytes will allow us to understand the potential of these cells in craniofacial regeneration.

Cephalic pericytes, such as those in the dental pulp, are neural crest derived, while pericytes in trunk tissues are mesodermal in origin (Crisan et al., 2008b) (Miletich and Sharpe, 2004) (Etchevers et al., 2001). Neural crest cells are a multipotent population of ectomesenchymal cells that originate on the dorsal edge of the neural tube, undergo an epithelial to mesenchymal transformation and migrate to their niche. *In vivo,* neural crest cells interpret many patterning signals to determine their fate. Importantly, only cranial neural crest can differentiate into bone and cartilage. In addition, a recent report showed that pericyte-derived mesenchymal cells were able to differentiate into odontoblast-like cells *in vivo* as demonstrated by genetic lineage tracing (Feng et al.). Therefore, we hypothesize that dental pulp pericytes may be comparable to mesodermal pericytes and could be a candidate source of stem cells for craniofacial tissue engineering. In this study, we have identified and isolated CD146+CD34-CD45-CD56- perivascular cells present in the human dental pulp. With immunohistochemistry assays, we first determined the presence and absence of above

cell surface markers that could be utilized to sort dental pulp pericytes and validated that sorted dental pericytes could be expanded in culture while maintaining the pericytes phenotype. We also confirmed that these pericytes are capable of differentiating down multiple lineages.

Self-assembled 3D scaffoldless engineered tissue constructs are a relevant 3D model to study endogenous tissue formation and the microenvironment that cells generate for themselves without the influence of exogenous materials. These engineered tissues are formed by culturing cells as a monolayer until they form a tissue sheet. At this point, the tissue sheet delaminates from the plate and is contracted by the cells towards the center of the dish. Two pins are placed in the center of the dish that act as anchors. The tissue sheet contracts around these pins and self assembles to form a solid cylindrical tissue. This tissue is produced and organized by the cells themselves without the use of any exogenous scaffold. Recently we have shown that when cultured in a self-assembled three dimensional scaffoldless engineered tissue construct, the total heterogeneous population of dental pulp cells forms a spatially organized dentin-pulp complex-like structure (Chapter 2). These samples express dentin proteins on the periphery and exhibit pulp properties in the core after both after *in vitro* culture and *in vivo* subcutaneous implantation. In this study, we culture dental pulp pericytes in self-assembled 3D scaffoldless constructs to characterize their behavior in tissue formation and organization and to further evaluate their potential for craniofacial tissue engineering.

3.3 MATERIALS AND METHODS

3.3.1 Antibodies

Unconjugated antibodies are mouse anti-human CD146, -CD34, -NG2, -CD56, -CD44, -CD90 (BD Biosciences), -CD45 (DAKO), rabbit anti-human CBFA-1/Runx-2, -osteocalcin, -PDGFR-β (Santa Cruz Biotechnology). Conjugated antibodies include mouse anti-human CD146-Alexa488 (Chemicon), -CD146-FITC (AbSerotec), -CD45-PE-Cy5, -CD56-PE-Cy7 (BD Biosciences), -α-SMA-FITC (Sigma), -CD34-PE (DAKO), -CD166-biotin (Ancell), sheep anti-human vWF-FITC (US Biological), rabbit anti-human CD144-biotin (BMedSystems), donkey anti-rabbit-Alexa488, donkey anti-rabbit-Alexa594 (Molecular Probes), goat anti-mouseIgG biotin (DAKO), goat anti-mouse-IgM biotin (μ) (Caltag Laboratories), mouse IgG-PE, mouse IgG-FITC (Chemicon), mouse IgG-PE-Cy7, mouse IgG-PE-Cy5 (BD Biosciences) and sheep IgG-FITC (US Biological).

3.3.2 Tooth procurement and cell isolation

We obtained 85 adult third molars (age 14-23 years) at the School of Dental Medicine, University of Pittsburgh, as approved by the Institutional Review Board (IRB number: 0312073). Dental pulp was digested with collagenases I, II, and IV (each at 1 mg/ml, Sigma) at 37 ˚C for 2 h under gentle agitation. Cell suspensions were passed through a 70-μm cell strainer (BD Falcon) to obtain single-cell suspensions.

3.3.3 Immunohistochemistry

Dental pulps were frozen in Tissue Freezing Medium (Triangle Biomedical Sciences) and cryosectioned at 5-μm thickness. Tissue sections were fixed in ice cold 50% methanol and 50% ethanol for 5 min, air dried for 15 min and then blocked with 5% goat serum (Gibco) in PBS for 1 h at ambient temperature. Tissue sections were incubated with primary antibody (1:100 dilution, same dilution for all primary antibodies) overnight at 4 ˚C. Appropriate secondary antibodies were used (1:1000 dilution) for 1 h followed by streptavidin coupled to Cy3 (1:1000 dilution, Amersham) for 30 min at RT. When two antibodies were used simultaneously, the sections were incubated for 1 h at RT with a second primary antibody that was already conjugated with either Alexa-488 or FITC. The sections were then stained with 4',6-diamidino-2-phenylindole (DAPI, 1:2000 dilution, Molecular Probes) for 5 min at RT to visualize nuclei. Coverslips were mounted with Gel/Mount mounting medium containing anti-fading agents (Biomeda Corp.). Fluorescent images were acquired by optical and confocal microscopy using Nikon Eclipse TE2000-U and Olympus FLUOVIEW FV1000 microscopes, respectively.

3.3.4 FACS and cell culture

Freshly digested dental pulp cells were washed with phosphate buffered saline (PBS, Gibco) and stained with CD146-FITC, CD34-PE, CD45-PECy5 and CD56-PE-Cy7 antibodies for 30 min at 4 ˚C (1:100 dilution). Cells were then washed with PBS and resuspended in 1ml of Endothelial Cell Growth Medium 2 (EGM-2, Cambrex Bioscience

Inc.). A FACSAria dual-laser fluorescence activated cell sorter (Becton-Dickinson) was used to isolate CD146+CD34-CD45-CD56- cells as previously described (Crisan et al.).

Sorted cells were cultured at 37 ˚C, 5% CO_2 in EGM-2 on 48-well tissue culture plates coated with 2% gelatin (Calbiochem) at 10,000 cells per cm^2. After cells attached to the culture plate, medium was changed to high-glucose DMEM high glucose (GIBCO) with 20% fetal bovine serum (FBS, Atlantic Biological) and 1% penicillin-streptomycin (GIBCO).

3.3.5 CFU-f assay

Cultured dental pulp perivascular cells were seeded at a density of 100 cells/10cm^2 and cultured for two weeks to test their clonogenic ability. Cells were fixed with 100% methanol for 5 min, air dried for 5 min and stained with 3% Crystal violet (Sigma) for 5 min at RT. Cells were washed with distilled water and colonies (>2.5 mm or 50 cells) were counted. Percentage of CFU was calculated as the number of colonies counted divided by the number of cells plated, then multiplied by 100. Pericytes isolated from dental pulp of three patients were analyzed. Six plates of colonies were counted and scored for each donor.

3.3.6 Immunocytochemistry

Sorted dental pulp cells were seeded in 48-well tissue culture plates. Cells were fixed in 1% paraformaldehyde (PFA) in PBS or a mixture of ice-cold acetone and methanol (1:1). Cells were washed with PBS, blocked with 5% goat serum, and then incubated

with primary and secondary antibodies. To detect Runx-2 protein, cells were permeabilized with 0.1% Triton X-100 (Sigma) during blocking and incubation with antibodies.

3.3.7 Osteogenic differentiation

Dental pulp perivascular cells were seeded at 25,000 cells/cm^2 in 6-well tissue culture plates and cultured in control medium (high-glucose DMEM with 20% FBS, 1% PS) or osteogenic medium for two weeks. Osteogenic medium is control medium supplemented with 50ug/ml L-ascorbic acid (Fisher Biotech), 100mM ß-glycerolphosphate (Sigma), and 100nM dexamethasone (Sigma). Medium was changed every 3 days. Cells were then fixed and subjected to alkaline phosphatase and von Kossa stainings. Cells were washed with PBS and fixed with 4% PFA for 15 min at 4 ˚C. For alkaline phosphatase staining, cells were incubated with a solution containing 5 mg naphtol AS MX-PO4 (Fisher Scientific) dissolved in 0.2 ml N,N-dimethylformamide, 25ml Tris-HCl (0.2 M, pH 8.3, Sigma), Red Violet LB salt (30mg, Sigma), and 25 ml distilled water for 45 min at RT. Cells were washed 3 times with distilled water, then incubated with 5% silver nitrate (Sigma) at RT for 30 min and then rinsed with distilled water 3 times. Cells were examined and imaged by bright field microscopy.

3.3.8 Chondrogenic differentiation

Dental pulp perivascular cells were centrifuged for 5min at 600g into 3-dimensional pellets (250,000 cells/pellet) and cultured for 14 days in chondrogenic medium that contains high glucose DMEM, 10ng/ml TGF-β1 (Peprotech), 10ul/ml ITS-plus premix (BD Biosciences Clonetech, final concentrations: 6.25 ug/ml insulin, 6.25 ug/ml transferrin, 6.25 ug/ml selenous acid, 1.25 mg/ml bovine serum albumin, and 5.35 ug/ml linoleic acid), 100nM dexamethasone (Sigma), 50 ug/ml ascorbic 2-phosphate (Sigma). Control medium was high-glucose DMEM containing ITS-plus premix. Medium was changed every 3 days. Each experiment was performed in triplicates. Cell pellets were fixed in 4% paraformaldehyde, dehydrated in ethanol/xylene series, and paraffin-embedded. Five-µm paraffin sections were stained with 1-Alcian blue with nuclear fast red counterstain or 2-Safranin O with fast green counterstain, using standard protocols.

3.3.9 Adipogenic differentiation

Dental pulp perivascular cells were seeded at 25,000 cells/cm^2 in 6-well tissue culture plates and cultured in control medium (high-glucose DMEM with 20% FBS, 1% PS) or adipogenic medium for two weeks. Adipogenic medium is control medium supplemented with 0.5 mM of 1-methyl-3-isobutylxanthine (Sigma), 1uM dexamethasone (Sigma), 0.01 mg/ml insulin (Cell Sciences), and 0.2 mM indomethacin (Sigma). Medium was changed every 3 days for 21 days. Each experiment was done in triplicates. Cells were fixed and stained with oil red-O (Sigma) using standard protocols.

3.3.10 Quantitative PCR

RNA was collected using an RNeasy Mini Kit (Qiagen) from monolayer cultures of human CD146+34-56-45- pulp cells treated with and without osteogenic media. Real-time RT-PCR was performed using TaqMan One-Step RT-PCR Master Mix Reagents (Applied Biosystems) and the following primers purchased from Applied Biosystems: alkaline phosphatase (Hs 01029144_m1) and RUNX2 (Hs 00298328_s1). The TaqMan Ribosomal RNA Control Reagents designed to detect the 18S ribosomal RNA gene(Applied Biosystems) was used as the endogenous control. Using a 7900 HT Fast Real-Time PCR System (Applied Biosystems) the RNA underwent reverse transcription for 30 minutes at 48°C, then polymerase activation for 10 minutes at 95°C, and finally PCR for 40 cycles with an initial denaturation for 15 seconds at 95°C then annealing/extending for 1 minute at 60°C.

3.3.11Scaffoldless construct formation

Scaffoldless three dimensional engineered tissues were created similar to previously described (Chapter 2). Briefly, tissue culture plastic dishes, 35 mm in diameter, were coated with SYLGARD (type 184 silicone elastomer). The SYLGARD was coated with 3 $\mu g/cm^2$ natural mouse laminin (Invitrogen) for cell adhesion. Human dental pulp pericytes were plated onto the construct dish at a density of 200,000 cells/dish in a media containing DMEM, 20% FBS, 1% P/S, 0.13 mg/ml L-ascorbic acid-2-phosphate (L-asc-2-phos; Sigma),10^{-9} M dexamethasone (Sigma), and 2 ng/ml basic fibroblast

growth factor (bFGF; Peprotech). Once the cells reach confluence, two minutien pins, 0.2 mm diameter and 1 cm long, were pinned onto the cell monolayer, 7 mm apart, and the culture medium was switched to DMEM, 5% FBS, 1% P/S, 0.13 mg/ml L-asc-2-phos,10^{-9} M dexamethasone, 2 ng/ml bFGF, and 2 ng/ml transforming growth factor- β1 (TGFβ1; Peprotech). Seven days after the constructs rolled up, samples were fixed in 4% paraformaldehyde and embedded in paraffin. The constructs were sliced longitudinally at a thickness of 5 µm and used for hematoxylin and eosin (H and E) staining or immunofluorescent staining for DMP-1 (LF148, provided by Dr. Larry Fisher, NIH), and DSP (LF151, provided by Dr. Larry Fisher, NIH).

3.3.12 Statistical Analysis

Data was represented as the average +/- standard error. Statistical comparisons were performed using SPSS software. Independent samples t-tests were used to compare means. Significance was considered at $p < .05$.

3.4 RESULTS

Perivascular cells that surround endothelial cells in capillaries and microvessels are anatomically defined as pericytes (Carlile et al., 2000; Provis, 2001; Shepro and Morel, 1993). We performed immunohistochemistry to identify the various cells that surround vascular areas in human dental pulp using the cell surface markers listed in **Table 3.1**.

We found that pericytes in the dental pulp co-express CD146, α-SMA and NG2 (**Fig 3.1a, b, g**) and were negative for CD56, CD34, vWF and CD45 expression (**Figure 3.1c, d, e, and h**). A population of non-pericyte cells express both CD146 and CD56 expression (**Figure 3.1f**) therefore the exclusion of CD56 expressing cells were included. We deduced that the CD146+ NG2+ CD34- CD45-CD56- cell surface phenotype typifies all pericytes within human dental pulp, as it does in other tissues analyzed so far (Crisan et al.).

Table 3.1: Markers Used for Immunohistochemistry

Pericytes	CD146, NG2, α-SMA, PDGFR-β
Endothelial cells	CD146, CD34, vWF
Hematopoietic cells	CD34, CD45
Myoblasts, NK cells	CD56

To isolate pericytes by flow cytometry from the enzymatically dissociated dental pulp, we first excluded CD45+ hematopoietic cells and CD56+ myogenic and NK cells (**Figures 3.2a, b**). The dental pulp cell suspension could then be fractionated into three distinct cell populations as shown in **Figure 3.2c** and outlined below:

- Endothelial cells: CD34+CD146-CD45-CD56- and CD34+CD146+CD45-CD56-
- Pericytes (Dental pulp perivascular cells) : CD146+CD34-CD45-CD56-
- Uncharacterized CD34-CD146-CD45-CD56- cells

CD146+CD34-CD45-CD56- pericytes were isolated. Pericytes represent 0.62 ± 0.41 %, whereas endothelial cells account for 3.43 ± 2.16 % of the total dental pulp cell population.

Sorted dental pulp perivascular cells were seeded in culture in EGM-2 medium on gelatin-coated plates. Cell viability was low when less than 1,000 cells were seeded after sorting. Cells attached to the bottom of the wells in approximately 48-72 h. One week after culture initiation, EGM-2 medium was replaced by DMEM supplemented with 20% FBS. Recently attached cells exhibited mixed elongated, spindle and polygonal shapes. After cells were passaged once, they exhibited star-like shapes with prominent nuclei and multiple cytoplasmic extensions (**Figure 3.2d**).

The clonogenic capacity of cultured pericytes was determined by using the CFU-f assay. Cells were seeded at a low density of 100 cells/10cm^2 and colonies were observed on day 14 by crystal violet staining. *In vitro* cultured dental pulp pericytes are highly clonogenic, 98±2% of these being CFU-f (**Figure 3.2e**). Cultured pericytes at passage 8, i.e. cultured for 2 months, maintained expression of the pericyte markers CD146, NG2 and α-SMA (**Figure 3.2f-h**) and remained negative for vWF, CD144, CD45 and CD56 expression (not shown). All cultured pericytes were also positive for PDGFR-ß (**Figure 3.2i**). These results showed that sorted pericytes were not contaminated by other cell types and did not change their antigenic characteristics when proliferating in culture. To further characterize cultured dental pulp pericytes, we tested their expression of several mesenchymal stem cell markers. Cultured pericytes express the MSC markers CD44, CD90 and CD166 (**Figure 3.2j, k, l**). Pericytes in culture also

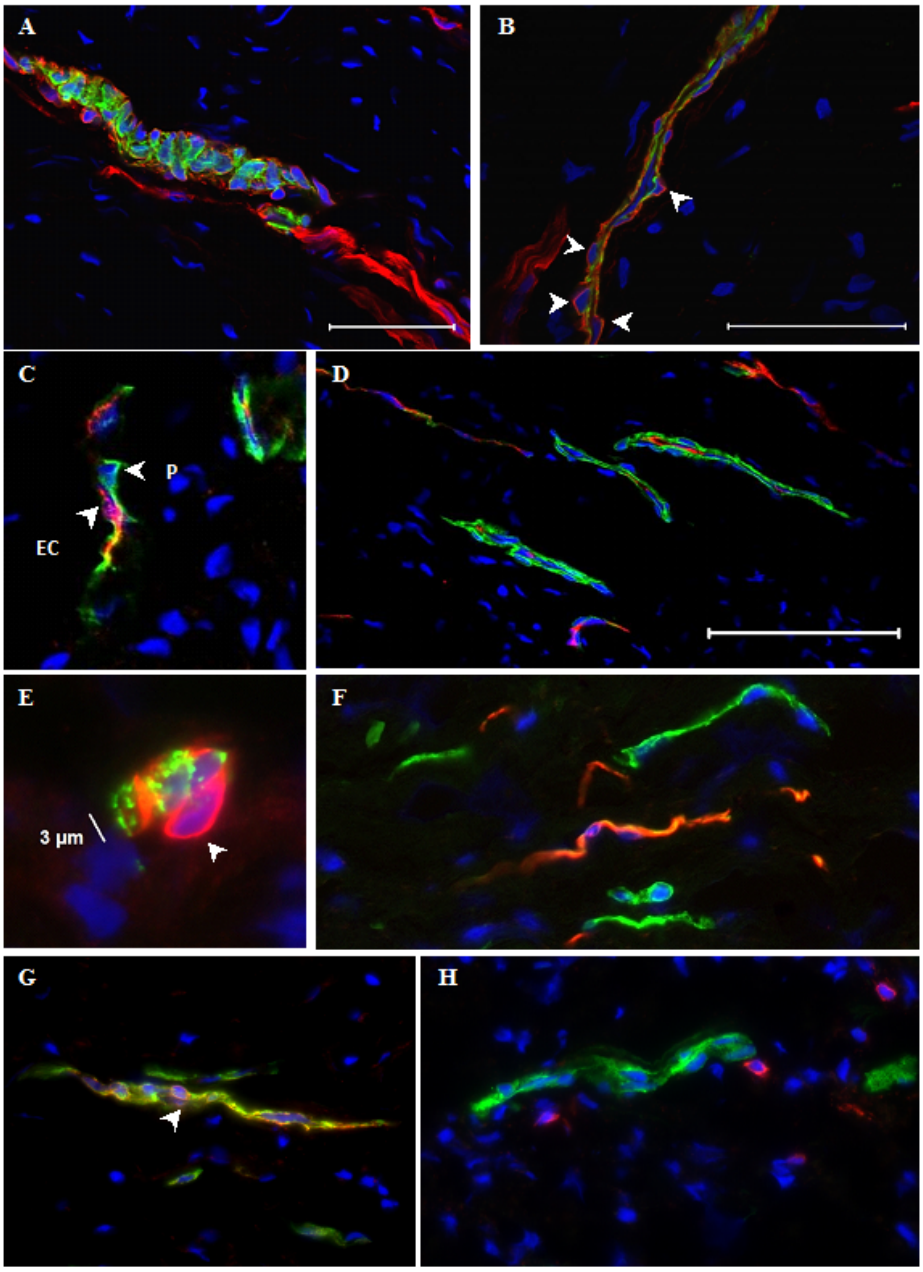

Figure 3.1: Immunodetection of pericytes in the human dental pulp
Frozen sections of dental pulp were stained with antibodies against pericytes, endothelial cells, neural cells, and hematopoietic cells. Pericytes are pointed with arrows. A, B - CD146 (red) α-SMA (green). C, D- CD146 (green), CD34 (red). Pericytes (P). Endothelial cells (EC). E - CD146 (red), vWF (green). F - CD146 (green), CD56 (red). G - CD146 (green) NG2 (red) H - CD146 (green) CD45 (red). Nuclei were stained blue with DAPI. Bar = 50µm. (Teng, 2009)

express both Runx2 and osteocalcin, suggesting their inherent osteogenic capability (**Figure 3.2m, n**).

We explored the multilineage differentiation potential of pericytes by culturing the FACS sorted and propagated cells in differentiation media that stimulates the differentiation of osteocytes, chondrocytes and adipocytes. Due to the inherent expression of transcription factor Runx2 in dental pulp pericytes cultured without β-glycerophosphate, we hypothesized that with the addition of ß-glycerol phosphate and dexamethasone would induce differentiation towards the osteoblast lineage. Alkaline phosphatase and von Kossa staining were used to characterize the progeny of pericytes grown in these conditions. Alkaline phosphatase is present in pericytes cultured in the control media and the staining remains present in cells cultured in the osteogenic media. After two weeks of culture, pericytes cultured in osteogenic medium differentiated into osteoblasts-like cells as seen by the formation of a mineralized matrix via von Kossa staining (**Figure 3.3a, b**). In addition to the staining, the mRNA expression of alkaline phosphatase and Runx2 were monitored after 7 and 14 days of culture by quantitative PCR analysis. Alkaline phosphatase (**Figure 3.4a**) and Runx2 (**Figure 3.4b**) were significantly upregulated when cultured in an osteogenic media compared to untreated control. This data demonstrates the osteo/odontogenic differentiation capability of dental pulp pericytes.

In addition to osteogenic differentiation, dental pulp pericytes were also induced to differentiate toward the chondrogenic and adipogenic lineages to further explore their multi-lineage potential. To induce chondrogenic differentiation, pericytes were cultured

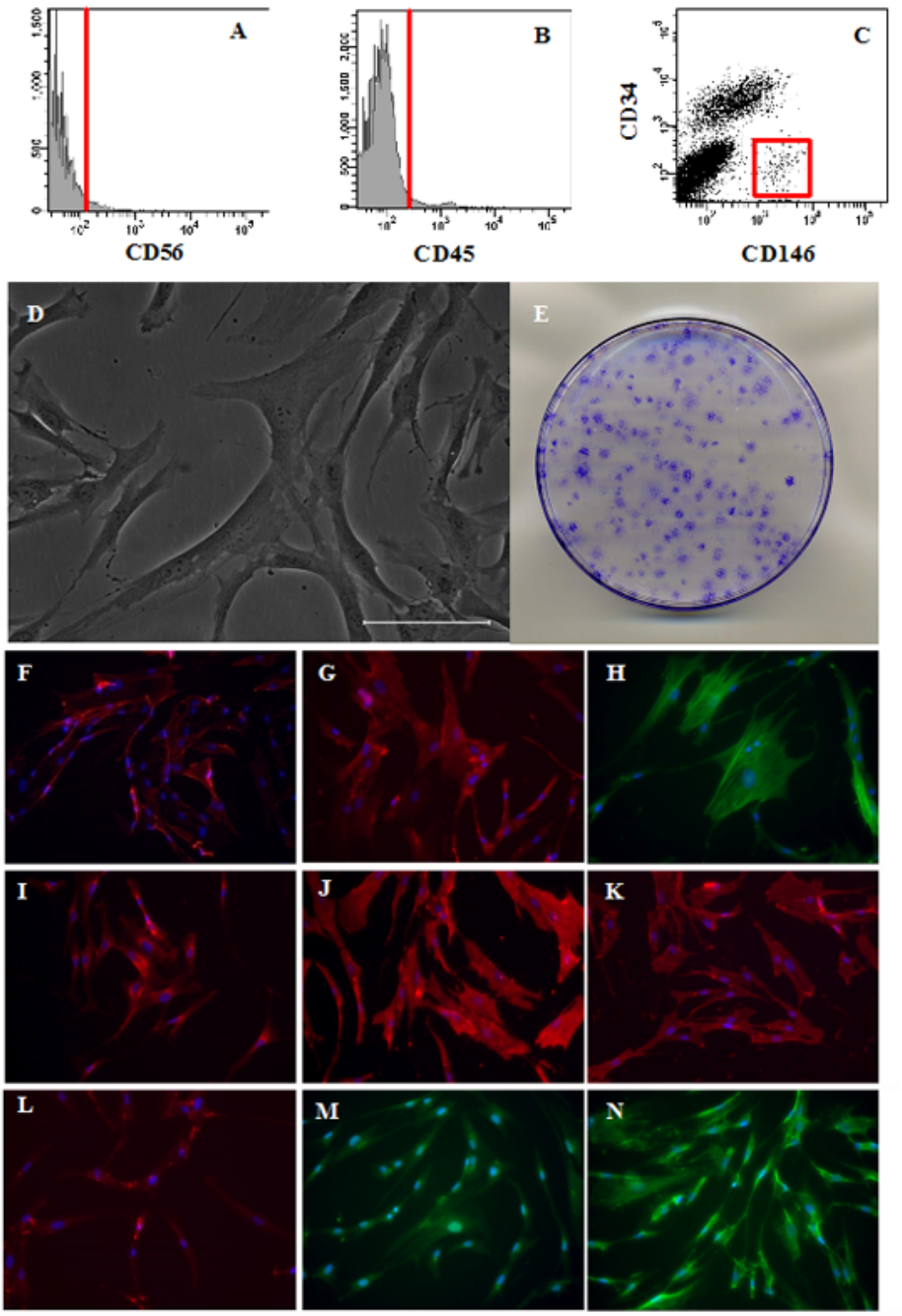

Figure 3.2: Flow cytometry sorting, morphology, CFU-f analysis, and immunocytochemistry of cultured dental pulp pericytes. Dental pulp tissues were digested and cells were stained with antibodies against CD146, CD34, CD56, and CD45. Cells were analyzed and sorted by FACS. Exclusion of A- CD56+ and B- CD45+ cells. C - selection of CD146+CD34- pericyte population. D - Dental pulp pericytes imaged by phase contrast microscopy. Bar = 100um. E - Colonies of dental pulp pericytes were stained by crystal violet. Cultured pericytes were characterized by immunocytochemistry. Pericyte markers: F - CD146 (red), G - NG2 (red), H - α-SMA (green), I - PDGF r-ß. Mesenchymal stem cell markers: J - CD44 (red), K - CD90 (red), L - CD166 (red). Osteoblast markers: M – Runx2 (green). N - Osteocalcin (green). Magnification: 20X. (Teng, 2009)

as pellets and maintained in differentiation medium containing TGF-β1. After 3 weeks, pellets exhibited cartilage-like morphology with round, smooth and shiny surfaces. Alcian blue and safranin O staining of sections of the pellets indicated the presence of proteoglycans surrounding lacuna confirming that the pericytes differentiated into chondrocytes (**Figure 3.3c, d, e**). For adipogenic differentiation**,** pericytes were cultured in medium containing 1-methyl-3-isobutylxanthin, dexamethasone, insulin and indomethacin. After three weeks of culture, we observed lipid vesicles in the cytoplasm and after five weeks of culture we found accumulated lipid droplets. Finally, we observed Oil red O stained mature adipocytes (**Figure 3.3f**).

We have demonstrated the feasibility of sorting pericytes from the human dental pulp. The sorted pericytes population can be expanded in culture and differentiated into three lineages including bone/dentin, cartilage and adipocytes. We therefore conclude that the CD146+CD34-CD45-CD56- cell population from the neural crest origin is comparable to those from the mesoderm origin.

To further explore the regenerative capacity of dental pulp pericyte stem cells, the FACS sorted and expanded DPSC were used to tissue engineer 3D self-assembled scaffoldless constructs. These tissues are formed by the cells themselves by the production and assembly of endogenous extracellular matrix. These constructs are cylindrical tissues that are approximately 7 mm in length (**Figure 3.5a**). H and E staining of sections of the engineered tissues revealed that the constructs are solid and cellular (Figure 4B). Immunostaining shows that the constructs also expressed dentin matrix protein 1 (DMP1) (**Figure 3.5c**) and dentin sialoprotein (DSP) (**Figure 3.5d**) indicating that the pericytes differentiated down an odontogenic lineage within these 3D

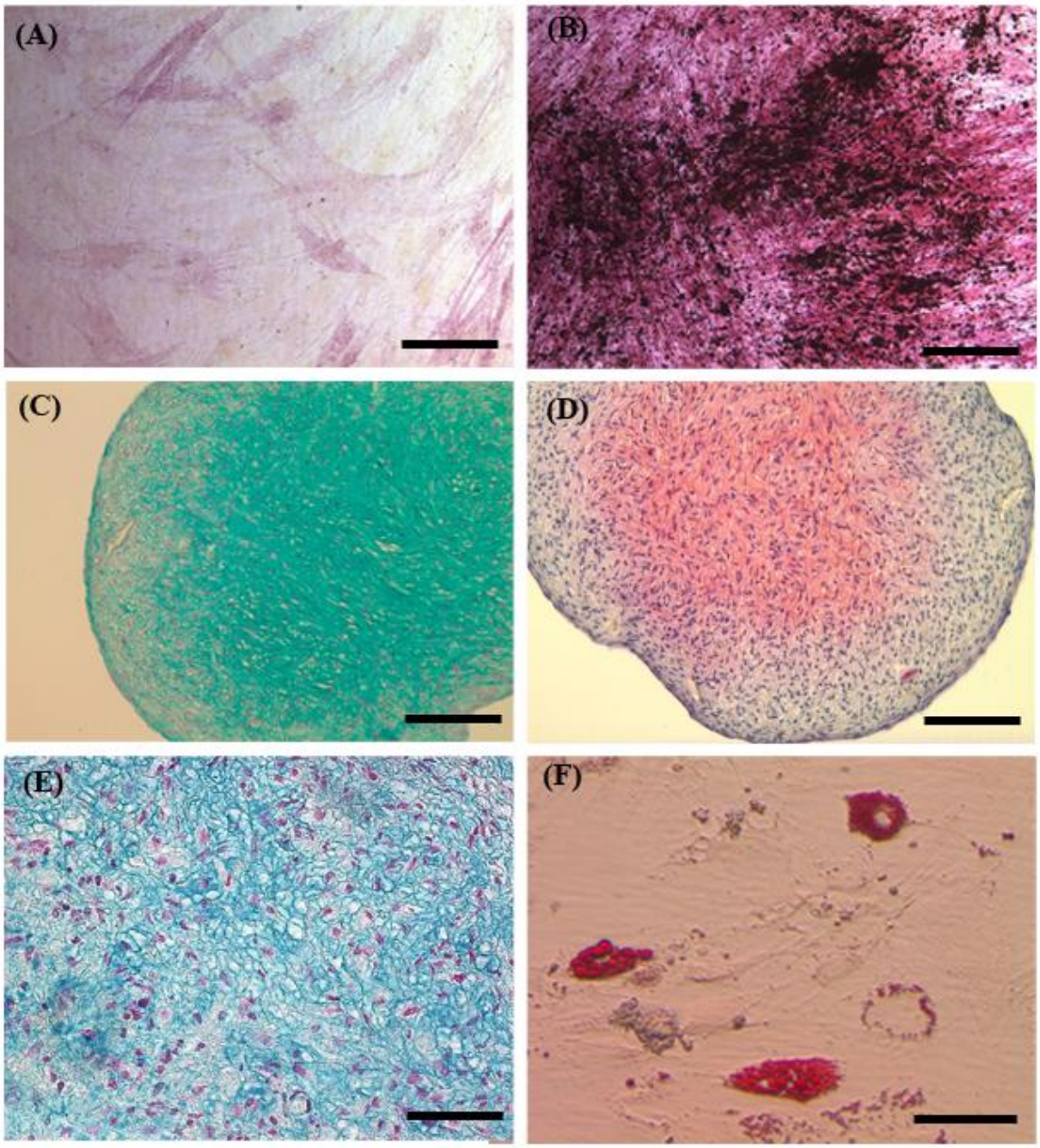

Figure 3.3 Multilineage differentiation of cultured dental pulp pericytes. Osteogenic differentiation: alkaline phosphatase (red) and von Kossa (black) staining of pericytes cultured in A – control medium, B - osteogenic medium. Chondrogenic differentiation: pellet sections stained with C - Alcian blue (counter stained with nuclear fast red), 20X and E-40X. D - Safranin-O (counter stained with fast green). Intense Alcian blue and Safranin O stainings were observed at the center of the pellets showing proteoglycans accumulation. Adipogenic differentiation: F - Oil red O staining. A-D: bar = 100µm. E-F: bar = 50µm. (Teng, 2009)

structures. This data indicates that dental pulp pericyte stem cells have the capacity to form 3D engineered tissues that could be used for dentin regeneration.

3.5 DISCUSSION

There is an enormous need to develop safe and effective methods to regenerate soft and hard tissues for craniofacial diseases such as head and neck cancers, trauma, birth defects, periodontal disease and pulp injuries. Cellular approaches provide an attractive option to develop therapies targeted for craniofacial regeneration. Engineering cellular therapies requires the understanding of the cells and their regenerative potential. Current studies have focused on isolating dental pulp stem cells by utilizing different enrichment techniques, markers and various multi-lineage differentiation assessments. Many such studies used the total population of dental pulp cells and only few reported the characterization and tentative isolation of dental pulp stem cells using flow cytometry. Additionally, differences between using the total heterogeneous population of cells versus sorted dental pulp stem cells for regenerative therapies is largely unknown.

Shi et al. were the first to characterize and compare different dental pulp candidate stem cell populations (Shi and Gronthos, 2003). They have isolated clonogenic populations of DPSCs by their ability to adhere to plastic, similar to bone marrow stromal cells (Gronthos et al., 2000). Colony-derived DPSCs formed mineralized nodules *in vitro* and generated dentin and pulp-like tissue *in vivo* (Batouli et al., 2003; Shi et al., 2005). Using similar methods, Shi's group also isolated stem cells

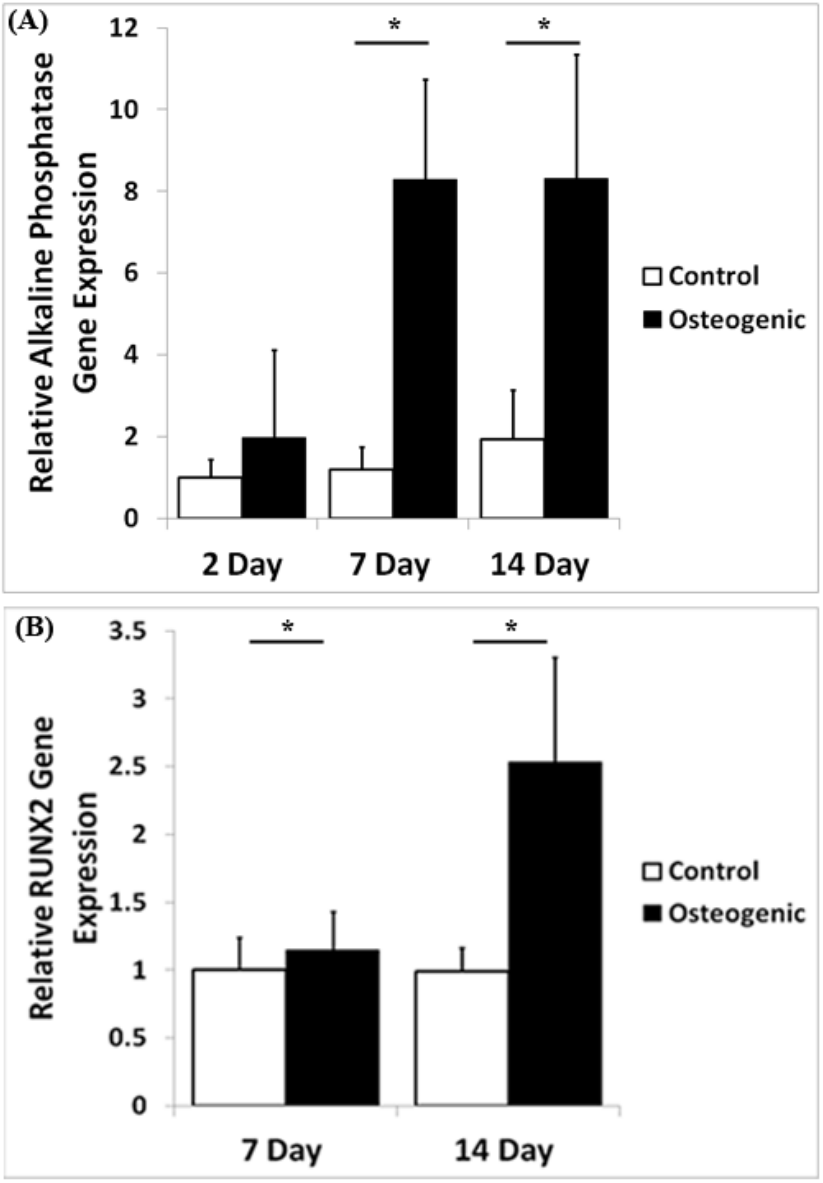

Figure 3.4: Increases in osteogenic gene expression of dental pulp pericytes by induction of differentiation. Alkaline phosphatase (A) and Runx2 (B) mRNA expressions were upregulated in dental pulp pericytes cultured with osteogenic media demonstrated by qPCR. * $p < 0.05$

from human exfoliated deciduous teeth (SHEDs) and showed that these cells are clonogenic and able to differentiate into neural cells, adipocytes and odontoblasts *in vitro* as well as osteogenic and odontogenic cells *in vivo* (Miura et al., 2003). Alliot-Licht et al. have utilized total pulp cells and have shown that a population of α-SMA positive cells can form mineralized nodules *in vitro*, suggesting that the bone/dentin progenitors are perivascular cells (Alliot-Licht et al., 2001; Alliot-Licht et al., 2005). The reports mentioned above suggested that the dental pulp stem cells reside in the perivascular niche.

Our group has recently demonstrated that one of the sources, if not the only one, of mesenchymal stem cells in multiple tissues is the pericyte (Crisan et al.). We now extend this notion and hypothesize that pericytes are, or include, a stem cell population in the dental pulp. However, the dental pulp differs from the tissues investigated in our previous study in that it originates from the neural crest not the mesoderm (Crisan et al., 2008b). Thus in this study, we have aimed to identify that one population of neural crest derived stem cells resides in the perivascular niche and assess how these stem cells compare to pericyte stem cells derived from mesodermal tissues. Our data demonstrated that dental pulp perivascular cells express the pericyte markers CD146, SMA and NG2, but not the endothelial cell markers CD34 and vWF. These data agree with previous studies by our group and others pertaining to the isolation of pericytes from other tissues (Crisan et al., 2008b; Crisan; Peault et al., 2007; Shi and Gronthos, 2003). We have shown that CD146+CD34-CD45-CD56- sorted dental pulp pericytes are highly clonogenic and multipotent, as was also demonstrated for pericytes derived from otherhuman tissues (Crisan et al., 2008b). Cultured pericytes express CD44, CD90

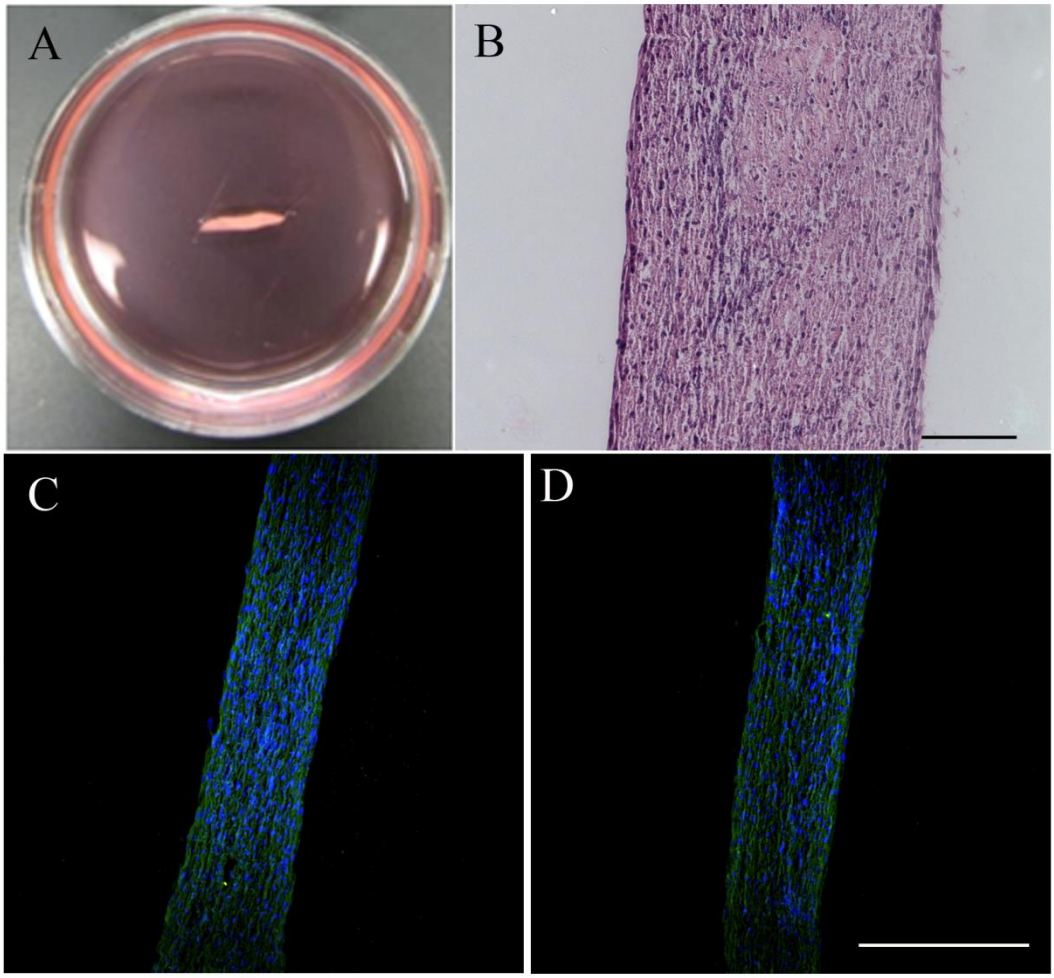

Figure 3.5: Dental pulp pericytes can generate engineered three dimensional dentin-like constructs A- Scaffoldless three dimensional tissue constructs were engineered from dental pulp pericytes in 35 mm diameter culture dishes, B- H and E of shows that cells organize into a solid tissue scale bar = 200 µm. The constructs express dentin proteins such as C- DMP1 (green), DAPI (blue), and D- DSP(green), DAPI (blue) indicating that the engineered tissues are expressing a dentin-like phenotype, scale bar = 500 µm.

and CD166, which also applies to mesenchymal stem cell populations from various tissues (Falanga et al., 2007; Gronthos et al., 2000; Jo et al., 2007; Mageed et al., 2007). This data indicates that pericytes derived from the neural crest behave similarly to those of the mesoderm and also suggests that all mesenchymal stem cells may reside in the perivascular niche.

We have shown that sorted dental pulp pericytes express Runx2 and osteocalcin without induction by osteogenic differentiation factors. This agrees with previous reports showing that perivascular cells naturally have an osteogenic predisposition *in vitro* (Canfield et al., 2000a; Schor et al., 1990). In the presence of ß-glycerolphosphate or dexamethasone, dental pulp pericytes become mineralized in a similar manner as perivascular cells from other tissues such as the retina, brain, epididymal fat pad, skin, lung, placenta and aorta (Bergers and Song, 2005; Doherty and Canfield, 1999; Howson et al., 2005; Peault et al., 2007; Proudfoot et al., 1998). Furthermore, pericytes from bovine retinal microvessels at different stages of differentiation express bone markers such as alkaline phosphatase, Runx-2, osteopontin, osteonectin, osteocalcin and bone sialoprotein (Canfield et al., 2000b; Doherty and Canfield, 1999). The studies above demonstrated the osteogenic potential of pericytes *in vitro*. *In vivo,* bovine retinal pericytes and CD146+CD34-CD45-CD56- sorted pericytes also formed bone (Crisan et al., 2008b). In addition, CD146+ dental pulp cells form ectopic dentin-like tissue in immunocompromised mice (Shi and Gronthos, 2003). Together, these results suggest the potential use of dental pulp pericytes for engineering mineralized tissues such as bone and dentin.

It is currently unclear how engineered tissues vary if regenerated from an isolated population of stem cells or from the total heterogeneous population of cells found in the originating tissue. In this study, we assessed the behavior of dental pulp pericyte stem cells in a 3D self-assembled scaffoldless model. These 3D constructs are formed completely by the cells themselves and therefore are a good model to study cell behavior and tissue assembly. Dental pulp pericytes formed 3D constructs that

expressed dentin proteins uniformly across the tissue. This, however, differs from the type of 3D scaffoldless tissue that forms from the total population of dental pulp cells. Previously, we have shown that scaffoldless self-assembled 3D constructs formed from the total population of dental pulp cells spatially express dentin proteins on the periphery of the construct to form a dentin-pulp complex-like structure (Chapter 2). The formation of these spatially organized tissues is controlled in part by proper cell-cell communication, specifically connexin 43 (Cx43) mediated gap junctions (Chapter 2). It is unknown whether the formation of two organized structures in the constructs engineered from the total population of dental pulp cells is due to spatial cell differentiation or the migration of a certain cell type to the periphery. Neural crestal cells are known for their migratory behavior which is in part controlled by proper Cx43 expression (Huang et al., 1998). Perhaps in the constructs formed from the total heterogeneous cell population, the stem cells are migrating to the periphery of the construct to form a dentin-like structure while the remaining pulp cells continue to form a pulp-like structure in the center. The scaffoldless 3D self-assembled engineered constructs clearly show that tissues regenerate differently when formed from an isolated population of stem cells versus the total heterogeneous population of cells of the originating tissue.

Our data clearly demonstrate that we have successfully isolated pericytes from human adult dental pulp as CD146+CD34-CD45-CD56- cells. This approach provides us with a well-characterized stem cell population of high purity that can be expanded, differentiated, and used to form 3D tissue engineered constructs. Dental pericytes should therefore be amenable to study and develop targeted dental therapies as well as

bone regeneration strategies. Specifically, cellular dental therapies have recently garnered a lot of attention. Dentin, dental pulp, and cementum-periodontal complex regeneration has been shown with DPSCs, SHEDs and periodontal ligament stem cells (Li et al., 2008). Root-periodontal complex regeneration has been shown with cells from apical papilla and periodontal ligament (Sonoyama et al., 2005). Hard tissue formation with rat dental pulp cells has also been shown *in vivo* (Yang et al., 2008). Dental pulp pericytes provide a unique population of stem cells since they originate from neural crest and not the mesoderm. Facial bones undergo intramembranous ossification where they directly differentiate into bone without going through a cartilage template. Using osteoblasts differentiated from dental pulp pericytes will allow the facial anomalies to be replaced with cells that share the same ontogeny. Due to the availability of milk teeth and extracted adult teeth, dental pulp pericytes can provide a convenient source of therapeutic cells to regenerate dental tissues as well as tissues of other mesodermal lineages such as bone, cartilage and fat.

3.6 ACKNOWLEDGEMENTS

I would like to thank Dr. Charles Sfeir and Dr. Pang-ning (Bonnie) Teng for their contributions to this research.

4.0 CHAPTER 4: SELF-ASSEMBLED 3D SCAFFOLDLESS TISSUE ENGINEERED DENTAL PULP CELL CONSTRUCTS FOR ENDODONTIC THERAPY

4.1 ABSTRACT

A major causes of tooth loss following endodontic treatment is the development of caries and loss of marginal integrity of dental restorations, leading to bacterial recontamination of the root canal system. The presence of a vital dental pulp would challenge these bacteria with an immunological response, minimizing bacterial contamination and the development of periapical pathology. In this study, self-assembled scaffoldless three-dimensional (3D) tissues were engineered from dental pulp cells (DPC) and assessed as a device for pulp regeneration. These engineered tissues were placed into the canal space of tooth root segments that were capped on one end with calcium phosphate cement. After 3 and 5 month subcutaneous implantation in mice, empty tooth roots lacking engineered DPC tissues remained predominately empty. Whereas tooth root constructs containing 3D scaffoldless DPC engineered tissues formed a vascular pulp-like tissue through the length of the canal with odontoblast-like cells forming against the dentin wall as seen by dentin protein expression. This study shows that 3D self-assembled scaffoldless DPC tissues can

regenerate a vital dental pulp-like tissue in a tooth root canal system and are therefore promising for an endodontic therapy.

4.2 INTRODUCTION

Regenerative therapies for endodontics would prolong the life of the entire tooth organ. The dental pulp is comprised of connective tissue with fibroblasts, blood vessels, nerves, and a population of stem cells that aid in the repair of the surrounding dentin (Liu et al., 2006). Current endodontic treatments involve the replacement of infected dental pulp with an inert material. Although these treatments have a high degree of success (Friedman et al., 2003), one of the main causes of the future extraction of treated teeth is the formation of caries that potentially could have been repaired by progenitor cells in the pulp (Zadik et al., 2008). Another common complication that necessitates the retreatment of a tooth or tooth extraction is the reintroduction of bacteria in the pulp space through the deterioration of dental restorations (Ray and Trope, 1995; Stockton, 1999; Torabinejad et al., 1990). The presence of a vital pulp would provide a biological defense and maintain interstitial pulp pressure to deter such invasions (Heyeraas and Berggreen, 1999). Also, the surrounding hard tissue of the pulp, the dentin, becomes mechanically altered after an endodontic treatment due potentially to the loss of moisture and interstitial pressure provided by the pulp tissue, which leads to higher fracture susceptibility to the tooth (Akkayan and Gulmez, 2002;

Heyeraas and Berggreen, 1999; Soares et al., 2007). Furthermore, the generation of a vital dental pulp would facilitate continued root development in immature teeth. A tissue engineered dental pulp could replace current methods of endodontic treatment and result in a physiologically functional pulp dentin complex.

A number of dental tissues contain populations of stem cells that could be used for regenerative therapies such as the dental pulp from adult or deciduous teeth, apical papilla, or periodontal ligament (Gronthos et al., 2000; Miura et al., 2003; Seo et al., 2004; Sonoyama et al., 2008). Dental pulp stem cells are able to differentiate to form both dentin and pulp tissues and therefore the combination of these cells with various scaffold materials are currently being investigated for use in endodontic treatments (Gronthos et al., 2000). Commonly used scaffolding materials include calcium phosphates, collagen gels, or polymeric materials due to their similarities with dentin or pulp tissues, and these systems have shown some success in the formation of dentin-like or pulp-like tissues (Cordeiro et al., 2008; Gronthos et al., 2000; Huang et al., 2010; Prescott et al., 2008). However, these methods involve the introduction of exogenous materials that could elicit a host response or adversely induce cell differentiation.

Recently we have engineered self-assembled three-dimensional (3D) scaffoldless tissues from human dental pulp cells (DPC). These samples are formed by culturing cells on dishes to generate cell sheets. These sheets lift from the substrate and are contracted by the cells towards two pins placed in the dish. The tissue sheet self-assembles into a cylindrical 3D engineered tissue that is anchored to the plate by the pins. These 3D tissues are formed by the cells themselves without any exogenous materials; therefore, the cells are able to generate their own preferred

microenvironment. Our previous results have shown that these samples express dentin proteins on the periphery and exhibit pulp properties in the core similar to a dentin-pulp complex after both *in vitro* culture and *in vivo* subcutaneous implantation in mice (Chapter 2).

The goal of this study is to investigate the use of scaffoldless 3D tissues engineered from DPC as a mechanism to regenerate dental pulp-like tissues in the root canals of human teeth. This study assesses the potential of scaffoldless 3D dental pulp cell engineered tissues for an endodontic therapy.

4.3 MATERIALS AND METHODS

4.3.1 Dental pulp cell isolation

Healthy, adult third molars were obtained from the University of Pittsburgh, School of Dental Medicine after routine extraction. All residual soft tissue was removed from the outer regions of the teeth, the teeth were cracked open, and the pulp was removed. The pulp was minced and then digested in an enzyme cocktail containing 3 mg/ml collagenase and 4 mg/ml dispase for 1.5-2 hours at 37°C. The total population of DPCs were plated and expanded in a growth medium (GM) containing Dulbecco's Modified Eagle Medium (DMEM; Gibco), with 20% fetal bovine serum (FBS; Atlanta Biologics), and 1% penicillin/streptomycin (P/S; Gibco). Cells were used at passage 4-5.

4.3.2 Tooth root segment preparation

Adult teeth were collected after extraction at the University of Pittsburgh, School of Dental Medicine. The crowns regions were removed and the roots were cut into radicular segments 5-7 mm in length using an IsoMet low speed saw (Buehler) with an IsoMet diamond blade (Buehler). The root canal space was opened to a diameter of 1 – 1.5 mm. Root segments were then subjected to a series of washes to remove the smear layer and for sterilization. First the roots were soaked in 0.5 M ethylenediamine tetraacetic acid (EDTA) for 1 minute, then rinsed in phosphate buffered saline (PBS) for 5 minutes, and finally soaked in 6.15% NaOCl for 10 minutes. The roots were then washed 3 times in sterile PBS and then soaked again in 0.5M EDTA for 10 minutes. The roots were again rinsed in PBS 3 times. To ensure sterility, the roots were kept incubated in GM at 37°C for 4 days and monitored for microbial growth. One end of each root was sealed with calcium phosphate cement.

4.3.3 Formation and delivery of DPC in three dimensional scaffoldless engineered tissues into tooth roots

Scaffoldless three dimensional samples were prepared from DPCs similarly to previously described (Chapter 2). Briefly, 35 mm diameter tissue culture plastic dishes were first filled with Sylgard 184 silicone elastomer (Dow Corning). The silicone was then coated with 3μg/cm^2 mouse laminin (Invitrogen). DPC were plated onto sample dishes at a density of 200,000 cells/dish in GM with 5 mg/ml L-ascorbic acid (Fisher

Scientific). At cell confluence, 2 minutien pins were placed into the center of each dish approximately 7 mm apart. Additionally, the culture medium was switched to one containing DMEM with 5% FBS, 1% P/S, and 2 ng/ml transforming growth factor beta 1 (TGFβ1). Cell sheets naturally delaminate from the edges of the dished and contract towards the pins to form 3D scaffoldless tissues. Two to four samples were placed into the canal of the tooth root segment prior to implantation.

4.3.4 Animal implantation

Prepared tooth root constructs containing scaffoldless DPC engineered tissues within the canal or kept empty were implanted subcutaneously in immunocompromised Balb/C nude male mice (Charles River). Incisions approximately 1 cm in length were made in the dorsal surface of the back and pockets were created using blunt dissection. Four samples were implanted into each mouse and samples were removed either after 3 or 5 months.

4.3.4 Histology

After extraction, specimens were fixed in 10% formalin for 24 hours. Samples were decalcified in 0.32M EDTA for 2-3 weeks, embedded in paraffin blocks and sectioned longitudinally. Sections were stained with hematoxylin and eosin or used for immunohistochemistry (IHC) using antibodies against dentin sialoprotein (DSP) (LF151, provided by Dr. Larry Fisher, NIH). IHC detection was performed using an EXPOSE IHC detection kit (Abcam).

4.4 RESULTS

In this study, human tooth roots were cut into segments 5-7 mm in length and the canal spaced opened to 1-1.5 mm in diameter as seen in **Figure 4.1a and b**. To enhance the clinical relevance of the model system, a calcium phosphate cement was placed on one end of the root segment to limit the infiltration of host tissue, similar to natural roots that are only open at the apex (**Figure 4.1c)**. These prepared roots were then either implanted subcutaneously in mice with an empty canal space as a control or the canal space was filled with scaffoldless DPC engineered tissues. **Figure 4.1d** shows an image of a 3D scaffoldless tissue engineered from DPC. These cylindrical samples are formed after cells are cultured to confluence and produce sufficient extracellular matrix for cell sheet formation. The sheet lifts from the substrate and contracts towards two pins in the dish to self-assemble into a cylindrical solid tissue. The scaffoldless engineered tissues are 7 mm in length. Our previous studies have shown that that these scaffoldless samples highly cellular, solid tissues (Chapter 2). Additionally, when cultured in an osteogenic medium containing ascorbic acid, dexamethasone, and beta glycerophosphate, these tissues exhibit the properties of a spatially organized dentin-pulp complex-like structure. **Figure4.1e** shows a schematic of the final assembled tooth root construct prior to implantation.

H and E staining of empty control samples after 3 months and 5 months of implantation can be seen in **Figure 4.2**. Some host tissue infiltration is seen from the open end of the root and exhibits an adipose-like morphology as seen in **Figure 4.2b** at 3 months and **Figure 4.2f** at 5 months. However, the majority of the length of the canal

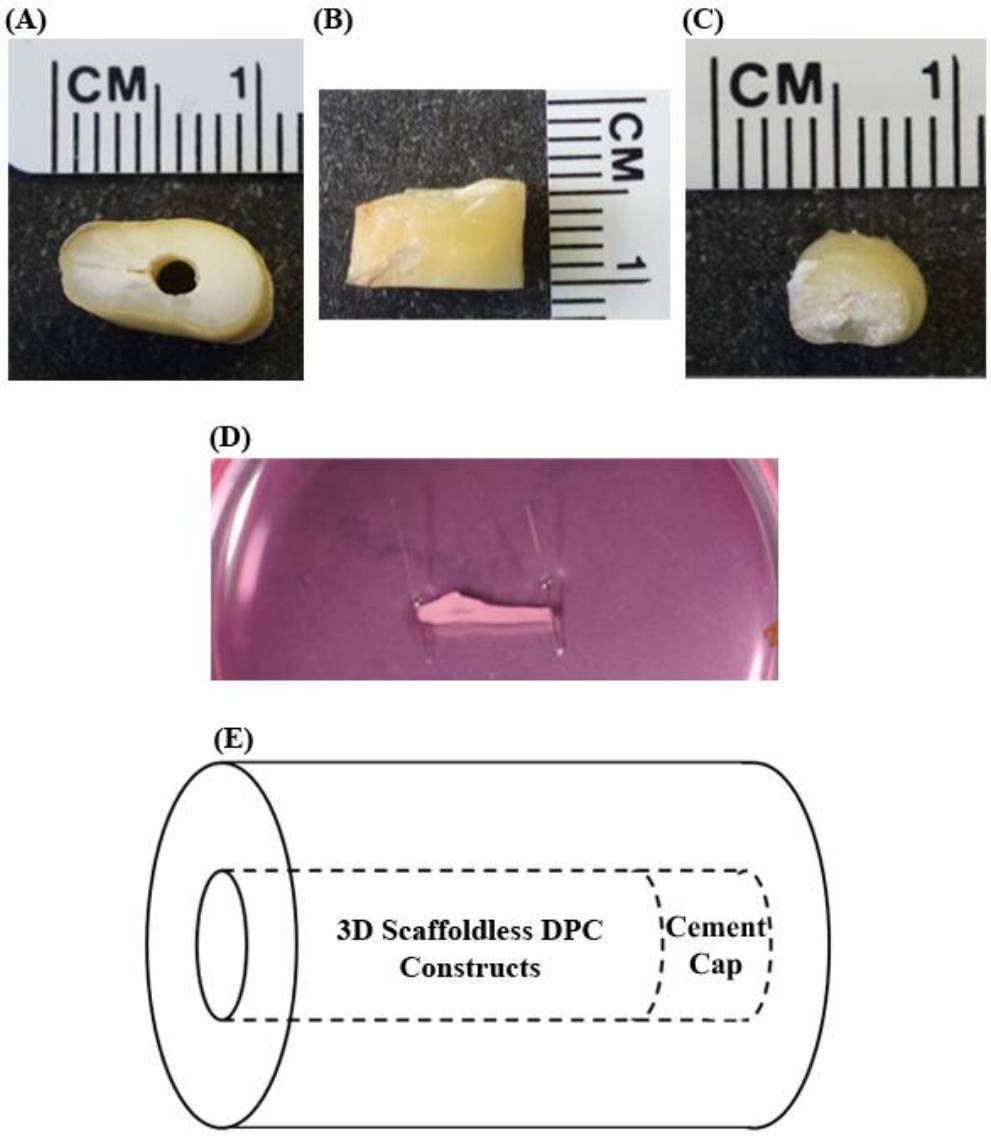

Figure 4.1: Images of tooth root samples from a coronal/apical and proximal view, respectively (A, B), photograph of tooth root from a coronal/apical view with cement cap (C), image of 3D scaffoldless tissue engineered from DPC (D), and schematic of final tooth root construct (E).

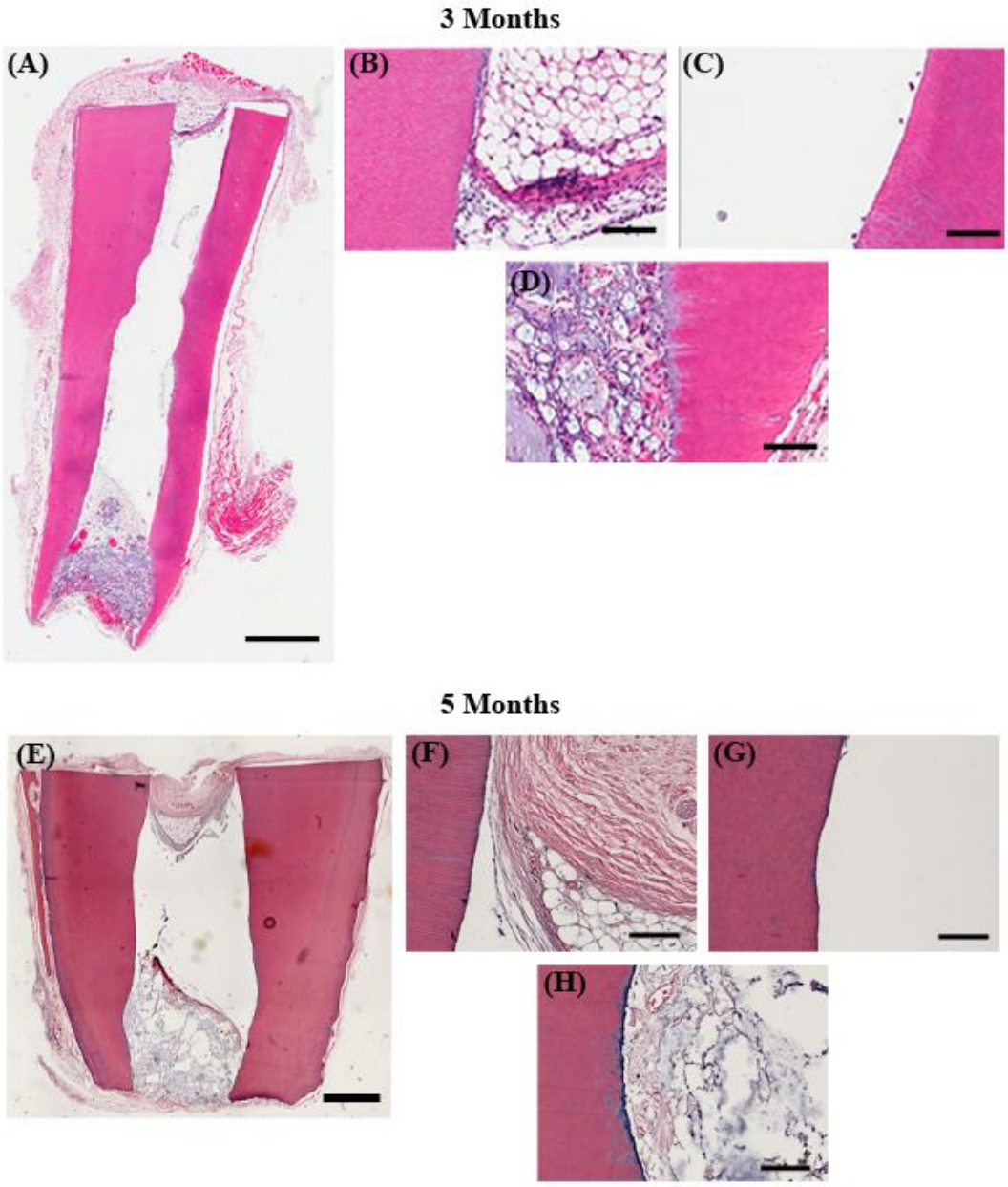

Figure 4.2 Empty tooth root constructs remain empty after 3 and 5 month implantations. Full image of H and E stained section of empty sample after 3 month implantation (A) and higher magnification images of region near the open end of root (B), center of root canal (C), and cement paste (D). Full image of H and E stained section of empty sample after 5 month implantation (E) and higher magnification images of region near the open end of root (F), center of root canal (G), and cement paste (H). Scale bars: A, E = 1 mm, B-D and F-H = 100 μm

space remains empty (**Figure 4.2c and g)**. The calcium phosphate cement supported the infiltration of host cells (**Figures 4.2d and h)**. At 3 months the spaces between the cement particles became highly cellular, and cells lined up along the dentin wall of the human tooth root (**Figure 4.2d**). After 5 months of implantation the tissue still remained in the cement region, but less cement is seen potentially due to cement resorption (**Figure 4.2h**)

Unlike the empty control samples, H and E shows that the tooth root constructs containing 3D scaffoldless DPC samples are filled with a vascular connective tissue throughout the root canal space after both 3 and 5 month implantations as seen in **Figure 3**. These constructs contain an adipose-like tissue near the open end of the root (**Figure 4.3b and f)** which is similar to the tissue seen near the open region of the empty tooth root constructs, therefore this is likely host mouse tissue. The centers of these tooth root constructs are filled with a vascular connective tissue that is adhering to the dentin wall and additionally cells can also be seen lining the dentin wall (**Figure 4.3c and g**). The cement paste cap is filled with cells and tissue **(Figure 4.3d and h)** similar to the empty tooth root samples, however, at 3 months a bone-like tissue formed at the interface of the cement and the scaffoldless DPC tissue indicating that the DPC maintain the potential for hard tissue generation (**Figure 4.3d**), a characteristic of the dental pulp. Immunostaining revealed dentin sialoprotein (DSP) expression at the dentin surface indicating odontoblast differentiation **(Figure 4.4)**. This is similar to natural dental pulp where odontoblasts line the pulp chamber. Together, these data indicate that the scaffoldless DPC constructs generated a pulp-like tissue after being placed into a tooth root.

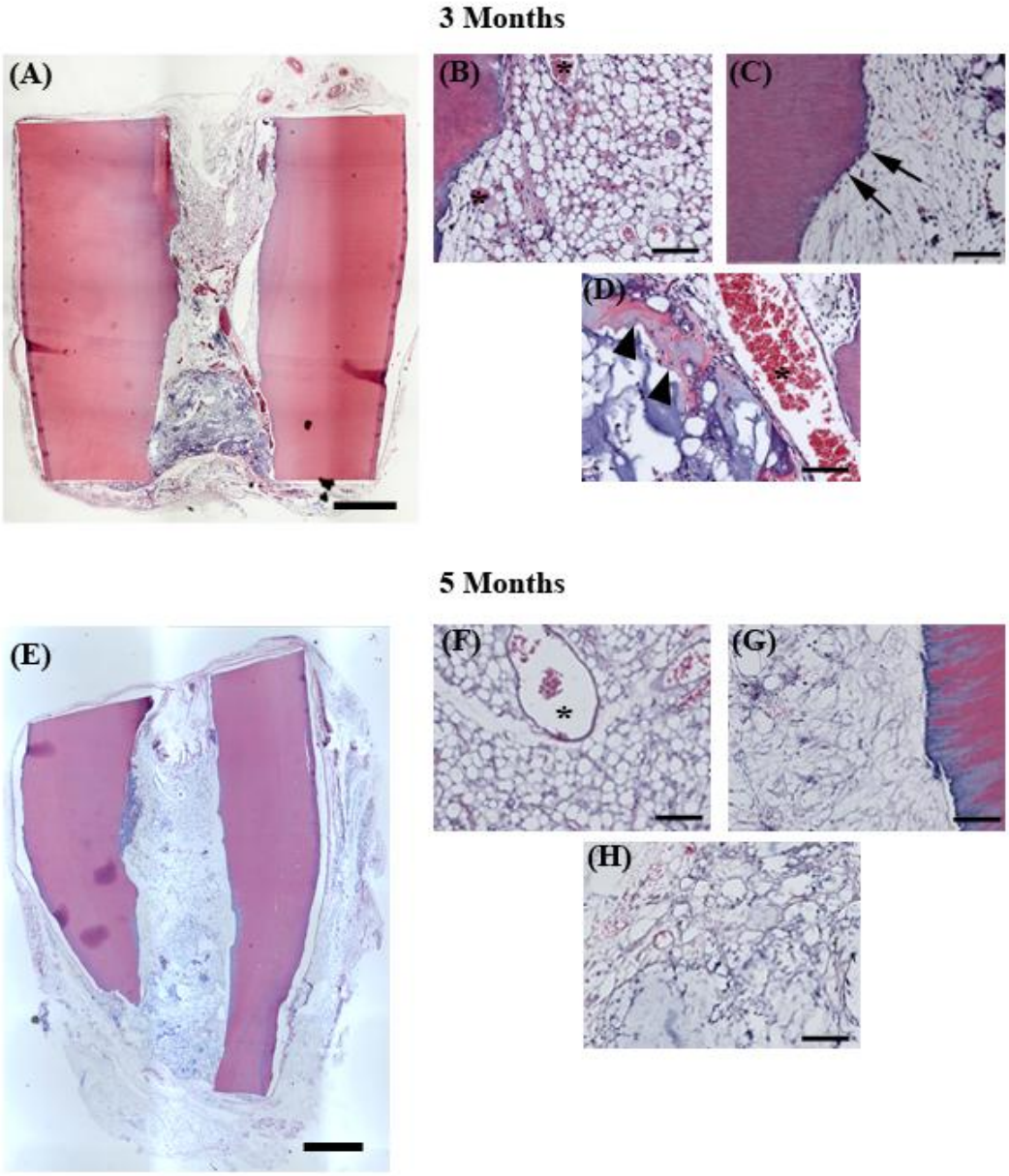

Figure 4.3: Tooth root constructs containing scaffoldless engineered DPC tissues form a vascular connective tissue in root canal after 3 and 5 month implantations. Full image of H and E stained section of tooth root construct containing scaffoldless DPC tissues after 3 month implantation (A) and higher magnification images of region near the open end of root (B), center of root canal (C), and cement paste (D). Full image of H and E stained section of tooth root constructs containing scaffoldless DPC tissues after 5 month implantation (E) and higher magnification images of region near the open end of root (F), center of root canal (G), and cement paste (H). Black arrow show cells lining the dentin, arrow heads show bone, and asterisk indicate blood vessels. Scale bars: A, E = 1 mm, B-D, F-H = 100 μm.

4.5 DISCUSSION

The regeneration of a vital dental pulp tissue during an endodontic treatment would prolong the life of the entire tooth organ. In this study, scaffoldless 3D tissues engineered from human DPC were assessed for pulp regeneration. When inserted within a human tooth root, these samples were able to form a dental pulp-like tissue that was vascular, capable of forming bone-like tissue, and differentiated into odontoblast-like cells against the dentin surface as seen by DSP expression. This study shows that 3D scaffoldless engineered tissues have potential for pulp regenerative therapies.

Different tooth root models have been designed to study dental pulp tissue engineering (Cordeiro et al., 2008; Goncalves et al., 2007; Huang, 2009; Huang et al., 2010). The tooth root constructs used in the current study are based off of the root fragment model described by Huang and colleagues (Huang, 2009; Huang et al., 2010). The tooth root segments in this reported model were dimensionally similar to those used in our current study. The length of the segments ranged between 5-7 mm and one end was sealed to mimic clinical conditions where vascular infiltration into the length of the root canal is only accessible at the apex. Huang et al. used mineral trioxide aggregate (MTA) to seal one end of the root segment whereas a calcium phosphate cement was used as capping material in our current study. Host tissue seemed to readily permeate the calcium phosphate cement therefore this end of the root contained more of a barrier than a seal. However, since the host tissue readily entered and filled the cement, more of a biological seal was created. Ongoing studies are being performed to investigate the use of this cement as a pulp capping material.

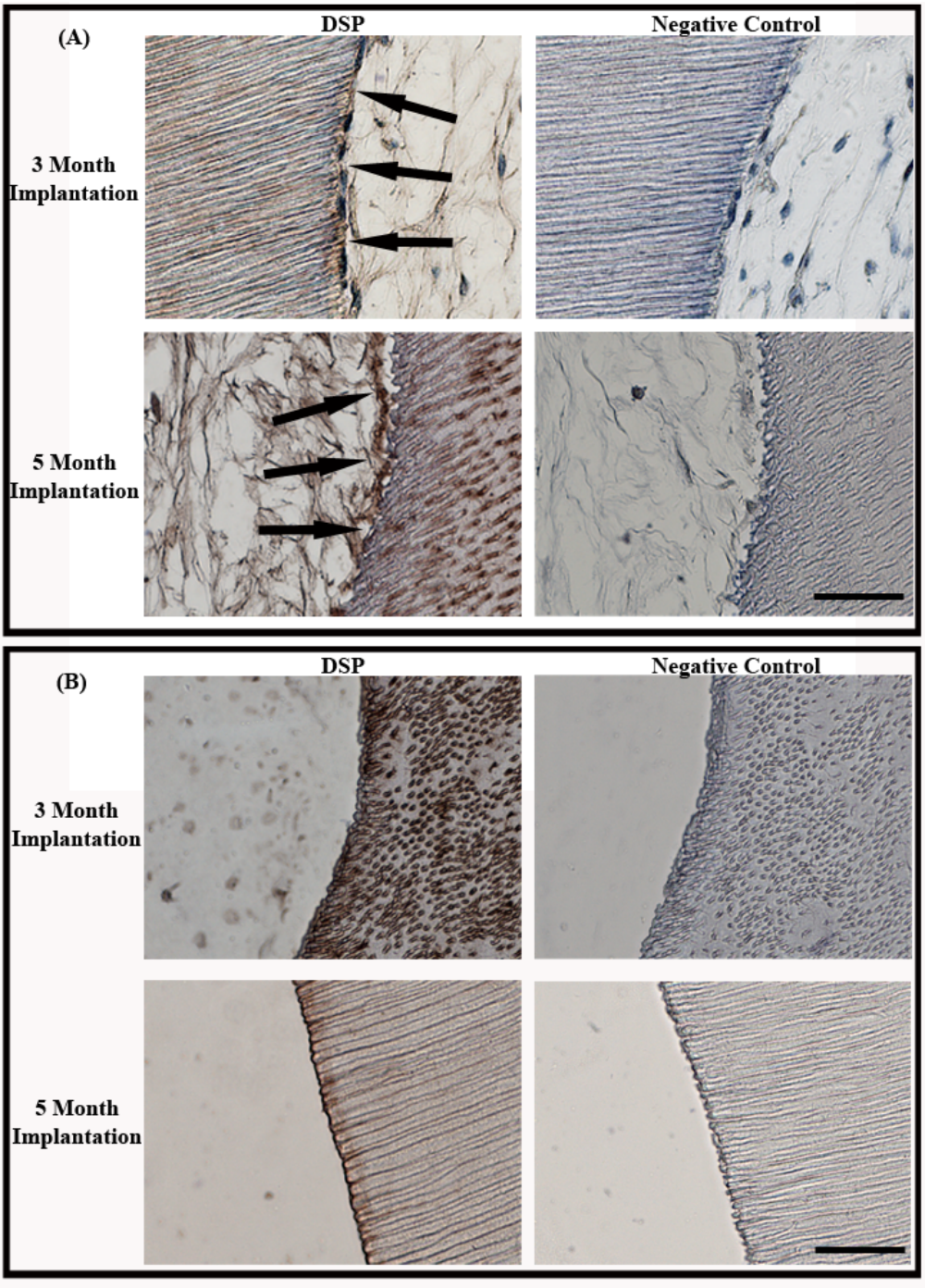

Figure 4.4: Immunostaining indicates strong DSP expression (brown) at interface of dentin and engineered pulp tissue (black arrows) in tooth root constructs containing 3D scaffoldless DPC tissues after 3 and 5 month implantation(A). This was not seen in the empty samples (B). Images are counterstained with hematoxylin (blue) to localize nuclei. Scale bars = 50 µm.

In this study DPCs were transplanted into the root canal space of human teeth via 3D engineered scaffoldless tissues. The cells secreted their own matrix to form an autogenous 3D structure which could then be delivered into the root lumen. Traditionally, cells are combined with exogenous materials before being transplanted into the body to facilitate the formation of a 3D structure, help localize the cells to the region of regeneration, or direct cell behavior. Scaffolds for dental pulp engineering have been designed mainly from polymeric materials (Cordeiro et al., 2008; Goncalves et al., 2007; Huang et al., 2010) or natural materials such as collagen or peptides (Galler et al., 2012; Prescott et al., 2008). However, exogenous materials are far from being able to recapitulate the multifaceted extracellular matrix scaffold that the cells generate for themselves. Other studies have been performed where DPC were cultured in a scaffoldless pellet form and then implanted into amputated pulp in dogs (Iohara et al., 2004). Pellet culture systems are formed by centrifuging cells to form aggregates. Although these systems are also considered to be scaffoldless, the cells are forced into a 3D structure by centrifugation which exerts additional external forces onto the cells that can effect on cell behavior. In our self-assembled system, in addition to producing their own endogenous matrix, the cells arrange their own preferred 3D structure themselves therefore fully controlling their environment and behavior. It has been hypothesized that the delivery of DPCs via aggregated cell sheets, similar to the scaffoldless delivery methods used in the current study, would result in limited cell adherence to the root canal walls and may not support vascular infiltration (Murray et al., 2007). However, in the current study it has been clearly shown that cells delivered

via 3D scaffoldless engineered tissues do adhere to the root canal wall and express odontoblast markers and that blood vessels can indeed penetrate the matrix.

This study shows that self-assembled 3D scaffoldless engineered tissues are a promising method to deliver cells into the root canal for pulp regenerative therapies. This self-assembled scaffoldless system warrants additional evaluation for tissue replacement in pulpotomy models in larger animals to further test its clinical potential.

4.6 ACKNOWLEDGMENTS

I would like to thank Dr. Charles Sfeir, Dr. Herbert Ray and Dr. Kostas Verdelis for their contributions to this research.

5.0 CHAPTER 5: RESORBABLE CALCIUM PHOSPOHATE PARTICLES AS A DENTAL MATERIAL FOR ENDODONTIC THERAPIES

5.1 ABSTRACT

The ideal endodontic material designed to protect an exposed pulp induce dentin bridge formation to prevent future bacterial invasions. In this study, a novel resorbable calcium phosphate cement termed ReCaPP is assessed for this application. Particles of ReCaPP were mixed with human dental pulp cells and placed into the canals of human tooth root segments. After 3 or 5 month subcutaneous implantations in mice, a mixture of dentin and pulp-like tissue formed within the root canals of the constructs. The dentin-like tissue formed tightly along the surface of original root surface generating a biological seal. These data indicate that ReCaPP has great potential as an endodontic material.

5.2 INTRODUCTION

A large focus of endodontics is the protection and maintenance of an exposed dental pulp using procedures such as pulp capping or apexogenesis (Bakland and Andreasen; Parirokh and Torabinejad). These treatments involve the use of dental materials to form a barrier between the vital pulp tissue and the oral flora. However, one of the main causes for the retreatment of the tooth is infection of the pulp from bacterial leakage through the capping material(Ray and Trope, 1995; Stockton, 1999; Zadik et al., 2008). An ideal endodontic material is biocompatible, bonds tightly to dental hard tissues, is able to set in a moist environment, and facilitates tissue growth and dentinogenesis from the pulp cells to induce the formation of a dentin bridge(Chong and Pitt Ford, 2005; Takita et al., 2006). This last requirement is of considerable importance since tissue infiltration and the generation of a dentin bridge creates a biological seal against bacterial invasion to the dental pulp.

Two of the most common materials currently used to treat pulpal complications are calcium hydroxide (CH) and mineral trioxide aggregate (MTA). For several decades, CH has been the main material used to protect exposed pulps. This material is considered to have antibacterial properties due to its high pH which is advantageous in disinfecting the exposure site. This material also facilitates the formation of a dentin bridge. However, CH has poor sealing to dentin or dental resins(Kiba et al.). Additionally, the dentin bridge formed with CH often contains integrated blood vessels. After the dissolution of CH, these vessel spaces become channels for bacterial invasion to the pulp (Bakland and Andreasen). MTA has started being used more recently for

endodontic therapies to overcome some of the limitations of CH. The main constituents of MTA are tricalcium silicate, tricalcium aluminate, calcium silicate, and tetracalcium aluminoferrite (Parirokh and Torabinejad). This material also has antibacterial effect on surrounding tissues and facilitates dentin bridge formation. However, dentin formation occurs faster with MTA than with CH, and contains less vasculature which therefore minimizes future bacterial invasion (Bakland and Andreasen). Although MTA has shown very promising results thus far for endodontic therapies, it does still have some limitations. One of the main disadvantages of MTA is its long setting time of approximately 4 hours (Torabinejad and Chivian, 1999). Additionally, some consider MTA to be difficult to handle for various clinical applications (Parirokh and Torabinejad).

Recently, our lab has created a novel resorbable calcium phosphate cement termed ReCaPP. This cement is more relevant than CH and MTA since calcium phosphate constitutes the inorganic component of vertebrate hard tissues. Thus far this material has mainly been studied for bone regeneration and has shown promising results in promoting hard tissue formation. ReCaPP is easy to handle in that the paste can be simply applied with a spatula or even loaded into a syringe and injected. Additionally, the ReCaPP has a quick final setting time of approximately 25 minutes. The aim of this study is to investigate the potential of ReCaPP as an endodontic material.

5.3 MATERIALS AND METHODS

5.3.1 Dental pulp cell isolation

Healthy, adult third molars were obtained from the University of Pittsburgh, School of Dental medicine after routine clinical extraction. All residual soft tissue was removed from the outer regions of the teeth after which the teeth were cracked open and the pulp removed. The pulp was minced and then digested in an enzyme cocktail containing 3 mg/ml collagenase and 4 mg/ml dispase for 1.5-2 hours at 37°C. The total population of DPCs were plated and expanded in a medium containing Dulbecco's Modified Eagle Medium (DMEM; Gibco), with 20% fetal bovine serum (FBS; Atlanta Biologics), and 1% penicillin/streptomycin (P/S; Gibco). Cells were used at passage 4-5.

5.3.2 Tooth root preparation

Adult teeth were collected after extraction at the University of Pittsburgh, School of Dental Medicine. The root canal space was opened to a diameter of 1 – 1.5 mm. The crowns regions were removed and the roots were cut into radicular segments 5-7 mm in length using an IsoMet low speed saw (Buehler) with an IsoMet diamond blade (Buehler). Root segments were then subjected to a series of washes to remove the smear layer and for sterilization. First the roots were soaked in 0.5 M ethylenediamine tetraacetic acid (EDTA) for 1 minute, rinsed in phosphate buffered saline (PBS) for 5 minutes, and then soaked in 6.15% NaOCl for 10 minutes. The roots were then washed

3 times in sterile PBS and then soaked again in 0.5M EDTA for 10 minutes. The roots were again rinsed in PBS 3 times. To ensure sterility, the roots were kept incubated in GM at 37°C for 4 days and monitored for microbial growth. One end of each root was sealed with ReCaPP.

5.3.3 Delivery of DPC with calcium phosphate particles

DPC cell suspension was added to the ReCaPP particles at a concentration of 5×10^6 cells/ 40 mg calcium phosphate. The cell-ReCaPP mixture was kept on a rotator in a humidified incubator at 37°C and 5% CO_2 for approximately an hour to allow for cell adhesion. The ReCaPP particles with cells were then inserted into the tooth root lumen.

5.3.4 Animal Implantation

Prepared tooth roots containing DPC with ReCaPP cement particles within the canal were implanted subcutaneously in immunocompromised Balb/C nude mice. Incisions approximately 1 cm in length were made in the dorsal surface of the back and pockets were created using blunt dissection. Four samples were implanted into each mouse and samples were removed either after 3 or 5 months.

5.3.5 Histology

After extraction, specimens were fixed in 10% formalin for 24 hours. Samples were decalcified in 0.32M EDTA for 2-3 weeks, embedded in paraffin blocks and sectioned longitudinally. Sections were stained with hematoxylin and eosin or used for immunohistochemistry using an antibody against dentin sialoprotein (DSP; LF151, kindly provided by Dr. Larry Fisher at NIDCR). Antibodies were detected using EXPOSE IHC Detection kit (Abcam).

5.4 RESULTS

DPC were combined with ReCaPP calcium phosphate cement particles and placed into tooth root fragments to assess the potential of this cement for endodontic therapies. Human tooth roots were cut into segments 5-7 mm in length and the canal space opened to a diameter of 1-1.5 mm. One end of the roots was first capped with the ReCaPP paste in an attempt to make the root model more clinically relevant by limiting host tissue infiltration to only one side. The root canal was then filled with particles of the ReCaPP with DPC. **Figure 5.1a** shows a schematic of the samples used in this study. Images of machined root segments prior to and after the addition of cement are seen in **Figures 5.1b and c**. These images show that the canal space was completely filled with the cement.

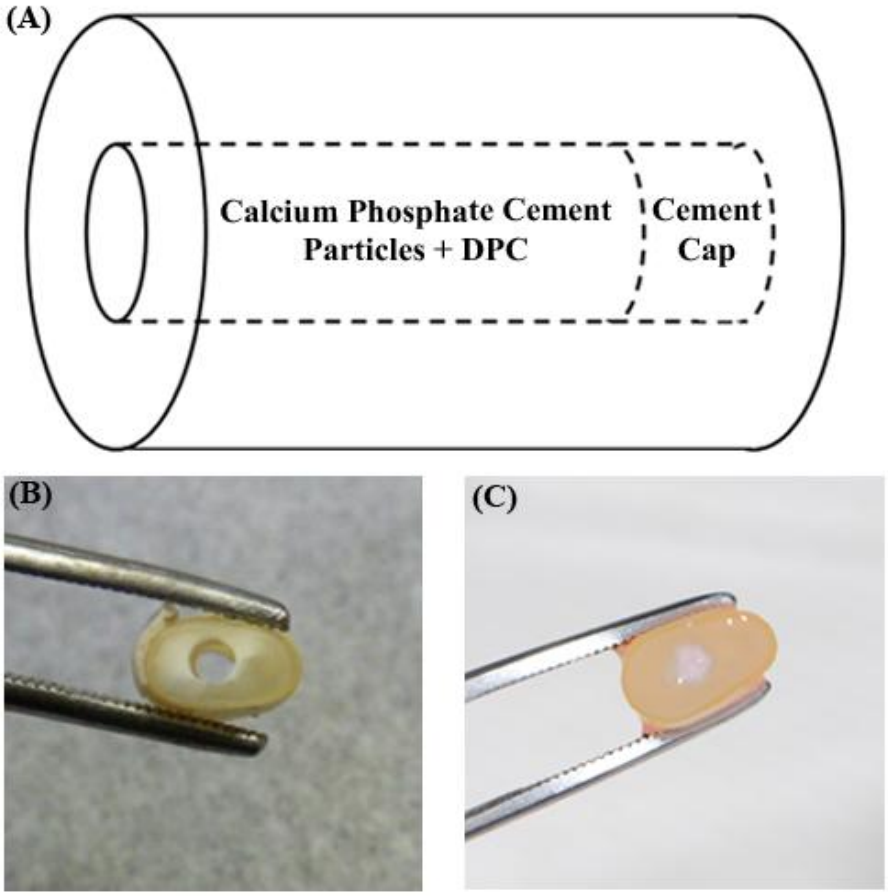

Figure 5.1: Schematic of tooth root construct (A) and images of tooth root segments from an apical/proximal view without (B) and with (C) cement particle in canal.

F**igures 5.2 and 5.3** show images of H and E staining on sections from samples implanted subcutaneously in mice for 3 and 5 months, respectively. The full root canal is filled with tissue (**Figure 5.2a and 5.3a**) in contrast to samples where the root canal was left empty as seen previously (Figures 4.2a and 4.2b). The center regions of these samples are filled with a mixture of dentin and pulp-like tissues (**Figures 5.2b and 5.3b**). Additionally, tissue is seen adhering tightly to the wall of the tooth root segment

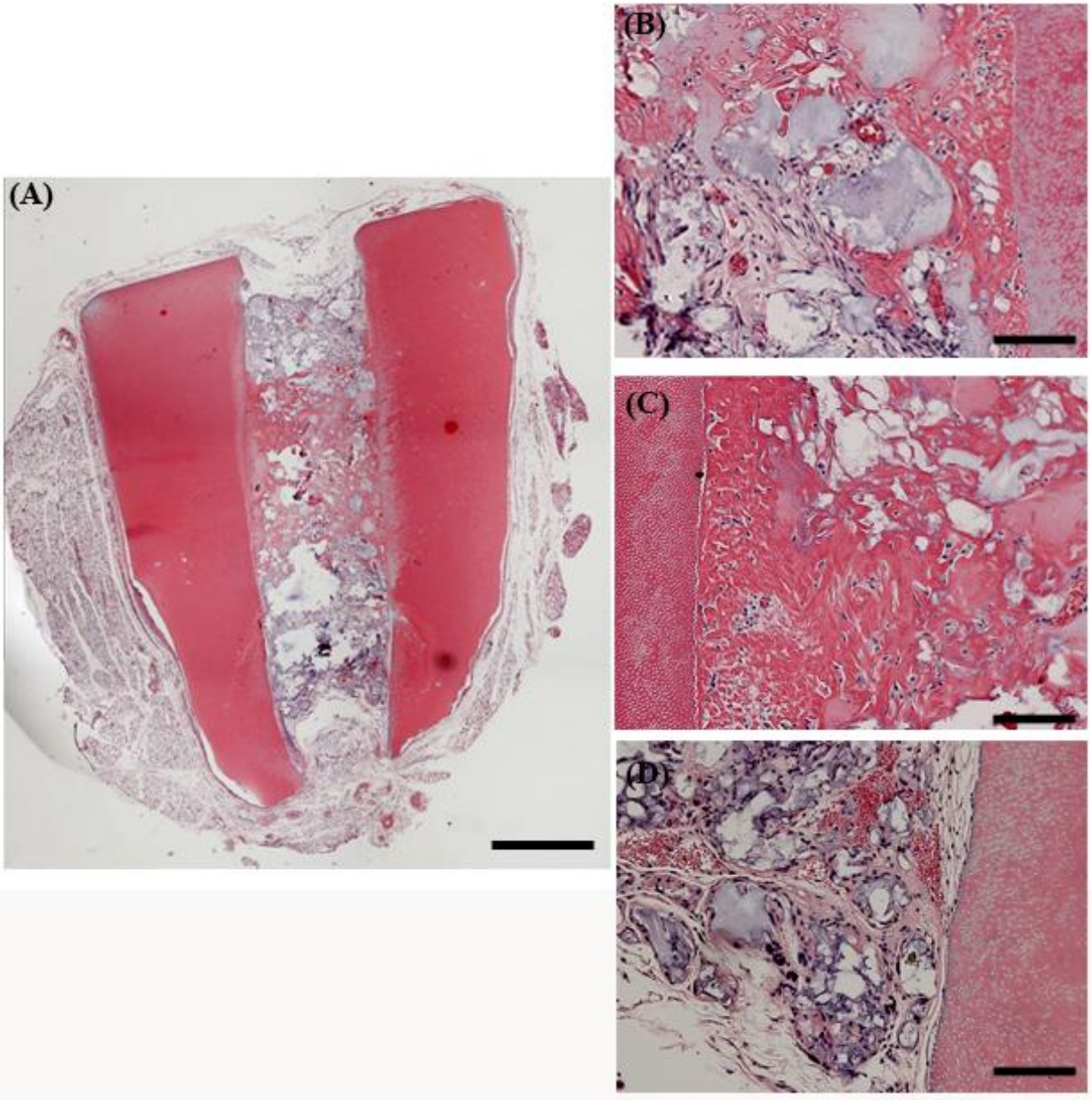

Figure 5.2: H and E of tooth root construct containing ReCaPP particles and DPC after 3 month implantation. Image of full sample (A) and higher magnification showing the formation of dentin and pulp-like tisues (B), dentin forming tightly along the root canal wall (C) and cell and tissue infiltration in the cement cap (D). Scale bars: A = 1 mm, B, C, D = 100 µm.

(**Figures 5.2c and 5.3c**). Lastly, dentin and pulp-like tissue formation are not seen in the ends of the canal that were capped with the cement paste (**Figure 5.2d and 5.3d**). These areas were not loaded with DPC prior to implantation, therefore it is postulated

that the implanted human DPC are critically involved in the formation of the dentin and pulp-like tissues.

To further verify dentin production, immunohistochemistry was used to localize the production of dentin sialoprotein (DSP), an extracellular matrix protein expressed highly in dentin. Cells can be seen expressing DSP in the regenerated tissue in the root canal space after both 3 and 5 months **(Figure 5.4)**.

5.5 DISCUSSION

In this study, a novel calcium phosphate cement called ReCaPP is described that achieves the many requirements of an effective endodontic material. This material will be easily translatable for clinical application due to its ease in handling and quick setting times. Finally, ReCaPP facilitates cell infiltration and induces dentin formation to form a biological seal which is critical to an endodontic material.

It is postulated that the dissolution of calcium based endodontic materials induces dentin bridge formation due to local increases in calcium concentration. Extracellular calcium has been shown to promote osteogenic differentiation in dental pulp cells(An et al., 2012; Matsuoka et al., 1999; Rashid et al., 2003), and we have previously shown that the osteogenic induction of DPC due to increases in calcium concentration is occurring due to modulations of connexin 43 (Chapter 2). The use of a

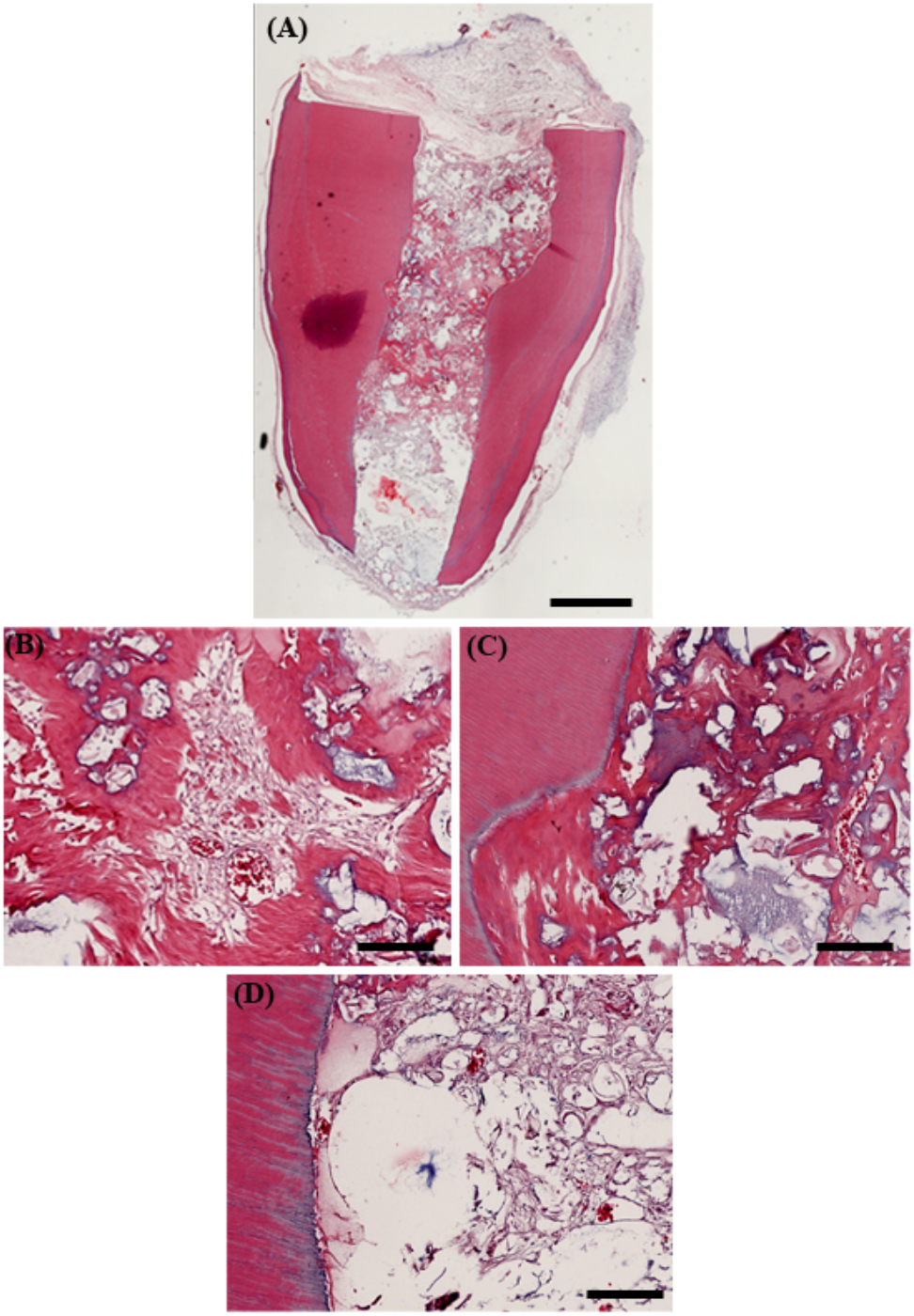

Figure 5.3: H and E of tooth root construct containing ReCaPP particles and DPC after 5 month implantation. Image of full sample (A) and higher magnification showing the formation of dentin and pulp-like tisues (B), dentin forming tightly along the root canal wall (C) and cell and tissue infiltration in the cement cap (D). Scale bars: A = 1 mm, B, C, D = 100 µm.

resorbable calcium phosphate in our current study likely caused the release of calcium and phosphate ions which induced dentin formation. In our previous studies, we showed that DPC delivery using scaffoldless three-dimensional constructs without a material carrier into the root canals of similar tooth root segments regenerated pulp-like tissues

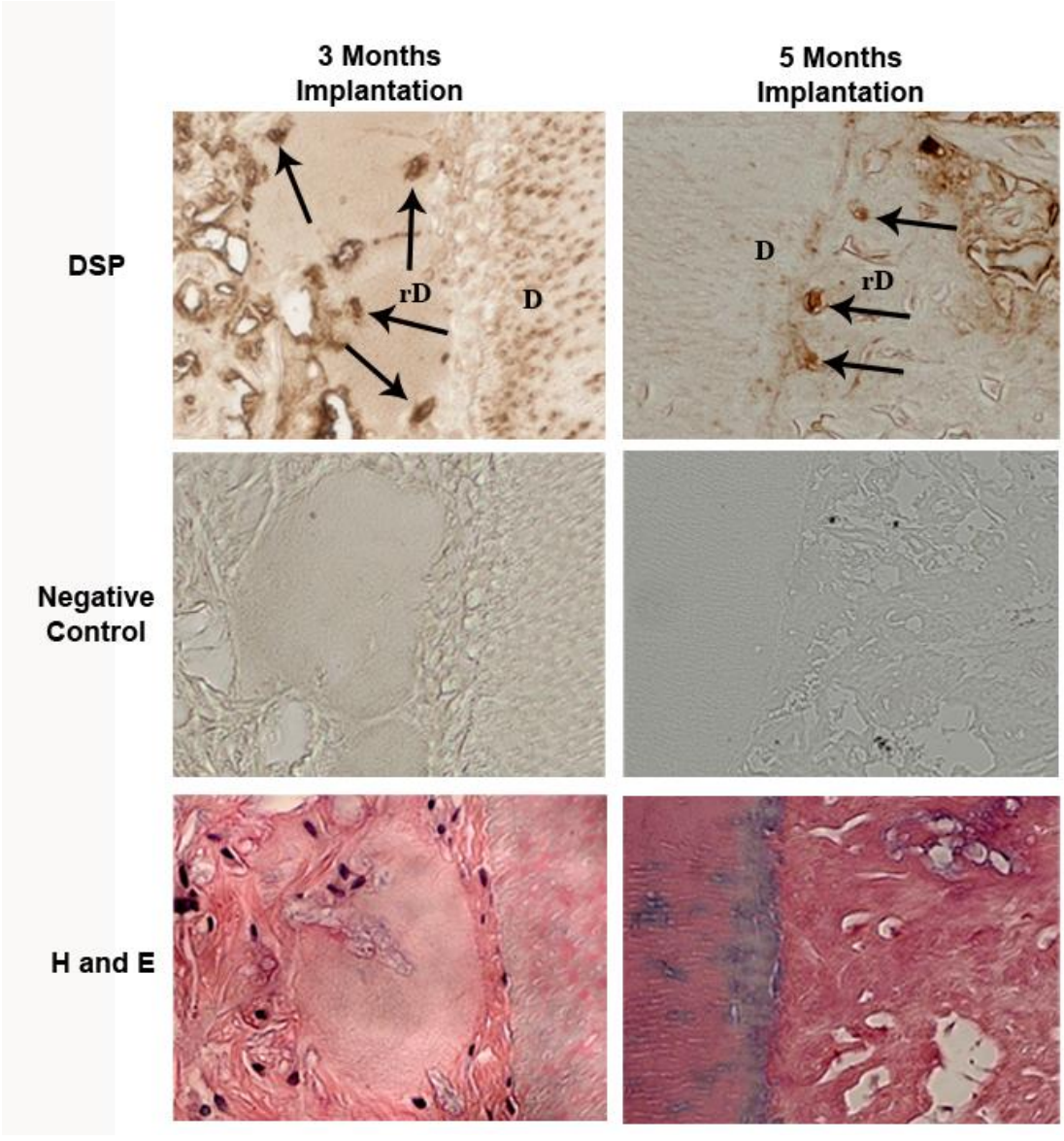

Figure 5.4: Immunostaining for dentin sialoprotein, corresponding negative control images, and matching H and E stained section. Scale bars = 50 μm

throughout (Chapter 4). This further supports that in the current study the ReCaPP is inducing dentin formation from DPC in the root canal system.

The tooth root constructs used in this current study were modeled after the root fragment model described by Huang and colleagues (Huang, 2009; Huang et al., 2010). In our present study we capped one end of the tooth root segment with ReCaPP paste to limit host tissue infiltration to one open end to make the model more clinically relevant since naturally the root canal is only open at the apex. However, ReCaPP did allow cell penetration so instead of generating a seal, more of a barrier was created. These data are intriguing in the sense that since host cells readily infiltrated this material and depositing matrix, potentially when used as an endodontic material, the ReCaPP may support the infiltration of stem cells from any remaining dental pulp in the root or even from periapical tissues. However, for the current investigation, a model system that truly sealed one end of the root canal would have been advantageous. In the original model described by Huang et al., MTA was used as a capping agent and completely blocked the invasion of host tissue. Ongoing are being performed where ReCaPP with or without DPC are transplanted into tooth root segments capped with MTA to evaluate tissue formation in a system with one true open end.

In these experiments, the ReCaPP cement was set, crushed into particles, and mixed with human DPC cells prior to being transplanted into the tooth root construct. These studies provide great preliminary data indicating the potential of ReCaPP as a material that can induce dentinogenesis in a root canal system. Since the current study was performed using set particles of ReCaPP with cells, additional studies are presently being performed with cement particles alone, without the addition of DPC. This aims to

assess host cell infiltration into the material through the entire length of the root canal of the construct. Also, during actual clinical application, likely the ReCaPP will be applied directly in the paste form, prior to setting; additional studies are currently being performed where the ReCaPP paste is being injected directly into the root canal of these constructs.

This study shows that ReCaPP has promise toward being a powerful endodontic material. Additional studies are being current performed using the same tooth root model used here to further assess the potential of this material. These data warrant future studies on ReCaPP in more clinically relevant pulpotomy models.

5.6 ACKNOWLEDGEMENTS

I would like to thank Dr. Charles Sfeir, Dr. Herbert Ray and Dr. Kostas Verdelis for their contributions to this research.

6.0 CHAPTER 6: REGENERATION AND CHARACTERIZATION OF FUNCTIONAL PERIOSTEUM USING CELL SHEET TECHNOLOGY

6.1 ABSTRACT

The presence of a functional periosteum accelerates healing in bone defects by providing a source of progenitor cells that aid in repair. In this study, bone marrow stromal cell (BMSC) sheets were used to engineer periosteal tissues. BMSC were cultured to hyperconfluence and produced sufficient extracellular matrix to form robust tissue sheets. The sheets were wrapped around calcium phosphate pellets and implanted subcutaneously in mice for 8 weeks. Calcium phosphate samples wrapped in BMSC sheets regenerated a bone-like tissue with a functional periosteum-like structure on the outer surface which was characterized morphologically and by periosteum protein expression. Whereas, control samples lacking BMSC sheets did not regenerate these osteogenic tissues. These data indicate that cell sheet technology can be used to regenerate a functional periosteum-like tissue which could aid hard tissue repair.

6.2 INTRODUCTION

There are approximately 6.3 million bone fractures each year in the United States (Stevens et al., 2008). The presence of a functional periosteum has been shown to accelerate bone healing by potentially providing a source of progenitor cells that facilitate repair (Eyre-Brook, 1984; Knothe Tate et al., 2007; Zhang et al., 2008). Periosteal tissue grafting has demonstrated successful results in bone regeneration (Fujii et al., 2006; Puckett et al., 1979; Reynders et al., 1999); however, autologous donor tissue availability is limited, grafting often leads to donor site morbidity, and allografts can transmit disease or elicit an immune response. Therefore, the generation of an engineered functional periosteum-like tissue could aid in bone regenerative therapies.

The periosteum is a connective tissue membrane enclosing bone that serves as an interface between bone and surrounding tissues and provides osteoblasts and precursor bone cells. The periosteum can be characterized through both structural and molecular mechanisms. The cambium layer of the periosteum directly lines the outer surface of the bone and can be morphologically characterized by the presence of cuboidal osteoblasts organized in rows (Allen et al., 2004; Ellender et al., 1988; Marks and Popoff, 1988). Periostin, also known as osteoblast-specific factor-2, is an extracellular matrix protein expressed by periosteal osteoblasts and pre-osteoblasts and is thought to be involved in cell adhesion (Horiuchi et al., 1999). Periostin is found in only a small number of tissues throughout the body and since it is not expressed in

other boney tissues like the bone matrix or endosteum, it can be used as a periosteum specific marker (Horiuchi et al., 1999; Kuhn et al., 2007).

Cell sheet engineering is an emerging technology that is being researched for several tissue regenerative therapies such as myocardial tissue repair (Masuda et al., 2008) and cornea regeneration (Nishida, 2003). This technique involves culturing cells to hyperconfluence and inducing matrix production for the formation of a robust tissue sheet (See et al.). At this point tissue sheets can be either peeled from the dish with forceps or released from the dish if cultured on a thermo-responsive polymer such as poly(N-isopropylacrylamide) (Akiyama et al., 2004). The periosteum is a tissue sheath surrounding the bone; therefore the addition of a cell sheet around a bone defect or regenerative scaffold may provide an avenue for periosteum engineering. Some studies have shown promising results for bone regeneration utilizing cell sheet techniques, however, the formation of a functional periosteum has not yet been structurally or molecularly characterized (Ma et al., 2011; Matsusaki et al., 2009; Ouyang et al., 2006; Zhao et al., 2011).

Bone marrow stromal cells (BMSC) are a promising cell source for bone engineering since they can be easily isolated from autologous tissue and contain a population of adult stem cells with osteogenic capacity (Pittenger et al., 1999). We hypothesized that engineered BMSC sheets can be used for the formation of a morphologically and molecularly relevant periosteum-like tissue. Calcium phosphates comprise the mineral component of vertebrate hard tissues, and therefore these materials are often used for scaffolding for bone regeneration (Hutmacher et al., 2007; Yuan et al., 1998). In this study, calcium phosphate scaffolds were wrapped in cell

sheets formed from human BMSC and the constructs were subcutaneously implanted into mice for eight weeks. The development of bone-like and periosteum-like tissues was histologically assessed.

6.3 MATERIALS AND METHODS

6.3.1 Human bone marrow stromal cell culture

Cadaveric human spinal bone marrow was received from the Donnenberg research group at the University of Pittsburgh. The marrow was plated onto tissue culture dishes in α-Modified Eagle Medium (αMEM) containing 20% fetal bovine serum (FBS, Atlanta Biologicals) 1% penicillin/streptomycin (P/S; Gibco), and 1% L-glutamine (Gibco). The adherent bone marrow stromal cells (BMSC) were expanded and frozen for future experiments. BMSC were used at passages 2-4 for experiments.

6.3.2 Engineered periosteum construct formation

BMSC were plated onto 35mm diameter tissue culture plastic dishes at a density of 200,000 cells per dish. The culture medium contained Dulbecco's Modified Eagle Medium (DMEM; Gibco), with 20% FBS, 1% P/S, 0.013 mg/ml L-ascorbic acid-2-phosphate (Sigma), 10^{-8} M dexamethasone (dex; Sigma), and 2 ng/ml basic fibroblast growth factor (bFGF; Peprotech). Once the BMSCs became confluent, the culture

medium was switched to DMEM with 5% FBS, 0.013 mg/ml L-ascorbic acid-2-phosphate, 10^{-8} M dex, 2 ng/ml bFGF, and 2 ng/ml of transforming growth factor beta 1 (TGFβ; Peprotech). Five days after confluence the cell sheets were wrapped around cylinderica beta tricalcium phosphate scaffolds that had a 3mm radius and a height of 3mm. The constructs were kept in tissue culture media until implantation in mice which was 20-30 minutes after wrapping.

6.3.3 Animal Implantation

All animal studies were approved by the University of Pittsburgh Institutional Animal Care and Use Committee. Cement pellets were subcutaneously implanted into Balb/C nude mice with or without BMSC sheet wrap. An incision of approximately 1cm in length was made through the skin on the dorsal surfaces of the animals and subcutaneous pockets were made using blunt dissection. One construct was placed into each pocket, and two samples were placed into each animal. The constructs were removed from the animals after 8 weeks.

6.3.4 Histology

After being dissected from the animals, the samples were fixed in 4% paraformaldehyde overnight and decalcified in 0.3M ethylenediaminetetraacetic acid (EDTA; Fisher Scientific) for approximately one week. Samples were then embedded and paraffin and sectioned transversely at a thickness of 5 μm. Sections were used for hematoxylin and

eosin (H and E) staining or immunofluorescent staining against periostin (Novus Biologicals). Immunostaining was detected using an EXPOSE immunohistochemistry detection kit (Abcam).

6.4 RESULTS

Tissue sheets were generated from human bone marrow stromal cells and wrapped around cylindrical beta tricalcium phosphate scaffolds. The cement was placed on top of the tissue sheet and the sheet was peeled from the dish using forceps and wrapped around the scaffold (**Figure 6.1**). These constructs were then implanted subcutaneously in mice, and after 8 weeks, bone and periosteum formation was assessed histologically.

Hematoxylin and eosin (H and E) staining shows that control scaffolds lacking tissue sheet wraps supported the infiltration of host mouse cells that generated a dense connective tissue within the scaffold (**Figure 6.2A and B**). The addition hBMSC tissue

Figure 6.1: Images of calcium phosphate before being wrapped with cell sheet (A), as its being wrapped with cell sheet (B), and calcium phosphate scaffold with cell sheet wrap (C) prior to implantation

sheet wraps facilitated the formation of a bone-like tissue around the perimeter of the cement containing osteocyte-like cells (**Figure 6.2C and D**). Furthermore, cuboidal osteoblast-like cells are seen organized in rows on the outer surface of the regenerated bone-like tissue, which is characteristic of a functional periosteum (Allen et al., 2004; Ellender et al., 1988; Marks and Popoff, 1988); this type of structure is not present in control samples.

Immunohistostaining was performed to localize periostin expression to further verify periosteum formation. A layer of tissue on the outer surface of the regenerated bone-like structure strongly expressed periostin in constructs containing hBMSC sheet wraps (**Figure 6.3**). Together, the expression of periostin and the organization of osteoblast-like cells on the outer surface of the bone-like tissue indicate the regeneration of a functional periosteum-like tissue.

6.5 DISCUSSION

In this study we show that cell sheets generated by human BMSC can be used to engineer functional periosteum-like tissues and facilitate bone formation. These findings are significant for bone regenerative therapies since a functional periosteum accelerates bone healing. Furthermore, cell sheet technology can be easily translatable for clinical application since these sheets can be generated from autologous cell sources, such as human bone marrow, without the addition of exogenous materials.

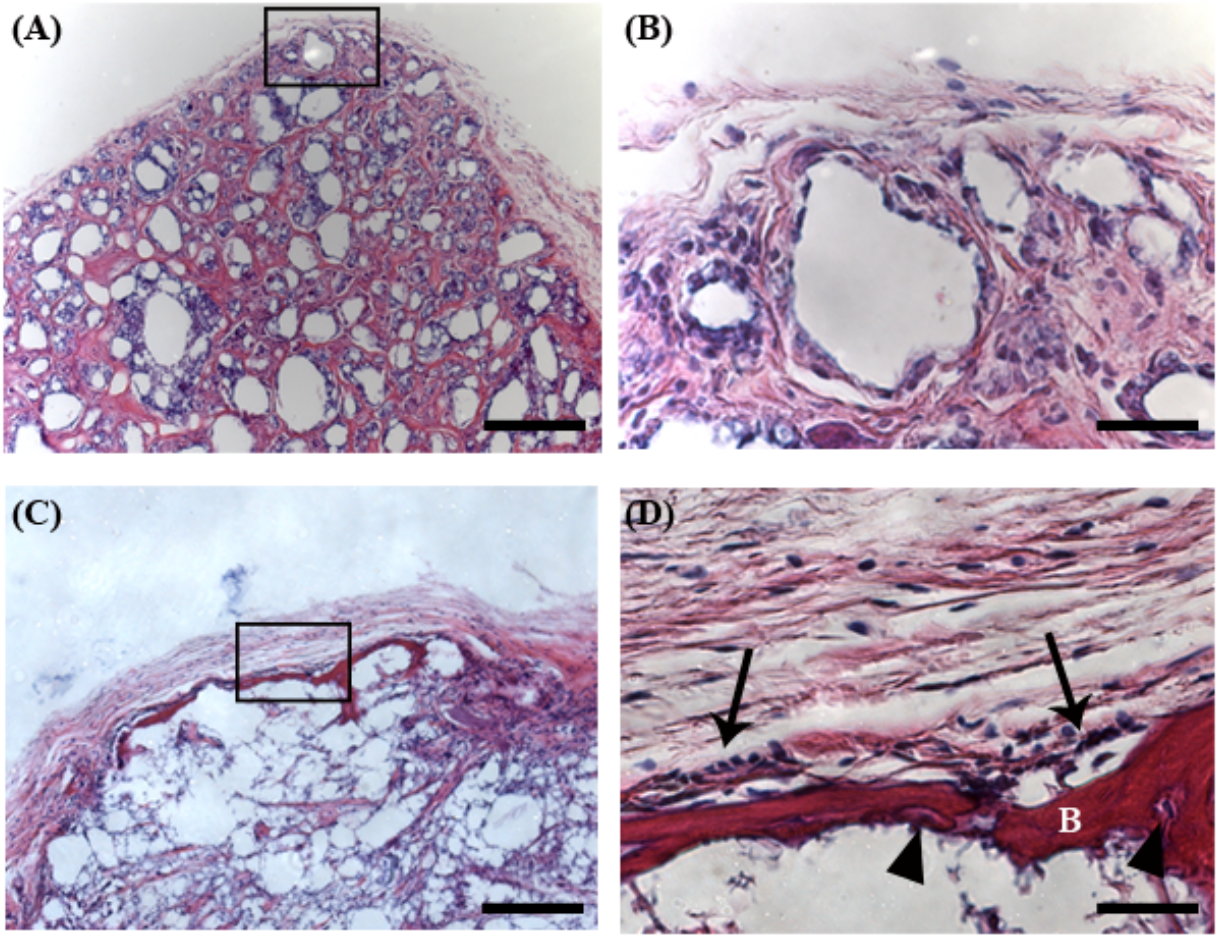

Figure 6.2: H and E staining shows that calcium phosphate scaffolds wrapped with BMSC sheet forms bone -like tissue with a periosteum-like structure on surface. (A) Control calcium phosphate samples lacking BMSC sheet wrap became infiltrated by host connective tissue, higher magnification of boxed area in (A) can be seen in (B) where the edge of control samples are shown to contain a fibrous tissue. (C) Bone-like tissue formed on the periphery of calcium phosphate scaffolds wrapped with BMSC sheet, higher magnification of boxed area in (C) can be seen in (D) where osteocyte-like cells are seen in lacunae in the regenerated bone (arrow heads) and rows of round osteoblast-like cells (arrows) can be seen on the outer surface of the bone-like tissue which is characteristic of a functional periosteum. Scale bars A, C = 200 μm; B, D = 33 μm.

To our knowledge this is the first reporting of the generation and characterization of a functional periosteum-like tissue in an engineered construct. Studies have reported periosteum engineering by combining human BMSC with either collagen gel scaffolding or matrix from small intestinal submucosa, or periosteum engineering using hBMSC

cells sheets (Fan et al., 2010; Ma et al., 2011; Zhao et al., 2011; Zhou et al., 2007). However, the focus of the analyses in these studies was the regeneration and characterization of bone-like tissues, the formation of a functional periosteum was not assessed. Although the formation of bone tissues is of great importance for regenerative therapies, the generation of a functional periosteum indicates that the regenerated bone is the actively forming in a natural manner and signifies continued

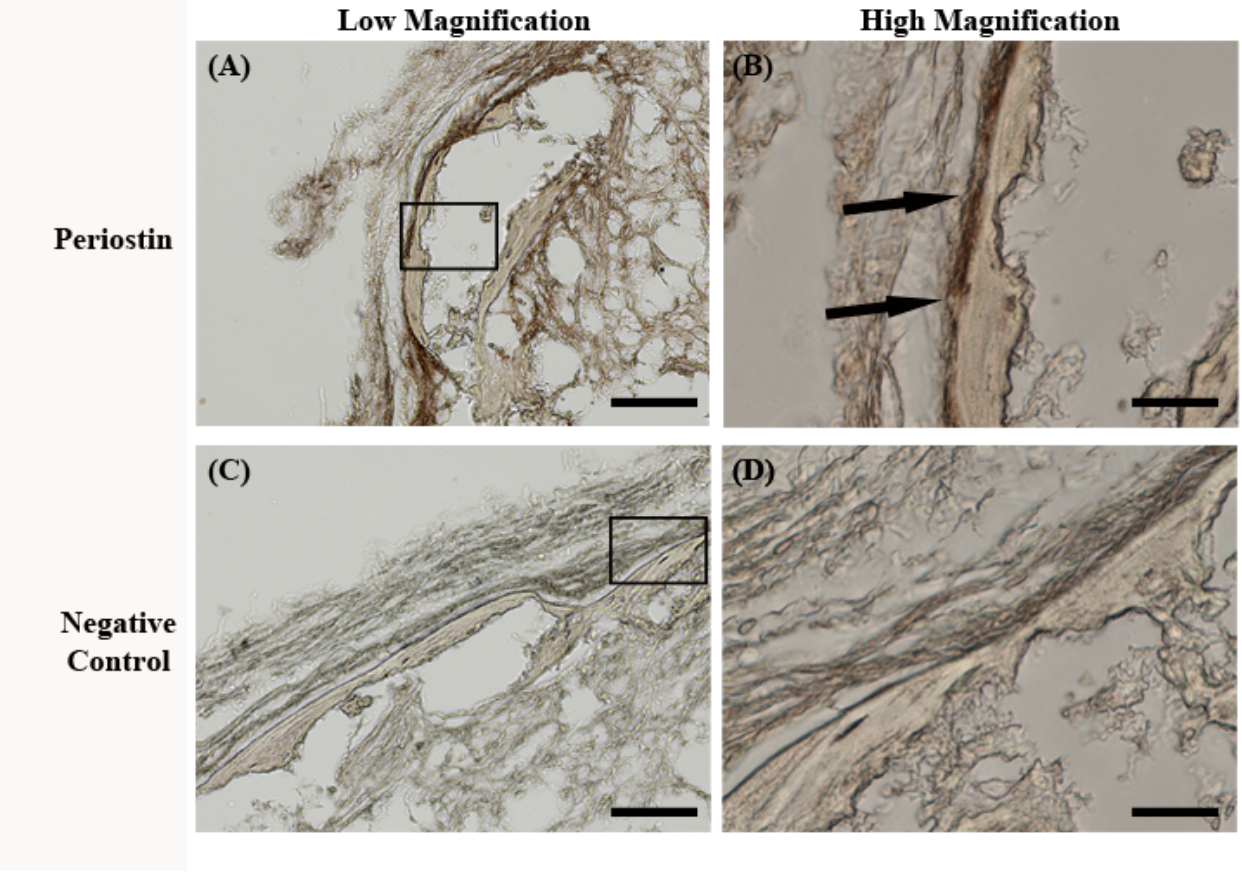

Figure 6.3: Immunostaining was used to localize periostin expression to characterize periosteum formation. (A) Image of edge of cement scaffold containing BMSC sheet wrap is positive for periostin expression (brown) on outer surface of regenerated bone-like tissues, higher magnification of boxed area in (A) is seen in (B) where tissue expressing periostin is tightly wrapping the outer surface of regenerated bone (arrows). (C) Image of negative control staining where primary antibody was omitted is shown, higher magnification of boxed area in (C) is shown in (D). Scalebars A, C = 100 μm and B,D = 33 μm.

radial bone growth. In a previous study, a periosteum-like tissue formed naturally on 3D scaffoldless bone-like construct engineered from rat bone marrow stromal cells and was morphologically characterized by the organization of osteoblast-like cells on the bone surface (Syed-Picard et al., 2009). In our current study the analysis of periosteum formation was similarly morphologically assessed and further verified by protein expression.

Transforming growth factor beta 1 (TGFβ1) has been shown to enhance periosteum formation. Studies have shown that the subperiosteal injections of TGFβ1 in rabbits increased cellularity of the cambium layer of the periosteum which would thereby provide more progenitor cells to bone defects (Olivos-Meza et al.; Reinholz et al., 2009). Additionally, periosteum grafts pretreated with TGFβ1 resulted in increased periosteum thickness in the site of regeneration (Olivos-Meza et al.). Futhermore, TGFβ1 has been shown to increase periostin expression (Horiuchi et al., 1999). In our current study, hBMSC sheets were cultured in the presence of TGFβ1 prior to being wrapped around the calcium phosphate pellets. Potentially, the addition of this factor in the culture medium enhanced the regeneration of a functional periosteum in our construct system.

This study conclusively shows the formation of a regenerated functional periosteum by the combination of a human BMSC sheet with a calcium phosphate cement scaffold. This study shows a promising method of cell delivery and engineered periosteum formation for bone regenerative therapies.

6.6 ACKNOWLEDGEMENTS

I would like to thank Dr. Charles Sfeir and Dr. Gaurav Shah for their contributions to this research.

7.0 CHAPTER 7: CONCLUSIONS AND FUTURE WORK

Traditional tissue engineering methods involve the combination of cells, growth factors and a scaffold to regenerate 3D tissues for therapeutic purposes. Naturally, cells develop and maintain their own 3D structure utilizing their endogenous matrix as a scaffold. The goals of this thesis were to coax cells to form scaffoldless self-assembled 3D constructs as a model to study tissue formation and as a device for dental and bone regenerative therapies. The following are the conclusions that can be drawn from these studies and potential future investigations motivated by these conclusions.

7.1 CALCIUM PHOSPHATES ARE OSTEOINDUCTIVE MATERIALS THAT ALTER CELL BEHAVIOR BY MODULATING CONNEXIN 43 MEDIATED GAP JUNCTIONS

Calcium phosphates are commonly used scaffold materials for hard tissue engineering since they constitute the mineral phase of vertebrate hard tissues. Only recently have some studies started to suggest that these material exhibit osteoinductive properties though the mechanisms facilitating this are largely unknown. In Chapter 2, scaffoldless self-assembled 3D constructs were used as a model to test the hypothesis that calcium

phosphates are osteoinductive and alter cell differentiation patterns and tissue organization in 3D engineered tissues. Scaffoldless 3D constructs produced from the total population of dental pulp cells formed an organized dentin-pulp complex-like structure where the outer periphery of the constructs expressed dentin proteins in contrast to the inner core that did not. The addition of amorphous calcium phosphate particles altered this spatial protein expression by inducing hard tissue protein expression throughout the 3D constructs. These results were seen both *in vitro* and *in vivo*. These data verify that calcium phosphates are osteoinducive materials that alter cell differentiation patterns and tissue organization.

In Chapter 2, we continued to further investigate the molecular mechanism facilitating the osteoinductive nature of calcium phosphates. During natural organ development, spatial tissue organization is dependent on proper cell-cell interactions including gap junctional intercellular communications (GJIC). We showed that amorphous calcium phosphate is altering GJIC, specifically connexin 43 mediated GJIC, and thereby altering cell differentiation patterns. Furthermore, we showed that these changes in connexin 43 expression and gap junction functionality were due to increases in local extracellular calcium concentration due to its release from the amorphous calcium phosphate. These data identify the mechanism of how calcium phosphate is molecularly altering cellular behavior. This study emphasizes the importance of tissue engineering scaffolding materials on cellular behavior and will lead the improved future scaffold design.

It is unknown whether the formation of two organized structures in the constructs engineered without ACP was due to spatial cell differentiation or the increased

proliferation of a certain cell type or the migration of a certain cell type to the periphery. The majority of craniofacial skeletal tissues are derived from neural crest cells. These cells are known for their migratory characteristic which is in part controlled by proper Cx43-mediated gap junctions. Perhaps the pulp stem cells are migrating to the periphery of the construct to form a dentin-like structure while the remaining pulp cell populations continue to form a pulp-like structure in the center. Since the addition of ACP alters Cx43 expression and gap junction formation, it may also be altering the migratory behavior of the DPCs. The addition of ACP may be altering cell migration or differentiation or a combination of both through the modulation of Cx43 expression.

In this study, it was shown that the osteoinductivity of calcium phosphate was due to the release of soluble calcium ions which modulated connexin 43 mediated GJIC. The amorphous calcium phosphate particles used in these investigations are a known degradable form of calcium phosphate (LeGeros, 1993) causing the release of calcium ions. In contrast, a more stable form of calcium phosphate, such as hydroxyapatite, is not degradable and therefore may not produce the similar osteoinductive results. This indicates that resorbable calcium phosphates may be more beneficial materials for hard tissue regeneration.

One of the complications with using calcium phosphates as scaffold materials for regenerative therapies is that they are mechanically brittle and therefore may not be able to withstand the loading environments of many hard tissues. However, in this study we learned that the osteoinductive nature of calcium phosphates is due in part to the release of calcium which induces connexin 43 expression. Potentially, future scaffolds could be designed with more appropriate mechanical properties for hard tissue

regeneration that could also release calcium ions similarly to resorbable calcium phosphates and emulate its osteoinductive nature. However, calcium is known to strongly influence several cellular processes. Since our data showed that the extracellular calcium is influencing connexin 43 GJIC, potentially a different approach is to design a scaffold that released factors known to regulate connexin 43 expression, like parathyroid hormone, TGFβs, bone morphogenic proteins, estrogen, vitamin D, or retinoic acid(Donahue, 2000; Rossello and Kohn, 2009).

7.2 DENTAL PULP PERICYTES ARE A POPULATION OF STEM CELLS THAT REGENERATE STRUCTURALLY DIFFERENT 3D TISSUES THAN THE TOTAL POPULATION OF DENTAL PULP CELLS

Identification of an easily available source of stem cells to repair and regenerate bone and teeth in the craniofacial complex is a clinically important goal for tissue engineering. Stem cells are subsets of the total heterogeneous population of cells comprising their tissue of origin. Currently, it is unknown whether stem cells should be isolated from the remaining population of cells for regenerative therapies or if the total heterogeneous population will provide additional support to the stem cells and enhance tissue assembly. In Chapters 2 and 3 of this thesis, the hypothesis that an isolated population of dental pulp stem cells will regenerate molecularly and structurally different tissues than those generated from the total population of dental pulp cells was tested using scaffoldless 3D self-assembled tissue engineered constructs as a model system. In Chapter 3, scaffoldless constructs were formed from a population of dental pulp cells

(CD146+34-45-56-) that were isolated and characterized as stem cells. These constructs were structurally and molecularly compared to scaffoldless constructs formed from the total population of dental pulp cells described in Chapter 2. Scaffoldless constructs formed from the total population of dental pulp cells regenerated a spatially organized multi-tissue construct that exhibited dentin properties on the periphery and pulp properties in the core; in contrast, the scaffoldless constructs formed from the CD146+34-45-56- population of dental pulp stem cells expressed dentin proteins uniformly throughout. This indicates that a stem cell population from the dental pulp regenerated a structurally and molecularly different 3D tissue than that generated by the total population of dental pulp cells thereby confirming the hypothesis. This study emphasizes the importance of not only tissue selection for the isolation of cells but also the population of cells used for future regenerative therapies.

7.3 SCAFFOLDLESS 3D SELF-ASSEMBLED TISSUES ENGINEERED FROM DENTAL PULP CELLS CAN REGENERATE A PULP-LIKE TISSUE IN ROOT CANALS OF HUMAN TOOTH ROOT SEGMENTS

Endodontic treatments involve the replacement of an infected dental pulp with an inert material. The removal of this vital tissue compromises the health of the remaining tooth organ. We hypothesized that scaffoldless tissue engineered constructs can be used as a device for regenerative dental and bone therapies.. In Chapter 4, we aimed to assess scaffoldless self-assembled 3D constructs engineered from dental pulp cells as a device

for pulp regenerative therapies without the use of calcium phosphate. Human tooth roots were machined into segments 5-7 mm in length, the canal was opened to a diameter of 1-1.5 mm, and one end was capped with a calcium phosphate cement to create a model system to assess tissue regeneration in a root canal space. Scaffoldless tissue engineered constructs generated from dental pulp cells were placed in the canals of these root segments and the entire system was implanted subcutaneously in mice. Our data from these studies indicated that scaffoldless self-assembled constructs have the potential of regenerating a pulp-like tissue in the canal space of tooth root segments. These studies, however, are extremely preliminary in assessing the full clinical translation of the tissue engineered devices. The next steps would include assessing the scaffoldless engineered dental pulp-like tissues in more clinically relevant pulpotomy animal models.

7.4 DENTAL PUPL CELLS DELIVERED INTO THE ROOT CANALS OF HUMAN TOOTH ROOT SEGMENTS WITH A CALCIUM PHOSPHATE CARRIER REGENERATE A MIXTURE OF DENTIN AND PULP-LIKE TISSUES

In Chapter 5, dental pulp cells were delivered with calcium phosphate particles into similar tooth root segments as those used in Chapter 4 to continue testing the hypothesis that scaffoldless tissue engineered constructs can be used as a device for regenerative dental and bone therapies. This study aimed to assess differences when dental pulp cells are delivered with calcium phosphate cement carrier versus within a

scaffoldless construct. Chapter 4 showed that the delivery of scaffoldless dental pulp constructs into the root canal space facilitated the regeneration of a dental pulp-like tissue. However, the data in Chapter 5 indicated that dental pup cells delivered with calcium phosphate results in the formation of a mixture of dentin and pulp-like tissues. These data support that calcium phosphates have a strong influence on cellular behavior and also confirm the hypothesis that regenerated tissues vary with and without the use of calcium phosphate.

The calcium phosphate used in Chapter 5 exhibits features of a promising endodontic material for use in protecting an exposed dental pulp. An important characteristic for materials in this application is the ability to induce formation of a dentin bridge at the exposure site. The generation of a dentin bridge would create a biological seal that will provide additional protection to the pulp in cases where the bacteria eventually leaks through the capping material. Since the data in Chapter 5 showed that the tricalcium phosphate can readily induce dentin formation, this material warrants further investigation as an endodontics material. An ideal enddontics material would also bond tightly with dental hard tissues and prevent bacterial penetration. Future studies required to evaluate the calcium phosphate include dye leakage assays as an assessment for the capacity of the material to block bacterial leakage and assays to measure the bonding of the material to dental hard tissues.

The studies in Chapter 5 evaluated calcium phosphate particles mixed with dental pulp cells and placed in a tooth root model system. Further evaluations of the cement also need to be performed of the cement alone, without the addition of dental pulp cells. This would not only serve as a control to gauge the contributions of the

dental pulp cells, but also provide insight on the behavior of the material alone. The data presented in this chapter have shown that the calcium phosphate particles have great potential for clinical applications and warrant further evaluations in more relevant pulpotomy models in larger animals.

7.5 CELL SHEETS GENERATED FROM BONE MARROW STROMAL CELLS CAN REGENERATE STRUCTURALLY AND MOLECULARLY RELEVANT PERIOSTEUM-LIKE AND BONE-LIKE TISSUES WHEN WRAPPED AROUND CALCIUM PHOSPHATE SCAFFOLDS

The presence of a functional periosteum has been shown to accelerate healing in bone defects (Eyre-Brook, 1984; Knothe Tate et al., 2007; Zhang et al., 2008). The goal of Chapter 6 was test the hypothesis that scaffoldless tissue engineered constructs can be used as a device for regenerative dental and bone therapies. In this study, scaffoldless cell sheets were assessed as a device to engineer a functional periosteum for bone regeneration. In this study, cell sheets were created from human bone marrow stromal cells and wrapped around calcium phosphate pellets. After 8 week subcutaneous implantation in mice, the cement pellets formed bone around the perimeter of the scaffolds with a structurally and molecularly relevant periosteum-like tissue. These data indicate that cell sheet technology have great promise for periosteum regeneration for bone therapies. Furthermore, cell sheet technology can be easily translatable for clinical

application since these sheets can be generated from autologous cell sources, such as human bone marrow, without the addition of exogenous materials. Future studies include using bone marrow stromal cell sheets to regenerate bone in larger animal bone defect models. These include potentially combining cells sheets around scaffolds and implanting in rabbit tibial critical sized defects or using cells sheets alone in non-load bearing critical sized calvarial defects.

The overall scope of this thesis was to use scaffoldless tissue engineered constructs as a 3D model to study tissue formation and cell differentiation and assess these constructs as a devices to for hard tissue regeneration. As a model system, these constructs were able to answer two important questions about the influence of scaffolding on cell differentiation and the regenerative differences of separate cell populations of a tissue. Additionally, these constructs were shown to have regenerative potential for use in endodontics and bone therapies. These studies show the significance of using engineered tissues generated and organized entirely by the cells themselves. The data presented in this thesis emphasize that scaffoldless engineered tissues are powerful tools for dental and bone research and regeneration, and future studies should utilize these systems for additional organ systems.

APPENDIX A:

SCAFFOLDLESS 3D TISSUE ENGINEERED DENTAL PULP CELL CONSTRUCT FOR CALVARIA REGENERATION

The following are results and conclusions from a set of experiments to assess the behavior of self assembled 3D scaffoldless dental pulp cell constructs in mouse calvarial defects. Two types of defects were created. The first defect type was circular critical sized defects (5 mm in diameter for mice) and the cylindercal scaffoldless samples were placed across the diameter of the defect (Figure A1(a)), this model was to assess if the scaffoldless constructs could regenerate a bone-like tissue when not directly surrounded by bone tissues. One critical sized defect was created per mouse. The second defect type created was slightly larger than the scaffoldless sample. This was used to assess if a scaffoldless construct could repair a hard tissue defect of similar size with the support of surrounding hard tissues. Two defects were formed per mouse, one was kept empty and the other was filled with a scaffoldless sample (Figure A1(b)).

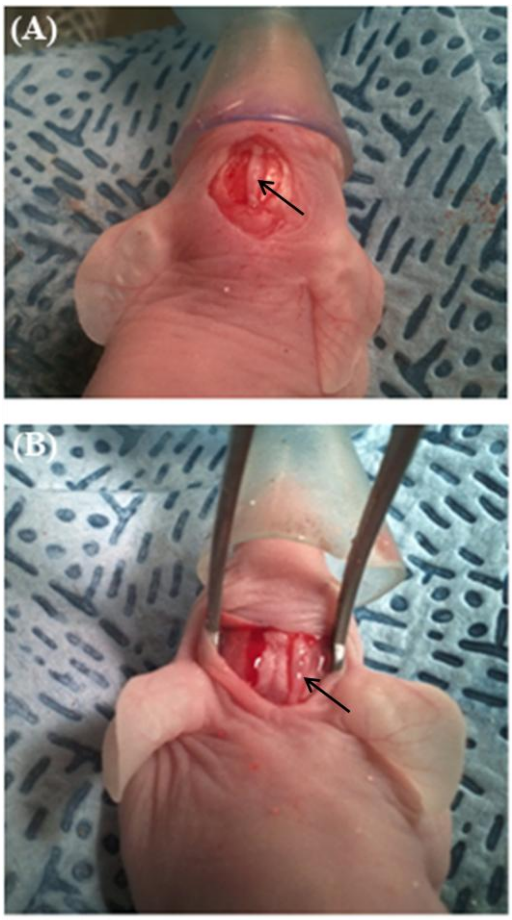

Figure A1: Images of mouse calvaria with circular critical sized defect (A) and defects with similar size as scaffoldless engineered tissues (B). Black arrows point to scaffoldless constructs.

Critical Sized Calvarial Defects

Micro computed tomography (microCT) was performed through the duration of the study. Figure A2 shows images of three dimensional reconstructions of the calvaria at 0 and 8 week time points of empty control defects (Figure A2(a)) and defects containing scaffoldless samples (Figure A2(b)). Ectopic mineral formed above calvarial bone outside of the defect in regions where scaffoldless samples would have been

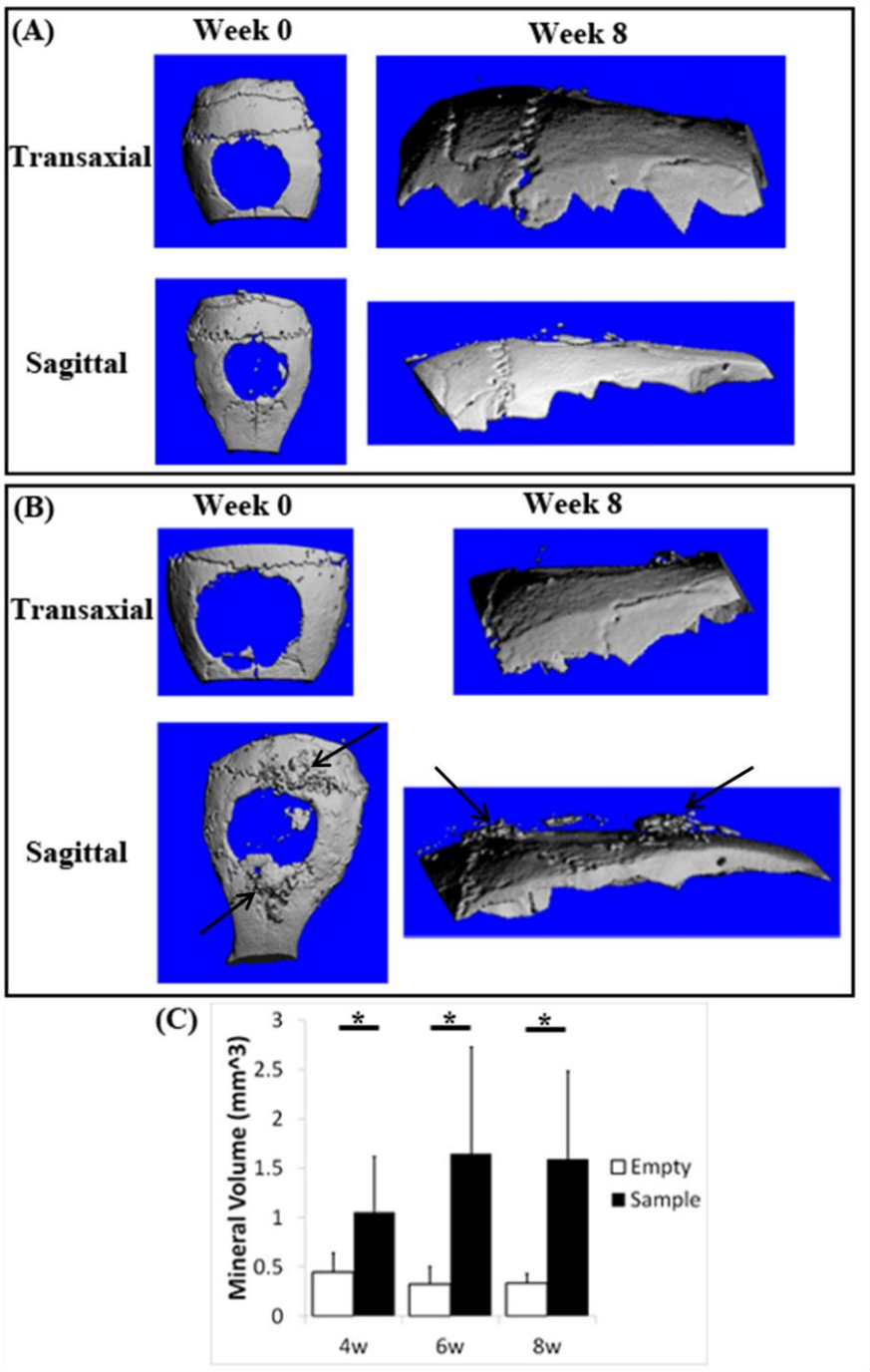

Figure A2: 3D microCT reconstruction of empty critical sized calvarial defects (A) and critical sized defects containing scaffoldless constructs (B) at 0 and 8 week timepoints, black arrows point to mineral formation above calvarial bone outside of the defect space. Quantification of mineral volume in defect space or above calvarial bone outside of defect (C). * $p < 0.05$

overlapping. The volume of mineral in the defect region or above the calvaria just outside the defect was quantified in all samples, and a significant increase was seen in mice containing scaffoldless constructs (Figure A2(c)).

Hematoxylin and eosin staining of sagittal sections revealed that empty defects did not regenerate any hard tissues and formed a thin connective tissue in the defect after 4 (Figure A3 (a-d)) and 12 (Figure A4 (a-d)) weeks. Scaffoldless constructs still remained in critical size defects after 4 (Figure A3 (e-h)) and 12 (not shown) weeks. At 4 weeks, bone-like tissue formed underneath the sample (Figure A3 (h)), and at 12 weeks the mineral that formed above the calvaria outside the defect is seen as bone-like (Figure A4 (g, h)). Immunohistochemistry showed that the cells in the scaffoldless construct seen at 4 weeks expressed the human specific, nuclear protein Ku80, which confirms that the location of the implanted scaffoldless tissue and that the human dental pulp cells remained in the engineered tissue (Figure A5 (a)). However, the bone beneath the samples at 4 weeks (Figure A5 (a)) and above the calvaria just outside the defect at 12 weeks (Figure A5(c)), do not express Ku80 indicating their formation from host mouse cells. Figure A5(e) indicates that scaffoldless tissue expressed a hard tissue protein throughout, dentin matrix protein 1 (DMP1).

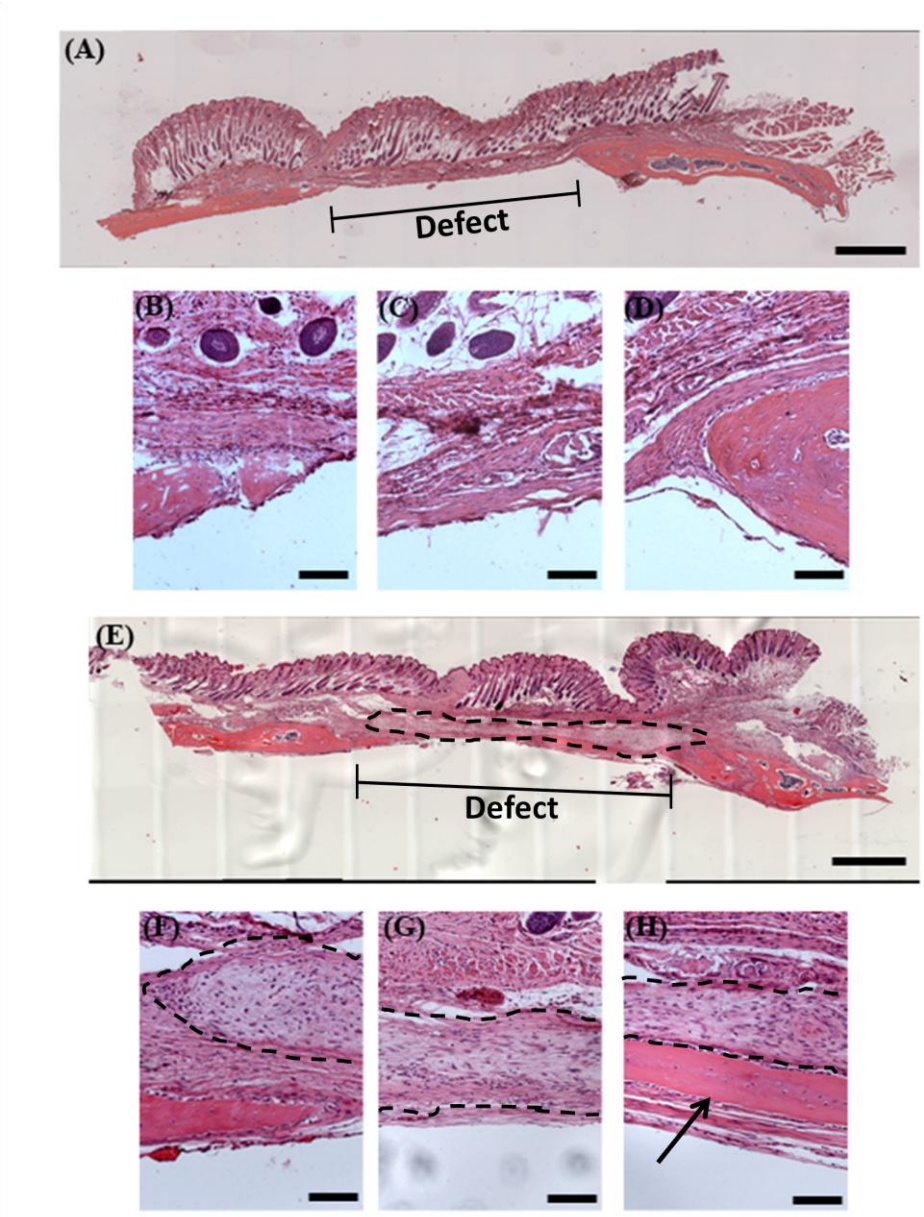

Figure A3: H and E of critical sized defect after 4 weeks. Image of full sagittal section of empty critical size defect (A), and higher magnifications of the left region (B), center (C) and right region (D) of the defect. H and E of full sagittal section of critical size defect with scaffoldless construct (E) and higher magnifications of left region (F), center (G) and right regions (H), dotted lines outline scaffoldless engineered tissue, and arrow points to bone forming beneath engineered tissue. Scale bars: A, E = 1 mm; B-D, F-H = 100 μm

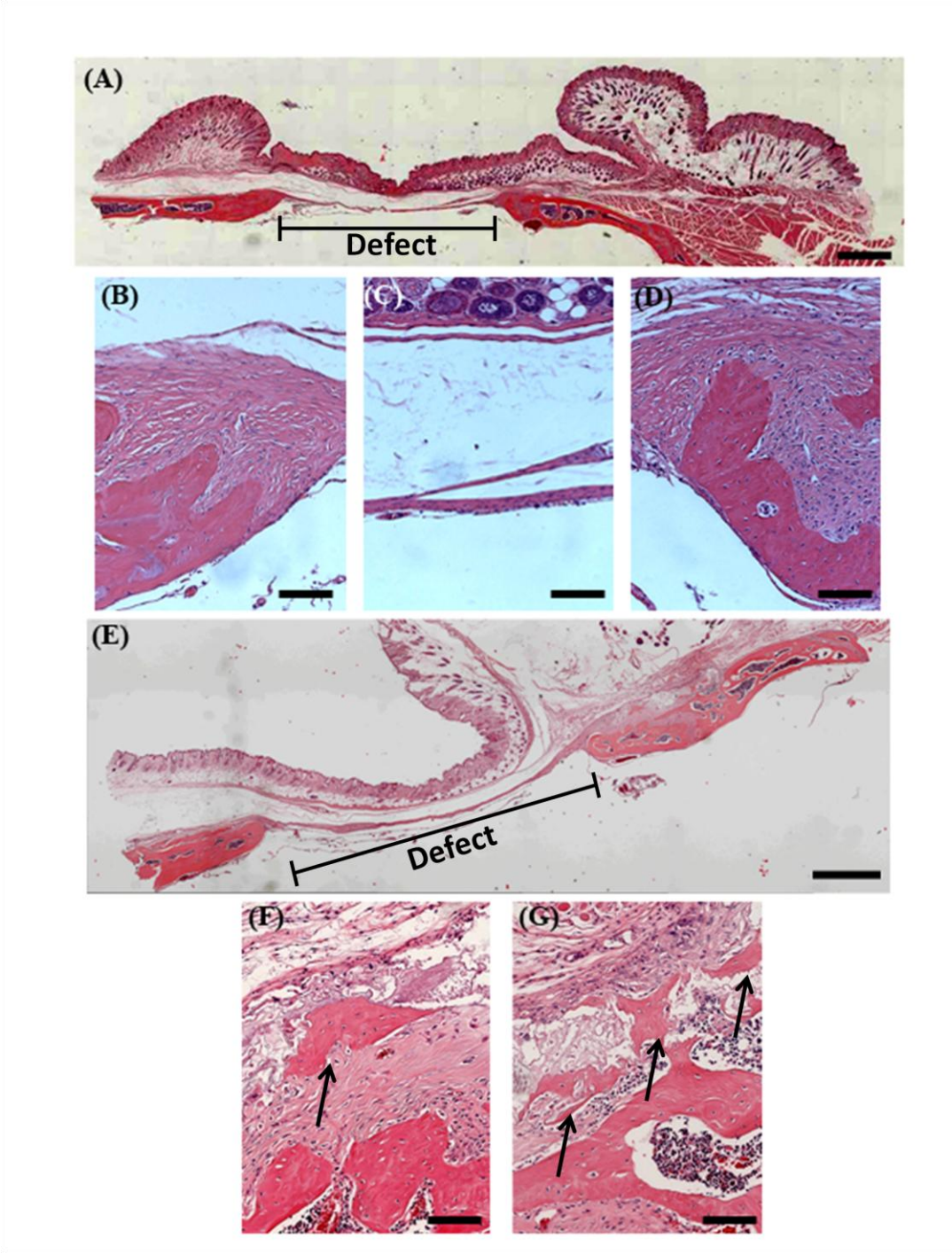

Figure A4: H and E of critical sized defects after 12 weeks. Image of full sagittal sections of empty critical size defect (A), and higher magnifications of the left region (B), center (C) and right region (D) of the defect. Image of full sagittal section of critical size defect with scaffoldless construct (E) and higher magnifications of regions above calvaria outside right side of defect (F and G) showing ectopic bone formation (black arrows). Scale bars: A, E = 1 mm; B-D, F, G = 100 μm

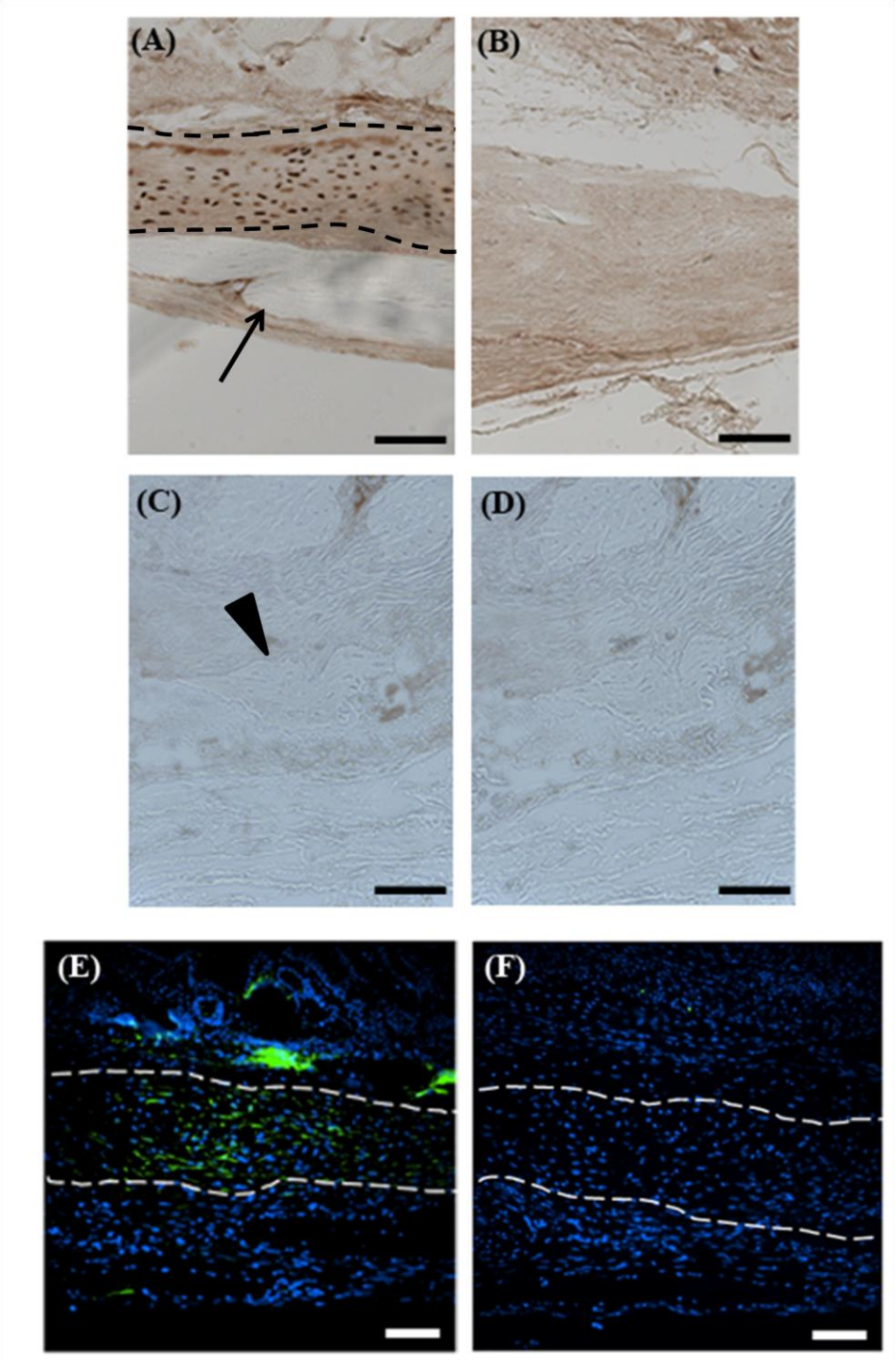

Figure A5: Immunostaining of critical sized defects containing scaffoldless constructs. Constructs (black dashed outline) seen after 4 week implantations express Ku80 (brown), a human specific nuclear protein, but the bone beneath the sample does not (arrow) (A) when compared to negative control (B), bone (black arrow head) formed above calvaria just outside defect at 12 weeks does not express Ku80 (brown) (C), when compared to negative control (D). Scaffoldless constructs (outlined with dashed white line) at 4 weeks express DMP1 (green) (E), when compared to negative control (F), DAPI nuclear stain is blue. Scale bars = 100 mm.

Calvarial Defects Slightly Larger than Scaffoldless Constructs

MicroCT reconstructions of the mouse calvaria with defects similar in size as the scaffoldless constructs show mineral formation over defects containing scaffoldless constructs at 8 weeks (Figure A6). H and E staining of coronal sections of the calvaria show both the empty defect and the defect with scaffoldless constructs at 4 (Figure A7(a-c)) and 12 (Figure A7(d-g)) weeks. The empty defects formed a thin connective tissue across opening, and scaffoldless engineered tissues are still present in their respective defects at both time points. At 12 weeks, defects containing scaffoldless constructs formed mineralized tissues protruding from the neighboring bone tissue (Figure A7(f,g)). Immunostaining for Ku80 show that human cells are still present in the scaffoldless constructs at 4 and 12 weeks (Figure A8(a,b)) and that these constructs are

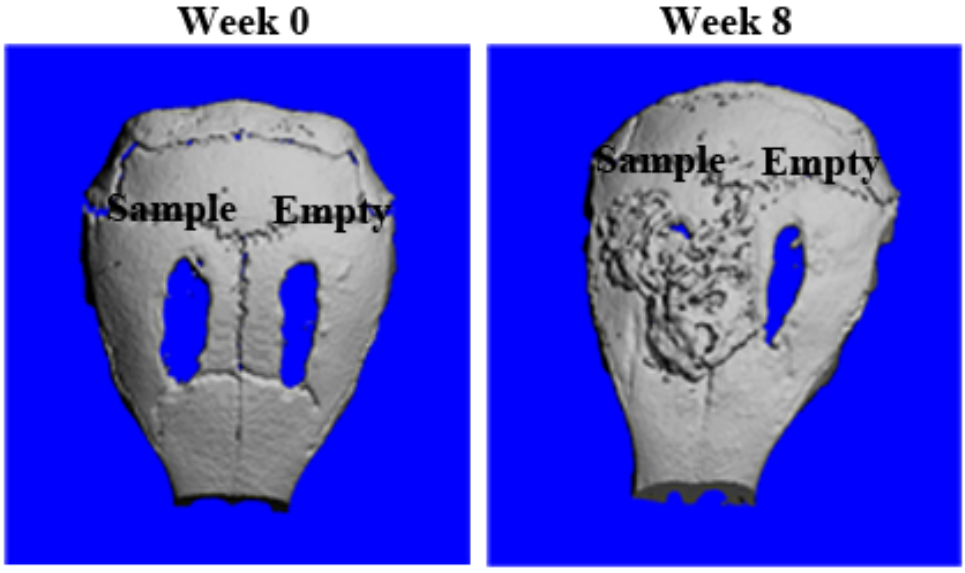

Figure A6: 3D microCT reconstruction of calvarial defects that are similar in size to scaffoldless construct at 0 and 8 week timepoints.

expressing DMP1 (Figure A8(c,d)). However, the regenerated bone lacks Ku80 expression indicating that the bone formed from host mouse tissue.

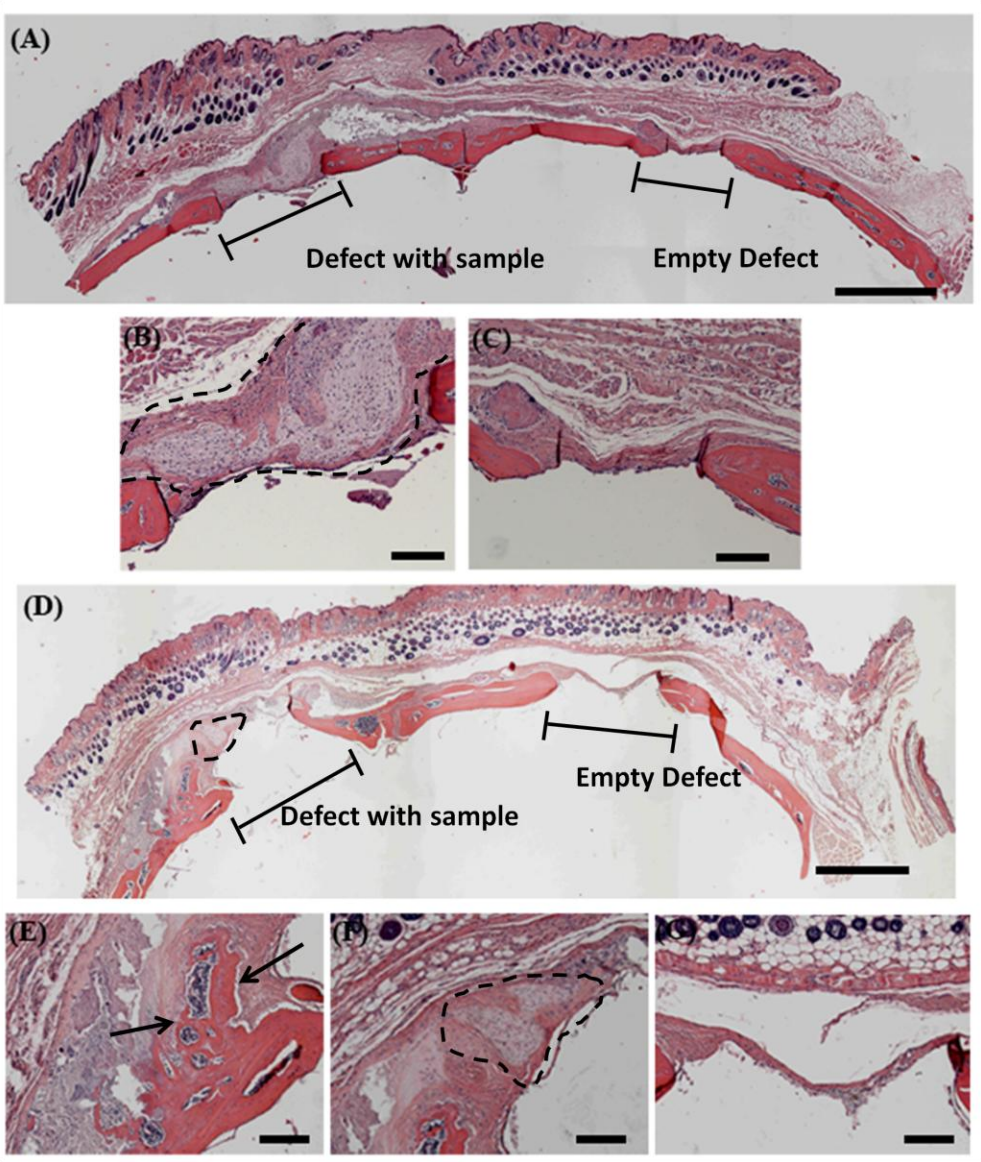

Figure A7: H and E of calvaria with defects similar in size to scaffoldless constructs. Image of full coronal section after 4 weeks (A) and higher magnifications of region with sample (outlined in dotted black line) (B), and empty defect (C). Image of full coronal section after 12 weeks (D) with sample outlined with dotted black line and higher magnification of region with scaffoldless sample (E, F) with sample outlined with dotted black lines and arrows pointing at regenerated bone, and higher magnification of empty defect (G). Scale bars: A, D = 1 mm; B, C, E-G = 100 mm

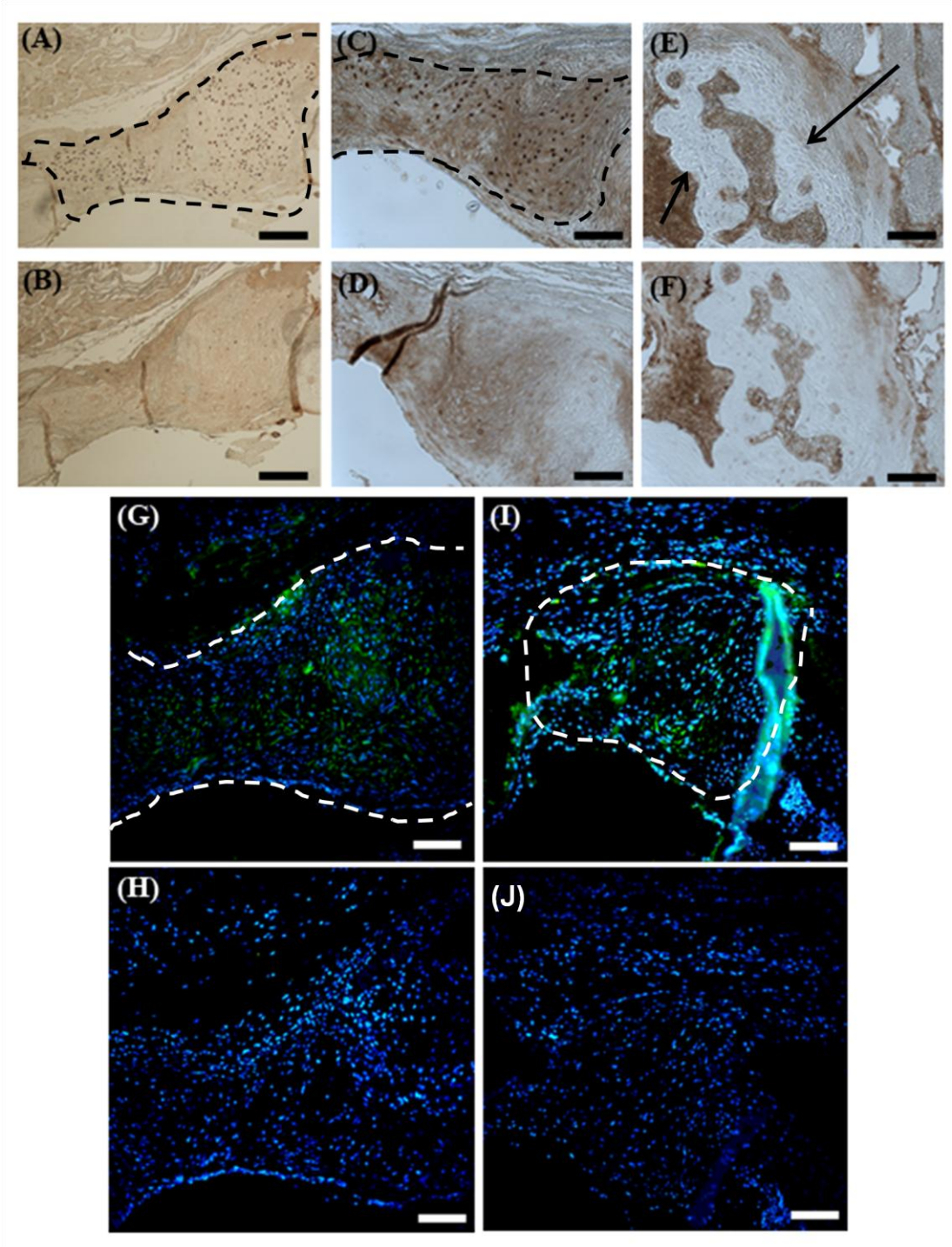

Figure A8: Immunostaining of calvarial defects similar in size as scaffoldless constructs. Constructs (black dashed outline) seen after 4 week (A) and 12 week (B) implantations express Ku80 (brown), a human specific nuclear protein , when compared to negative control (B and D, respectively), regenerated bone (black arrow) at 12 weeks does not express Ku80 (brown) (E), when compared to negative control (F). Scaffoldless constructs (outlined with dashed white line) at 4 (G) and 12 weeks (I) express DMP1 (green), when compared to negative control (H and J, respectively), DAPI nuclear stain is blue. Scale bars = 100 mm.

Conclusions

In this study, scaffoldless 3D tissues engineered from human dental pulp cells were implanted into calvarial defects in mice. A similar result was seen in both defect types where the presence of scaffoldless constructs induced ectopic host mouse bone formation over regions of natural mouse bone. The regenerated bone was not generated from the implanted cells. However, the cells within the scaffoldless construct produced a matrix containing a hard tissue protein, DMP1. Potentially, these matrix proteins facilitated an appropriate microenvironment to promote bone formation or outgrowth of the previously present bone tissue.

Acknowledgments

I would like to thank Dr. Charles Sfeir, Dr. Samer Zaky, Dr. Pamela Robey, and Ms. Tong Liu for their contributions to this research.

APPENDIX B:

CHARACTERIZATION OF RECAPP CALCIUM PHOSPHATE CEMENT

The following are results on a series of assays performed to characterize the ReCaPP calcium phosphate cement.

Protein release profile of ReCaPP

A release profile of adsorbed bovine serum albumin (BSA) from the ReCaPP cement was generated. The wells of a 96 well dish coated with either ReCaPP, commercially available cement, or contained no cement. The three substrates were coated with fluorescently labeled bovine serum albumin (BSA) using a solution containing 0.8 mg/ml of BSA in PBS. Two hundred and fifty µl were added to the different substrates resulting in 0.2 mg BSA/well, with an n = 3. The BSA solutions were left on the substrates for 2 days at 37°C. The wells were then rinsed for 1 minute with release medium containing α-MEM with 10% fetal bovine serum, 1% penicillin-streptomyocin, and 1% L-glutamine the release medium was then refreshed. Release medium was removed from each well and fluorescence was measured using a Perkin Elmer 1420 Victor^{3}V multilabel spectofluorometer after 1 and 4 hours and 1, 4, 7, 13, 21, 28, and 46 days. The

cumulative BSA released was calculated by taking the sum of BSA measured from all time points.

Figure B1 shows the release of profile of BSA from ReCaPP, the commercially available cement, and tissue culture plastic. The commercial cement and empty wells adsorbed lower amounts of BSA in comparison to ReCaPP. The commercial cement

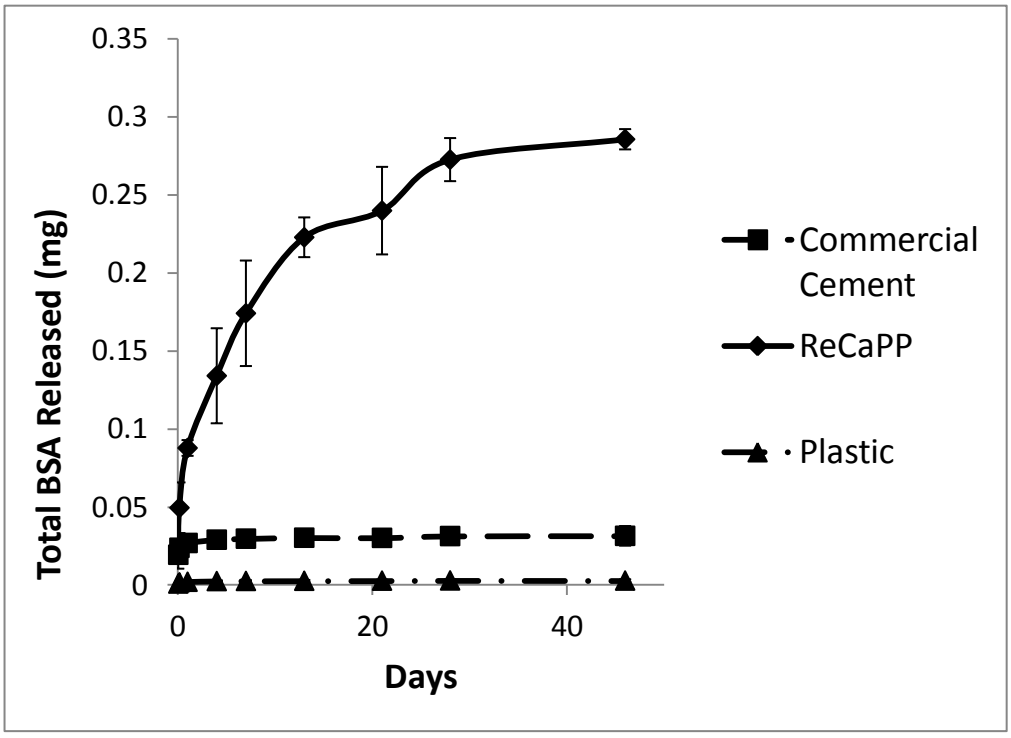

Figure B1: Release profile of fluorescently labeled BSA from ReCaPP cement, commercial cement and empty plastic culture wells.

and empty wells released all of the absorbed BSA at a very early time point whereas ReCaPP cement had a high initial release of BSA and continued to release small amounts of the protein over a span of 46 days.

Effects of set Recap and Recap paste on cell viability

Unlike the set cements, unreacted calcium phosphate pastes are generally considered toxic to cells due to fluctuations in pH during the setting process (Simon et al., 2004). Here, we assessed the effects of ReCaPP paste and set ReCaPP cement on MC3T3

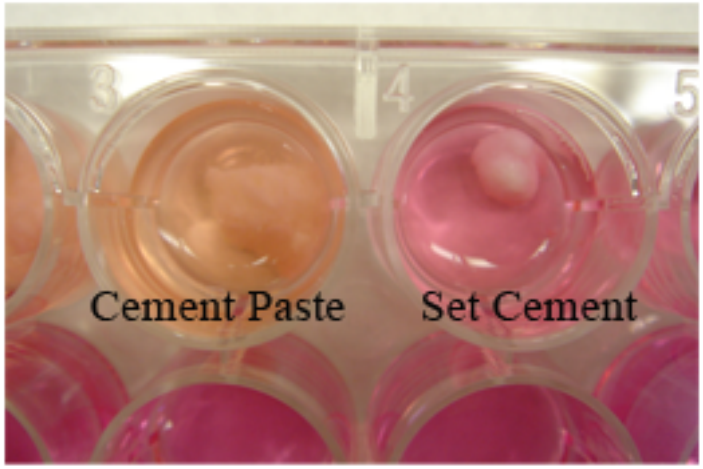

Figure B2: The media color differs from cultures with ReCaPP paste versus set ReCaPP cement which is indicative of a difference in pH.

cells, an osteoblast cell line. In this study, MC3T3 cells were cultured on 24 well dishes and either not set ReCaPP paste formed into balls or set ReCaPP cement was placed on top of the monolayer of cells. After 24 hours the first notable difference observed between cultures with cement paste versus cultures with set cement was the tissue culture media color which is indicative of differences in the pH (Figure B2). At this time,

the viability of the cells was assessed using a Live/Dead staining kit that uses calcein-AM to stain live cells green and ethidium homodimer to stain dead cells red (Figure B3). The region beneath the set cement predominately contained live cells whereas the region beneath the cement paste contained a mixture of live and dead cells. Simon et al. performed a similar assay and reported that the majority of cells did not survive when cultured with tetracalcium phosphate cement paste; their results are described in Figure B4 (Simon et al., 2004). Since some cells did survive when cultured with ReCaPP paste suggests that potentially ReCaPP cement paste may not be as toxic as other calcium phosphate pastes.

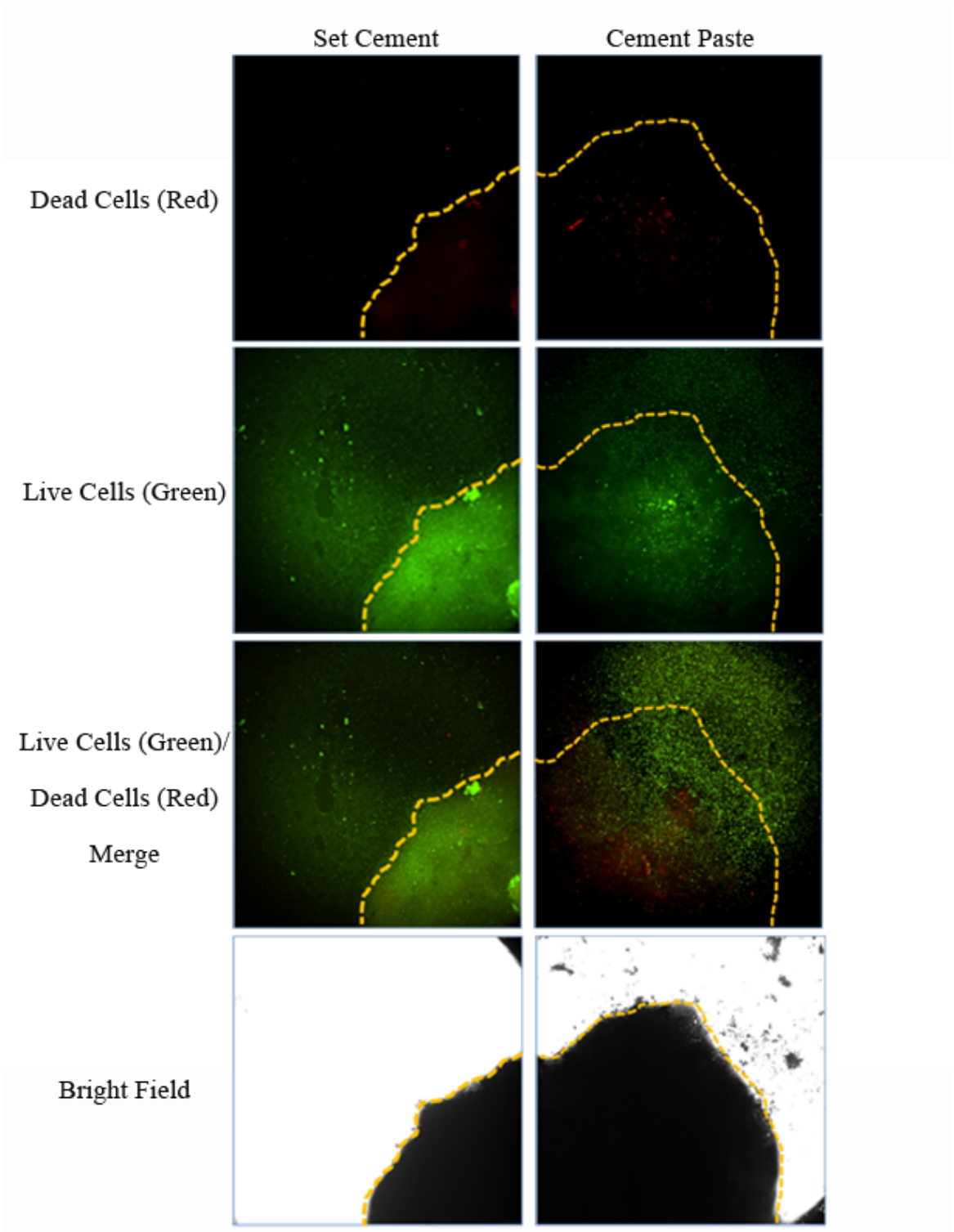

Figure B3: Images of cells cultured with either set ReCaPP cement or with ReCaPP paste and stained with Live/Dead stains. Yellow dotted line outlines location of ReCaPP as defined by brightfield images.

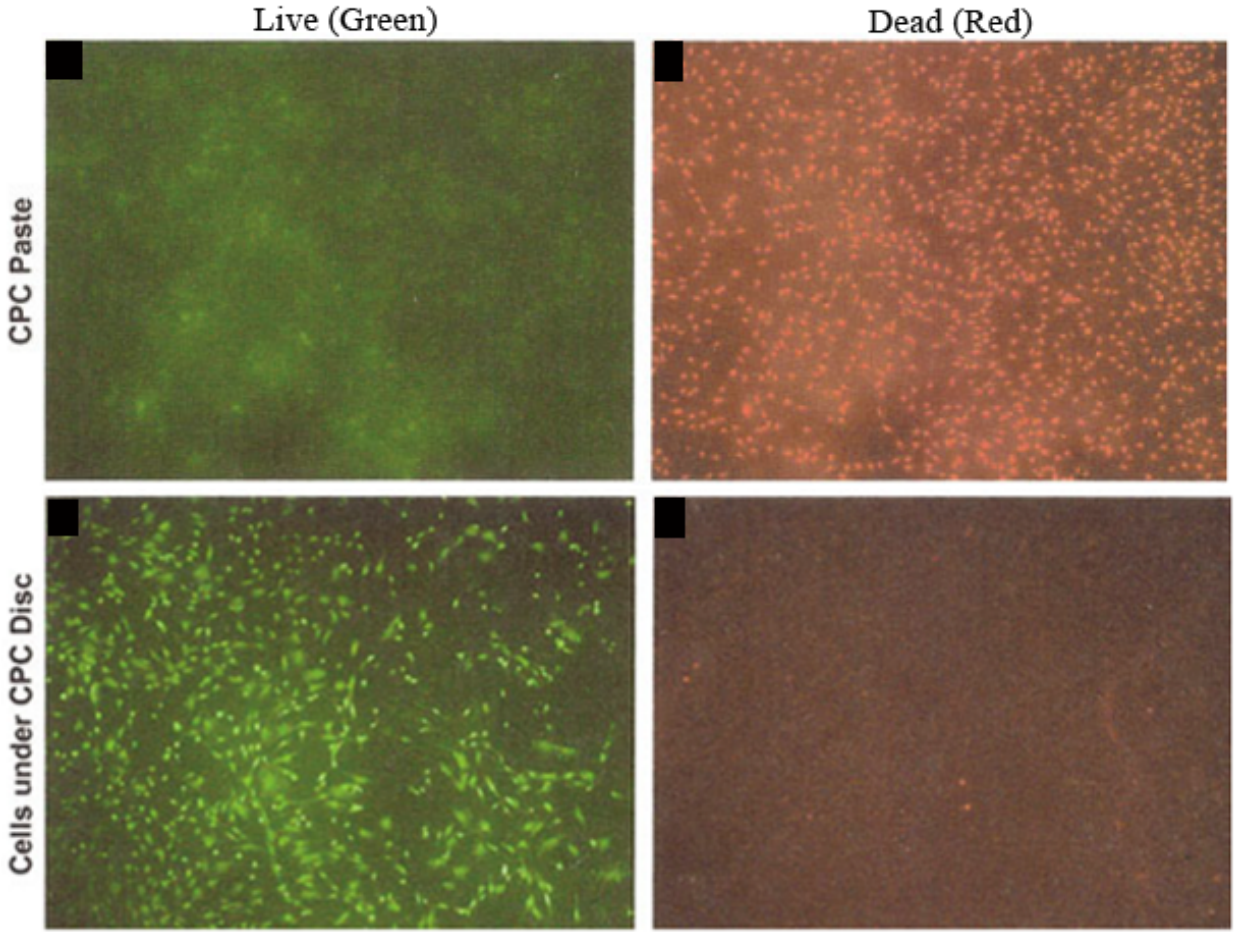

Figure B4: Live/Dead staining of cells cultured with either set tetracalcium phosphate or tetracalcium phosphate paste. Image modified from Simon et al. (Simon et al., 2004)

BIBLIOGRAPHY

About I, Proust JP, Raffo S, Mitsiadis TA, Franquin JC (2002). In vivo and in vitro expression of connexin 43 in human teeth. *Connect Tissue Res* 43(2-3):232-7.

Adams AM, Arruda EM, Larkin LM Use of adipose-derived stem cells to fabricate scaffoldless tissue-engineered neural conduits in vitro. *Neuroscience* 201(349-56.

Akiyama Y, Kikuchi A, Yamato M, Okano T (2004). Ultrathin poly(N-isopropylacrylamide) grafted layer on polystyrene surfaces for cell adhesion/detachment control. *Langmuir* 20(13):5506-11.

Akkayan B, Gulmez T (2002). Resistance to fracture of endodontically treated teeth restored with different post systems. *J Prosthet Dent* 87(4):431-7.

Allen MR, Hock JM, Burr DB (2004). Periosteum: biology, regulation, and response to osteoporosis therapies. *Bone* 35(5):1003-12.

Alliot-Licht B, Hurtrel D, Gregoire M (2001). Characterization of alpha-smooth muscle actin positive cells in mineralized human dental pulp cultures. *Arch Oral Biol* 46(3):221-8.

Alliot-Licht B, Bluteau G, Magne D, Lopez-Cazaux S, Lieubeau B, Daculsi G, et al. (2005). Dexamethasone stimulates differentiation of odontoblast-like cells in human dental pulp cultures. *Cell Tissue Res* 321(3):391-400.

An S, Gao Y, Ling J, Wei X, Xiao Y (2012). Calcium ions promote osteogenic differentiation and mineralization of human dental pulp cells: implications for pulp capping materials. *J Mater Sci Mater Med* 23(3):789-95.

Armulik A, Abramsson A, Betsholtz C (2005). Endothelial/pericyte interactions. *Circ Res* 97(6):512-23.

Bakland LK, Andreasen JO Will mineral trioxide aggregate replace calcium hydroxide in treating pulpal and periodontal healing complications subsequent to dental trauma? A review. *Dent Traumatol* 28(1):25-32.

Batouli S, Miura M, Brahim J, Tsutsui TW, Fisher LW, Gronthos S, et al. (2003). Comparison of stem-cell-mediated osteogenesis and dentinogenesis. *J Dent Res* 82(12):976-81.

Beniash E, Metzler RA, Lam RS, Gilbert PU (2009). Transient amorphous calcium phosphate in forming enamel. *J Struct Biol* 166(2):133-43.

Bergers G, Song S (2005). The role of pericytes in blood-vessel formation and maintenance. *Neuro-oncol* 7(4)*:*452-64.

Boskey AL (1998). Biomineralization: conflicts, challenges, and opportunities. *J Cell Biochem Suppl* 30-31(83-91.

Bosnakovski D, Mizuno M, Kim G, Ishiguro T, Okumura M, Iwanaga T, et al. (2004). Chondrogenic differentiation of bovine bone marrow mesenchymal stem cells in pellet cultural system. *Experimental Hematology* 32(5)*:*502-509.

Calve S, Dennis RG, Kosnik PE, 2nd, Baar K, Grosh K, Arruda EM (2004). Engineering of functional tendon. *Tissue Eng* 10(5-6)*:*755-61.

Canfield AE, Doherty MJ, Kelly V, Newman B, Farrington C, Grant ME, et al. (2000a). Matrix Gla protein is differentially expressed during the deposition of a calcified matrix by vascular pericytes. *FEBS Lett* 487(2)*:*267-71.

Canfield AE, Doherty MJ, Wood AC, Farrington C, Ashton B, Begum N, et al. (2000b). Role of pericytes in vascular calcification: a review. *Z Kardiol* 89 Suppl 2(20-7.

Carlile MJ, Sturrock MG, Chisholm DM, Ogden GR, Schor AM (2000). The presence of pericytes and transitional cells in the vasculature of the human dental pulp: an ultrastructural study. *Histochem J* 32(4)*:*239-45.

Chatterjee K, Sun L, Chow LC, Young MF, Simon CG, Jr. Combinatorial screening of osteoblast response to 3D calcium phosphate/poly(epsilon-caprolactone) scaffolds using gradients and arrays. *Biomaterials* 32(5)*:*1361-9.

Chong BS, Pitt Ford TR (2005). Root-end filling materials: rationale and tissue response. *Endodontic Topics* 11(114-130.

Chung CK, Muramatsu T, Uekusa T, Sasaki H, Shimono M (2007). Inhibition of connexin 43 expression and function in cultured rat dental pulp cells by antisense oligonucleotide. *Cell Tissue Res* 329(2)*:*295-300.

Clarke B (2008). Normal bone anatomy and physiology. *Clin J Am Soc Nephrol* 3 Suppl 3(S131-9.

Cordeiro MM, Dong Z, Kaneko T, Zhang Z, Miyazawa M, Shi S, et al. (2008). Dental pulp tissue engineering with stem cells from exfoliated deciduous teeth. *J Endod* 34(8)*:*962-9.

Covas DT, Panepucci RA, Fontes AM, Silva WA, Jr., Orellana MD, Freitas MC, et al. (2008). Multipotent mesenchymal stromal cells obtained from diverse human tissues share functional properties and gene-expression profile with CD146(+) perivascular cells and fibroblasts. *Exp Hematol*.

Crane NJ, Popescu V, Morris MD, Steenhuis P, Ignelzi MA, Jr. (2006). Raman spectroscopic evidence for octacalcium phosphate and other transient mineral species deposited during intramembranous mineralization. *Bone* 39(3)*:*434-42.

Crisan M, Casteilla L, Lehr L, Carmona M, Paoloni-Giacobino A, Yap S, et al. (2008a). A Reservoir of Brown Adipocyte Progenitors in Human Skeletal Muscle. ***Stem Cells*****.**

Crisan M, Yap S, Casteilla L, Chen CW, Corselli M, Park TS, et al. (2008b). A Perivascular Origin for Mesenchymal Stem Cells in Multiple Human Organs. ***Cell Stem Cell*** **3(3)*:*301-313.**

Crisan M, Sun, B., Casteilla, Louis., Zheng B., Gavina, M., Yap, S., Norotte, C., Logar, A., Tavian, M., Sinka, L., Teng, PN., Giacobino, JP., Torrente, Y., Huard, J., Peault, B. Vascular pericytes in human skeletal muscle development and regeneration. ***Paper Submitted*****.**

Cukierman E, Pankov R, Stevens DR, Yamada KM (2001). Taking cell-matrix adhesions to the third dimension. ***Science*** **294(5547)*:*1708-12.**

Cukierman E, Pankov R, Yamada KM (2002). Cell interactions with three-dimensional matrices. ***Curr Opin Cell Biol*** **14(5)*:*633-9.**

Damien CJ, Parsons JR (1991). Bone graft and bone graft substitutes: a review of current technology and applications. ***J Appl Biomater*** **2(3)*:*187-208.**

Dellavalle A, Sampaolesi M, Tonlorenzi R, Tagliafico E, Sacchetti B, Perani L, et al. (2007). Pericytes of human skeletal muscle are myogenic precursors distinct from satellite cells. ***Nat Cell Biol*** **9(3)*:*255-67.**

Dennis RG, Kosnik PE, 2nd (2000). Excitability and isometric contractile properties of mammalian skeletal muscle constructs engineered in vitro. ***In Vitro Cell Dev Biol Anim*** **36(5)*:*327-35.**

Dennis RG, Kosnik PE, 2nd, Gilbert ME, Faulkner JA (2001). Excitability and contractility of skeletal muscle engineered from primary cultures and cell lines. ***Am J Physiol Cell Physiol*** **280(2)*:*C288-95.**

Doherty MJ, Ashton BA, Walsh S, Beresford JN, Grant ME, Canfield AE (1998). Vascular pericytes express osteogenic potential in vitro and in vivo. ***J Bone Miner Res*** **13(5)*:*828-38.**

Doherty MJ, Canfield AE (1999). Gene expression during vascular pericyte differentiation. ***Crit Rev Eukaryot Gene Expr*** **9(1)*:*1-17.**

Donahue HJ (2000). Gap junctions and biophysical regulation of bone cell differentiation. ***Bone*** **26(5)*:*417-22.**

Ehrlich PJ, Lanyon LE (2002). Mechanical strain and bone cell function: a review. ***Osteoporos Int*** **13(9)*:*688-700.**

Ellender G, Feik SA, Carach BJ (1988). Periosteal structure and development in a rat caudal vertebra. ***J Anat*** **158(173-87.**

Elloumi Hannachi I, Itoga K, Kumashiro Y, Kobayashi J, Yamato M, Okano T (2009). Fabrication of transferable micropatterned-co-cultured cell sheets with microcontact printing. ***Biomaterials*** **30(29)*:*5427-32.**

Etchevers HC, Vincent C, Le Douarin NM, Couly GF (2001). The cephalic neural crest provides pericytes and smooth muscle cells to all blood vessels of the face and forebrain. *Development* 128(7)*:*1059-68.

Eyre-Brook AL (1984). The periosteum: its function reassessed. *Clin Orthop Relat Res* 189)*:*300-7.

Falanga V, Iwamoto S, Chartier M, Yufit T, Butmarc J, Kouttab N, et al. (2007). Autologous Bone Marrow-Derived Cultured Mesenchymal Stem Cells Delivered in a Fibrin Spray Accelerate Healing in Murine and Human Cutaneous Wounds. *Tissue Eng*.

Fan W, Crawford R, Xiao Y (2010). Enhancing in vivo vascularized bone formation by cobalt chloride-treated bone marrow stromal cells in a tissue engineered periosteum model. *Biomaterials* 31(13)*:*3580-9.

Feng J, Mantesso A, De Bari C, Nishiyama A, Sharpe PT Dual origin of mesenchymal stem cells contributing to organ growth and repair. *Proc Natl Acad Sci U S A* 108(16)*:*6503-8.

Fitzgerald M, Chiego DJ, Jr., Heys DR (1990). Autoradiographic analysis of odontoblast replacement following pulp exposure in primate teeth. *Arch Oral Biol* 35(9)*:*707-15.

Frankel VH, Nordin, M., editor (2001). Biomechanics of bone. In: Basic biomechanics of musculoskeletal system. Baltimore: Lippincott Williams and Wilkins.

Friedman S, Abitbol S, Lawrence HP (2003). Treatment outcome in endodontics: the Toronto Study. Phase 1: initial treatment. *J Endod* 29(12)*:*787-93.

Fujii T, Ueno T, Kagawa T, Sakata Y, Sugahara T (2006). Comparison of bone formation ingrafted periosteum harvested from tibia and calvaria. *Microsc Res Tech* 69(7)*:*580-4.

Galler KM, Hartgerink JD, Cavender AC, Schmalz G, D'Souza RN (2012). A customized self-assembling Peptide hydrogel for dental pulp tissue engineering. *Tissue Eng Part A* 18(1-2)*:*176-84.

Goldberg M, Smith AJ (2004). Cells and Extracellular Matrices of Dentin and Pulp: A Biological Basis for Repair and Tissue Engineering. *Crit Rev Oral Biol Med* 15(1)*:*13-27.

Goncalves SB, Dong Z, Bramante CM, Holland GR, Smith AJ, Nor JE (2007). Tooth slice-based models for the study of human dental pulp angiogenesis. *J Endod* 33(7)*:*811-4.

Gronthos S, Mankani M, Brahim J, Robey PG, Shi S (2000). Postnatal human dental pulp stem cells (DPSCs) in vitro and in vivo. *Proc Natl Acad Sci U S A* 97(25)*:*13625-30.

Hairfield-Stein M, England C, Paek HJ, Gilbraith KB, Dennis R, Boland E, et al. (2007). Development of self-assembled, tissue-engineered ligament from bone marrow stromal cells. *Tissue Eng* 13(4)*:*703-10.

Hall BK, editor (2000). The periosteum and bone growth. Boca Raton: CRC Press, Inc.

Heyeraas KJ, Berggreen E (1999). Interstitial fluid pressure in normal and inflamed pulp. *Crit Rev Oral Biol Med* 10(3)*:*328-36.

Hildebrand C, Fried K, Tuisku F, Johansson CS (1995). Teeth and tooth nerves. *Prog Neurobiol* 45(3)*:*165-222.

Horiuchi K, Amizuka N, Takeshita S, Takamatsu H, Katsuura M, Ozawa H, et al. (1999). Identification and characterization of a novel protein, periostin, with restricted expression to periosteum and periodontal ligament and increased expression by transforming growth factor beta. *J Bone Miner Res* 14(7)*:*1239-49.

Howson KM, Aplin AC, Gelati M, Alessandri G, Parati EA, Nicosia RF (2005). The postnatal rat aorta contains pericyte progenitor cells that form spheroidal colonies in suspension culture. *Am J Physiol Cell Physiol* 289(6)*:*C1396-407.

Huang GT (2009). Pulp and dentin tissue engineering and regeneration: current progress. *Regen Med* 4(5)*:*697-707.

Huang GT, Yamaza T, Shea LD, Djouad F, Kuhn NZ, Tuan RS, et al. (2010). Stem/progenitor cell-mediated de novo regeneration of dental pulp with newly deposited continuous layer of dentin in an in vivo model. *Tissue Eng Part A* 16(2)*:*605-15.

Huang GY, Cooper ES, Waldo K, Kirby ML, Gilula NB, Lo CW (1998). Gap junction-mediated cell-cell communication modulates mouse neural crest migration. *J Cell Biol* 143(6)*:*1725-34.

Hughes S, Chan-Ling T (2004). Characterization of smooth muscle cell and pericyte differentiation in the rat retina in vivo. *Invest Ophthalmol Vis Sci* 45(8)*:*2795-806.

Hutmacher DW, Schantz JT, Lam CX, Tan KC, Lim TC (2007). State of the art and future directions of scaffold-based bone engineering from a biomaterials perspective. *J Tissue Eng Regen Med* 1(4)*:*245-60.

Hwang YC, Hwang IN, Oh WM, Park JC, Lee DS, Son HH (2008). Influence of TGF-beta1 on the expression of BSP, DSP, TGF-beta1 receptor I and Smad proteins during reparative dentinogenesis. *J Mol Histol* 39(2)*:*153-60.

Iohara K, Nakashima M, Ito M, Ishikawa M, Nakasima A, Akamine A (2004). Dentin regeneration by dental pulp stem cell therapy with recombinant human bone morphogenetic protein 2. *J Dent Res* 83(8)*:*590-5.

Jager C, Welzel T, Meyer-Zaika W, Epple M (2006). A solid-state NMR investigation of the structure of nanocrystalline hydroxyapatite. *Magn Reson Chem* 44(6)*:*573-80.

Jo YY, Lee HJ, Kook SY, Choung HW, Park JY, Chung JH, et al. (2007). Isolation and characterization of postnatal stem cells from human dental tissues. *Tissue Eng* 13(4)*:*767-73.

Kamijo M, Haraguchi T, Tonogi M, Yamane GY (2006). The function of connexin 43 on the differentiation of rat bone marrow cells in culture. *Biomed Res* 27(6)*:*289-95.

Kiba W, Imazato S, Takahashi Y, Yoshioka S, Ebisu S, Nakano T Efficacy of polyphasic calcium phosphates as a direct pulp capping material. *J Dent* 38(10)*:*828-37.

Knaack D, Goad ME, Aiolova M, Rey C, Tofighi A, Chakravarthy P, et al. (1998). Resorbable calcium phosphate bone substitute. *J Biomed Mater Res* 43(4):399-409.

Knabe C, Berger G, Gildenhaar R, Meyer J, Howlett CR, Markovic B, et al. (2004). Effect of rapidly resorbable calcium phosphates and a calcium phosphate bone cement on the expression of bone-related genes and proteins in vitro. *J Biomed Mater Res A* 69(1):145-54.

Knabe C, Houshmand A, Berger G, Ducheyne P, Gildenhaar R, Kranz I, et al. (2008). Effect of rapidly resorbable bone substitute materials on the temporal expression of the osteoblastic phenotype in vitro. *J Biomed Mater Res A* 84(4):856-68.

Knothe Tate ML, Ritzman TF, Schneider E, Knothe UR (2007). Testing of a new one-stage bone-transport surgical procedure exploiting the periosteum for the repair of long-bone defects. *J Bone Joint Surg Am* 89(2):307-16.

Kosnik PE, Faulkner JA, Dennis RG (2001). Functional development of engineered skeletal muscle from adult and neonatal rats. *Tissue Eng* 7(5):573-84.

Kuhn B, del Monte F, Hajjar RJ, Chang YS, Lebeche D, Arab S, et al. (2007). Periostin induces proliferation of differentiated cardiomyocytes and promotes cardiac repair. *Nat Med* 13(8):962-9.

Lecanda F, Towler DA, Ziambaras K, Cheng SL, Koval M, Steinberg TH, et al. (1998). Gap junctional communication modulates gene expression in osteoblastic cells. *Mol Biol Cell* 9(8):2249-58.

Lecanda F, Warlow PM, Sheikh S, Furlan F, Steinberg TH, Civitelli R (2000). Connexin43 deficiency causes delayed ossification, craniofacial abnormalities, and osteoblast dysfunction. *J Cell Biol* 151(4):931-44.

Lee YL, Liu J, Clarkson BH, Lin CP, Godovikova V, Ritchie HH (2006). Dentin-pulp complex responses to carious lesions. *Caries Res* 40(3):256-64.

LeGeros RZ (1993). Biodegradation and bioresorption of calcium phosphate ceramics. *Clin Mater* 14(1):65-88.

LeGeros RZ (2002). Properties of osteoconductive biomaterials: calcium phosphates. *Clin Orthop Relat Res* 395):81-98.

LeGeros RZ (2008). Calcium phosphate-based osteoinductive materials. *Chem Rev* 108(11):4742-53.

Li X, Liu H, Niu X, Fan Y, Feng Q, Cui FZ, et al. (2011). Osteogenic differentiation of human adipose-derived stem cells induced by osteoinductive calcium phosphate ceramics. *J Biomed Mater Res B Appl Biomater* 97(1):10-9.

Li Y, Jin F, Du Y, Ma Z, Li F, Wu G, et al. (2008). Cementum and Periodontal Ligament-Like Tissue Formation Induced Using Bioengineered Dentin. *Tissue Eng Part A*.

Liu H, Gronthos S, Shi S (2006). Dental pulp stem cells. *Methods Enzymol* 419(99-113.

Lo CW (1996). The role of gap junction membrane channels in development. *J Bioenerg Biomembr* 28(4)*:*379-85.

Lo CW, Cohen MF, Huang GY, Lazatin BO, Patel N, Sullivan R, et al. (1997). Cx43 gap junction gene expression and gap junctional communication in mouse neural crest cells. *Dev Genet* 20(2)*:*119-32.

Lombaert IM, Brunsting JF, Wierenga PK, Faber H, Stokman MA, Kok T, et al. (2008). Rescue of salivary gland function after stem cell transplantation in irradiated glands. *PLoS One* 3(4)*:*e2063.

Ma D, Yao H, Tian W, Chen F, Liu Y, Mao T, et al. (2011). Enhancing bone formation by transplantation of a scaffold-free tissue-engineered periosteum in a rabbit model. *Clin Oral Implants Res* 22(10)*:*1193-9.

Mageed AS, Pietryga DW, DeHeer DH, West RA (2007). Isolation of large numbers of mesenchymal stem cells from the washings of bone marrow collection bags: characterization of fresh mesenchymal stem cells. *Transplantation* 83(8)*:*1019-26.

Mahamid J, Sharir A, Addadi L, Weiner S (2008). Amorphous calcium phosphate is a major component of the forming fin bones of zebrafish: Indications for an amorphous precursor phase. *Proc Natl Acad Sci U S A* 105(35)*:*12748-53.

Marks SC, Jr., Popoff SN (1988). Bone cell biology: the regulation of development, structure, and function in the skeleton. *Am J Anat* 183(1)*:*1-44.

Marshall GW, Jr., Marshall SJ, Kinney JH, Balooch M (1997). The dentin substrate: structure and properties related to bonding. *J Dent* 25(6)*:*441-58.

Masuda S, Shimizu T, Yamato M, Okano T (2008). Cell sheet engineering for heart tissue repair. *Adv Drug Deliv Rev* 60(2)*:*277-85.

Matsuoka H, Akiyama H, Okada Y, Ito H, Shigeno C, Konishi J, et al. (1999). In vitro analysis of the stimulation of bone formation by highly bioactive apatite- and wollastonite-containing glass-ceramic: released calcium ions promote osteogenic differentiation in osteoblastic ROS17/2.8 cells. *J Biomed Mater Res* 47(2)*:*176-88.

Matsusaki M, Kadowaki K, Tateishi K, Higuchi C, Ando W, Hart DA, et al. (2009). Scaffold-free tissue-engineered construct-hydroxyapatite composites generated by an alternate soaking process: potential for repair of bone defects. *Tissue Eng Part A* 15(1)*:*55-63.

Miletich I, Sharpe PT (2004). Neural crest contribution to mammalian tooth formation. *Birth Defects Res C Embryo Today* 72(2)*:*200-12.

Minkoff R, Rundus VR, Parker SB, Hertzberg EL, Laing JG, Beyer EC (1994). Gap junction proteins exhibit early and specific expression during intramembranous bone formation in the developing chick mandible. *Anat Embryol (Berl)* 190(3)*:*231-41.

Miura M, Gronthos S, Zhao M, Lu B, Fisher LW, Robey PG, et al. (2003). SHED: stem cells from human exfoliated deciduous teeth. *Proc Natl Acad Sci U S A* 100(10)*:*5807-12.

Moore KA, Lemischka IR (2006). Stem cells and their niches. *Science* 311(5769):1880-5.

Muller P, Bulnheim U, Diener A, Luthen F, Teller M, Klinkenberg ED, et al. (2008). Calcium phosphate surfaces promote osteogenic differentiation of mesenchymal stem cells. *J Cell Mol Med* 12(1):281-91.

Muraglia A, Corsi A, Riminucci M, Mastrogiacomo M, Cancedda R, Bianco P, et al. (2003). Formation of a chondro-osseous rudiment in micromass cultures of human bone-marrow stromal cells. *Journal of Cell Science* 116(14):2949-2955.

Murray PE, Garcia-Godoy F, Hargreaves KM (2007). Regenerative endodontics: a review of current status and a call for action. *J Endod* 33(4):377-90.

Nanci A, editor (2003). Ten Cate's Oral Histology: Development, Structure, and Function. St. Louis: Mosby.

Nayak RC, Berman AB, George KL, Eisenbarth GS, King GL (1988). A monoclonal antibody (3G5)-defined ganglioside antigen is expressed on the cell surface of microvascular pericytes. *J Exp Med* 167(3):1003-15.

Nishida K (2003). Tissue engineering of the cornea. *Cornea* 22(7 Suppl):S28-34.

Olivos-Meza A, Fitzsimmons JS, Casper ME, Chen Q, An KN, Ruesink TJ, et al. Pretreatment of periosteum with TGF-beta1 in situ enhances the quality of osteochondral tissue regenerated from transplanted periosteal grafts in adult rabbits. *Osteoarthritis Cartilage* 18(9):1183-91.

Ouyang HW, Cao T, Zou XH, Heng BC, Wang LL, Song XH, et al. (2006). Mesenchymal stem cell sheets revitalize nonviable dense grafts: implications for repair of large-bone and tendon defects. *Transplantation* 82(2):170-4.

Parirokh M, Torabinejad M Mineral trioxide aggregate: a comprehensive literature review--Part III: Clinical applications, drawbacks, and mechanism of action. *J Endod* 36(3):400-13.

Parirokh M, Torabinejad M Mineral trioxide aggregate: a comprehensive literature review--Part I: chemical, physical, and antibacterial properties. *J Endod* 36(1):16-27.

Peault B, Rudnicki M, Torrente Y, Cossu G, Tremblay JP, Partridge T, et al. (2007). Stem and progenitor cells in skeletal muscle development, maintenance, and therapy. *Mol Ther* 15(5):867-77.

Pittenger MF, Mackay AM, Beck SC, Jaiswal RK, Douglas R, Mosca JD, et al. (1999). Multilineage potential of adult human mesenchymal stem cells. *Science* 284(5411):143-7.

Pleshko N, Boskey A, Mendelsohn R (1991). Novel infrared spectroscopic method for the determination of crystallinity of hydroxyapatite minerals. *Biophys J* 60(4):786-93.

Prescott RS, Alsanea R, Fayad MI, Johnson BR, Wenckus CS, Hao J, et al. (2008). In vivo generation of dental pulp-like tissue by using dental pulp stem cells, a collagen scaffold, and dentin matrix protein 1 after subcutaneous transplantation in mice. *J Endod* 34(4):421-6.

Proudfoot D, Skepper JN, Shanahan CM, Weissberg PL (1998). Calcification of human vascular cells in vitro is correlated with high levels of matrix Gla protein and low levels of osteopontin expression. *Arterioscler Thromb Vasc Biol* 18(3):379-88.

Provis JM (2001). Development of the primate retinal vasculature. *Prog Retin Eye Res* 20(6):799-821.

Puckett CL, Hurvitz JS, Metzler MH, Silver D (1979). Bone formation by revascularized periosteal and bone grafts, compared with traditional bone grafts. *Plast Reconstr Surg* 64(3):361-5.

Qin C, D'Souza R, Feng JQ (2007). Dentin matrix protein 1 (DMP1): new and important roles for biomineralization and phosphate homeostasis. *J Dent Res* 86(12):1134-41.

Rashid F, Shiba H, Mizuno N, Mouri Y, Fujita T, Shinohara H, et al. (2003). The effect of extracellular calcium ion on gene expression of bone-related proteins in human pulp cells. *J Endod* 29(2):104-7.

Ray HA, Trope M (1995). Periapical status of endodontically treated teeth in relation to the technical quality of the root filling and the coronal restoration. *Int Endod J* 28(1):12-8.

Reinholz GG, Fitzsimmons JS, Casper ME, Ruesink TJ, Chung HW, Schagemann JC, et al. (2009). Rejuvenation of periosteal chondrogenesis using local growth factor injection. *Osteoarthritis Cartilage* 17(6):723-34.

Reynders P, Becker JH, Broos P (1999). Osteogenic ability of free periosteal autografts in tibial fractures with severe soft tissue damage: an experimental study. *J Orthop Trauma* 13(2):121-8.

Reynolds EC (1997). Remineralization of enamel subsurface lesions by casein phosphopeptide-stabilized calcium phosphate solutions. *J Dent Res* 76(9):1587-95.

Rezwan K, Chen QZ, Blaker JJ, Boccaccini AR (2006). Biodegradable and bioactive porous polymer/inorganic composite scaffolds for bone tissue engineering. *Biomaterials* 27(18):3413-31.

Rossello RA, Kohn DH (2009). Gap junction intercellular communication: a review of a potential platform to modulate craniofacial tissue engineering. *J Biomed Mater Res B Appl Biomater* 88(2):509-18.

Ruch JV (1998). Odontoblast commitment and differentiation. *Biochem Cell Biol* 76(6):923-38.

Saber-Samandari S, Gross KA Amorphous calcium phosphate offers improved crack resistance: a design feature from nature? *Acta Biomater* 7(12):4235-41.

Scheller EL, Krebsbach PH, Kohn DH (2009). Tissue engineering: state of the art in oral rehabilitation. *J Oral Rehabil* 36(5):368-89.

Schor AM, Allen TD, Canfield AE, Sloan P, Schor SL (1990). Pericytes derived from the retinal microvasculature undergo calcification in vitro. *J Cell Sci* 97 (Pt 3)(449-61.

See EY, Toh SL, Goh JC Multilineage potential of bone-marrow-derived mesenchymal stem cell cell sheets: implications for tissue engineering. *Tissue Eng Part A* 16(4)*:*1421-31.

Seo BM, Miura M, Gronthos S, Bartold PM, Batouli S, Brahim J, et al. (2004). Investigation of multipotent postnatal stem cells from human periodontal ligament. *Lancet* 364(9429)*:*149-55.

Sharpe PT, Young CS (2005). Test-tube teeth. *Sci Am* 293(2)*:*34-41.

Shepro D, Morel NM (1993). Pericyte physiology. *Faseb J* 7(11)*:*1031-8.

Shi S, Gronthos S (2003). Perivascular niche of postnatal mesenchymal stem cells in human bone marrow and dental pulp. *J Bone Miner Res* 18(4)*:*696-704.

Shi S, Bartold PM, Miura M, Seo BM, Robey PG, Gronthos S (2005). The efficacy of mesenchymal stem cells to regenerate and repair dental structures. *Orthod Craniofac Res* 8(3)*:*191-9.

Shih IM (1999). The role of CD146 (Mel-CAM) in biology and pathology. *J Pathol* 189(1)*:*4-11.

Simon CG, Jr., Guthrie WF, Wang FW (2004). Cell seeding into calcium phosphate cement. *J Biomed Mater Res A* 68(4)*:*628-39.

Soares CJ, Santana FR, Silva NR, Preira JC, Pereira CA (2007). Influence of the endodontic treatment on mechanical properties of root dentin. *J Endod* 33(5)*:*603-6.

Solan JL, Lampe PD (2009). Connexin43 phosphorylation: structural changes and biological effects. *Biochem J* 419(2)*:*261-72.

Sonoyama W, Coppe C, Gronthos S, Shi S (2005). Skeletal stem cells in regenerative medicine. *Curr Top Dev Biol* 67(305-23.

Sonoyama W, Liu Y, Yamaza T, Tuan RS, Wang S, Shi S, et al. (2008). Characterization of the apical papilla and its residing stem cells from human immature permanent teeth: a pilot study. *J Endod* 34(2)*:*166-71.

Stains JP, Civitelli R (2005). Gap junctions in skeletal development and function. *Biochim Biophys Acta* 1719(1-2)*:*69-81.

Stevens B, Yang Y, Mohandas A, Stucker B, Nguyen KT (2008). A review of materials, fabrication methods, and strategies used to enhance bone regeneration in engineered bone tissues. *J Biomed Mater Res B Appl Biomater* 85(2)*:*573-82.

Stockton LW (1999). Vital pulp capping: a worthwhile procedure. *J Can Dent Assoc* 65(6)*:*328-31.

Sun JS, Chang WH, Chen LT, Huang YC, Juang LW, Lin FH (2004). The influence on gene-expression profiling of osteoblasts behavior following treatment with the ionic products of sintered beta-dicalcium pyrophosphate dissolution. *Biomaterials* 25(4)*:*607-16.

Suzuki S, Sreenath T, Haruyama N, Honeycutt C, Terse A, Cho A, et al. (2009). Dentin sialoprotein and dentin phosphoprotein have distinct roles in dentin mineralization. *Matrix Biol* 28(4)*:*221-9.

Syed-Picard FN, Larkin LM, Shaw CM, Arruda EM (2009). Three-dimensional engineered bone from bone marrow stromal cells and their autogenous extracellular matrix. *Tissue Eng Part A* 15(1)*:*187-95.

Takita T, Hayashi M, Takeichi O, Ogiso B, Suzuki N, Otsuka K, et al. (2006). Effect of mineral trioxide aggregate on proliferation of cultured human dental pulp cells. *Int Endod J* 39(5)*:*415-22.

Tecles O, Laurent P, Zygouritsas S, Burger AS, Camps J, Dejou J, et al. (2005). Activation of human dental pulp progenitor/stem cells in response to odontoblast injury. *Arch Oral Biol* 50(2)*:*103-8.

Teng PN (2009). Mineralized tissue engineering, stem cell therapies and proteomics approaches. Pittsburgh, University of Pittsburgh.

Termine JD, Posner AS (1966). Infra-red determinaion of the percentage of crystallinity in apatitic calcium phosphates. *Nature* 211(5046)*:*268-70.

Torabinejad M, Ung B, Kettering JD (1990). In vitro bacterial penetration of coronally unsealed endodontically treated teeth. *J Endod* 16(12)*:*566-9.

Torabinejad M, Chivian N (1999). Clinical applications of mineral trioxide aggregate. *J Endod* 25(3)*:*197-205.

Wang C, Duan Y, Markovic B, Barbara J, Howlett CR, Zhang X, et al. (2004). Phenotypic expression of bone-related genes in osteoblasts grown on calcium phosphate ceramics with different phase compositions. *Biomaterials* 25(13)*:*2507-14.

Watt FM, Hogan BL (2000). Out of Eden: stem cells and their niches. *Science* 287(5457)*:*1427-30.

Weiner S, Addadi L (1997). Design strategies in mineralized biological materials. *Journal of Materials Chemistry* 7(5)*:*689-702.

Weiner S, Sagi I, Addadi L (2005). Structural biology. Choosing the crystallization path less traveled. *Science* 309(5737)*:*1027-8.

Yamato M, Konno C, Utsumi M, Kikuchi A, Okano T (2002). Thermally responsive polymer-grafted surfaces facilitate patterned cell seeding and co-culture. *Biomaterials* 23(2)*:*561-7.

Yang X, Walboomers XF, van den Beucken JJ, Bian Z, Fan M, Jansen JA (2008). Hard Tissue Formation of STRO-1-Selected Rat Dental Pulp Stem Cells In Vivo. *Tissue Eng Part A*.

Yu JH, Deng ZH, Shi JN, Zhai HH, Nie X, Zhuang H, et al. (2006). Differentiation of dental pulp stem cells into regular-shaped dentin-pulp complex induced by tooth germ cell conditioned medium. *Tissue Engineering* 12(11)*:*3097-3105.

Yuan H, Yang Z, Li Y, Zhang X, De Bruijn JD, De Groot K (1998). Osteoinduction by calcium phosphate biomaterials. *J Mater Sci Mater Med* 9(12)*:*723-6.

Yuan H, Li Y, de Bruijn JD, de Groot K, Zhang X (2000). Tissue responses of calcium phosphate cement: a study in dogs. *Biomaterials* 21(12)*:*1283-90.

Yuan H, Fernandes H, Habibovic P, de Boer J, Barradas AM, de Ruiter A, et al. (2010). Osteoinductive ceramics as a synthetic alternative to autologous bone grafting. *Proc Natl Acad Sci U S A* 107(31)*:*13614-9.

Zadik Y, Sandler V, Bechor R, Salehrabi R (2008). Analysis of factors related to extraction of endodontically treated teeth. *Oral Surg Oral Med Oral Pathol Oral Radiol Endod* 106(5)*:*e31-5.

Zandstra PW, Nagy A (2001). Stem cell bioengineering. *Annu Rev Biomed Eng* 3(275-305.

Zhang X, Awad HA, O'Keefe RJ, Guldberg RE, Schwarz EM (2008). A perspective: engineering periosteum for structural bone graft healing. *Clin Orthop Relat Res* 466(8)*:*1777-87.

Zhao L, Zhao J, Wang S, Wang J, Liu J (2011). Comparative study between tissue-engineered periosteum and structural allograft in rabbit critical-sized radial defect model. *J Biomed Mater Res B Appl Biomater* 97(1)*:*1-9.

Zhou Y, Chen F, Ho ST, Woodruff MA, Lim TM, Hutmacher DW (2007). Combined marrow stromal cell-sheet techniques and high-strength biodegradable composite scaffolds for engineered functional bone grafts. *Biomaterials* 28(5)*:*814-24.